FTIR-Spectroscopic Studies of Plasma Nitrogenation of Polyethylene Surfaces in Flowing DBD Post-Discharges in Nitrogen-Containing Gas Mixtures

Von der Fakultät Lebenswissenschaften
der Technischen Universität Carolo-Wilhelmina
zu Braunschweig
zur Erlangung des Grades einer
Doktorin der Naturwissenschaften
(Dr. rer. nat.)
genehmigte

D i s s e r t a t i o n

Von Zohreh Khosravi-Beringer
aus Esfahan / Iran

1. Referent: Professor Dr. Claus-Peter Klages
2. Referent: Professor Dr. Henning Menzel
eingereicht am: 03.02.2017
Mündliche Prüfung (Disputation) am: 23.06.2017

Druckjahr 2017

Vorveröffentlichungen der Dissertation

Teilergebnisse aus dieser Arbeit wurden mit Genehmigung der Fakultät für Lebenswissenschaften, vertreten durch den Mentor der Arbeit, in folgenden Beiträgen vorab veröffentlicht:

Publikationen

Klages, C.-P., Khosravi, Z. & Hinze, A. Some remarks on chemical derivatization of polymer surfaces after exposure to nitrogen-containing plasmas.
Plasma Process. Polym. 10: 307-312 (2013).

Klages, C.-P., Hinze, A. & Khosravi, Z. Nitrogen plasma modification and chemical derivatization of polyethylene surfaces - An in situ study using FTIR-ATR spectroscopy.
Plasma Process. Polym. 10: 948-958 (2013).

Khosravi, Z. & Klages, C.-P. Nucleophilic derivatization of polyethylene surfaces treated in ambient-pressure N_2-H_2 DBD post discharges.
Plasma Chem. Plasma Process. 34: 661-669 (2014).

Tagungsbeiträge

Khosravi, Z., Hinze, A. & Klages, C.-P.: In situ FTIR-ATR spectroscopic investigations of atmospheric-pressure plasma modification of polyolefin thin films. (Poster) presented at 13^{th} International Conference on Plasma Surface Engineering - PSE, Garmisch-Partenkirchen, Germany (2012).

Khosravi, Z. & Klages, C.-P.: Investigation of imine formation on PE surfaces treated in ambient-pressure nitrogen/hydrogen DBD afterglow, (Poster and extended abstract) at 14^{th} International Conference on Plasma Surface Engineering - PSE, Garmisch-Partenkirchen, Germany (2014).

Khosravi, Z., Kotula, S. & Klages, C.-P.: Electrophilic character of PE surfaces plasma-treated in N_2 or N_2-H_2 mixtures at atmospheric pressure, (Lecture) presented at the ISPC 22-22nd International Symposium on Plasma Chemistry, Antwerp, Belgium (2015).

I dedicate this thesis to my lovely parents

Zusammenfassung

Ziel dieser Arbeit ist es, ein besseres Verständnis der chemischen Eigenschaften von Polymeroberflächen zu erhalten, welche in praktisch sauerstoff-freien N_2-, NH_3- oder N_2-H_2- Gasmischungen bei Atmosphärendruck plasmabehandelt wurden. Solche Plasmabehandlungen führen zu Oberflächeneigenschaften, die in vielen Anwendungen (z.B. in der Biochemie) gewünscht sind.

Im Rahmen dieser Arbeit wurde gezeigt, dass einige Methoden, die zur Analyse von Oberflächen mit stickstoffhaltigen funktionellen Gruppen angewendet werden, falsch sind. Seit Jahrzehnten wird angenommen, dass individuelle funktionelle Gruppen auf plasma-modifizierten Oberflächen durch selektiv reagierende Derivatisierungsreagenzien detektiert und quantifiziert werden könnten. Für Oberflächen, die in stickstoffhaltigen Gasen plasmabehandelt wurden, wird allgemein anerkannt, dass Aminogruppen selektiv durch elektrophile Reagenzien wie Benzaldehyde (z. B. TFBA) oder Essigsäureanhydride (z. B. TFAA) analysiert werden könnten. Diese beiden Annahmen wurden bis heute fälschlicherweise zu Grunde gelegt.

Zur Untersuchung der Plasmabehandlung wurde ein Aufbau entwickelt, der FTIR-ATR-Analysen *in situ* von mit Polyethylen beschichteten ATR-Kristallen erlaubt. Die Behandlung erfolgt durch den Afterglow einer N,H-haltigen Entladung. Zusätzlich zu den Änderungen der Oberfläche durch Wechselwirkung mit Plasmaspezies wurden auch verschiedene Gase (z.B. feuchte Luft, Derivatisierungsreagenz) über die (plasmabehandelte) Oberfläche geleitet und die dadurch induzierten Änderungen konnten im IR-Spektrum *in situ* verfolgt werden. Die Oberflächen zeigten eine Reaktion mit TFBA, die zur Anbindung von etwa zwei 4-Trifluoromethylbenzaldimin-Gruppen pro Quadratnanometer führten. Trotzdem konnten mittels einer Isotopen-Austauschtechnik (Nachweisgrenze ca. 0,3 nm^{-2}) keine Aminogruppen gefunden werden.

Es wurde die Hypothese aufgestellt, dass die Aldehydreaktivität solcher Oberflächen in dem Vorhandensein von Iminen begründet ist, oder allgemeiner durch die Präsenz von N=C-Gruppen. Eine Literaturrecherche sowie eigene Experimente zeigten, dass aliphatische Imine tatsächlich mit aromatischen Adelhyden reagieren können. Neben der nukleophilen Reaktivität zeigen Imine aber auch elektrophile Eigenschaften. Daher wurden im Rahmen dieser Arbeit erstmals N,H-plasma-behandelte Oberflächen mit drei nukleophilen Reagenzien derivatisiert. Mittels XPS und FTIR-ATR (beides *ex situ*) wurde gezeigt, dass die behandelten Oberflächen tatsächlich mit nukleophilen Reagenzien reagieren, was unsere Imino-Hypothese untermauerte. Dafür sprachen auch NEXAFS-Untersuchungen (Röntgen-Nahkanten-Absorptionsspektroskopie), welche das Vorhandensein von N=C bestätigten.

Schlussendlich kann gefolgert werden, dass die chemische Reaktivität von Polyethylenoberflächen nach einer Plasmabehandlung hauptsächlich durch Iminogruppen und nicht durch Aminogruppen bestimmt wird, wie bisher allgemein angenommen wurde.

Dieses Ergebnis und auch TFAA-Experimente zeigen, dass weder TFBA-Reaktionen noch Derivatisierungen mit TFAA brauchbar sind, um Konzentrationen und Dichten von primären und sekundären Aminogruppen zu quantifizieren. Die Derivatisierung einer Oberfläche gibt lediglich Aufschluss darüber wie viel eines elektrophilen oder nukleophilen Reaktionspartners an eine Oberfläche gebunden werden kann.

Abstract

The aim of this work is to provide a better insight into the chemical properties of polymer surfaces treated with dielectric barrier discharge (DBD) plasmas in well-defined virtually oxygen-free N_2, NH_3, N_2-H_2 gas mixtures at ambient pressure. Plasma treatments under such atmospheric conditions lead to the creation of surfaces with properties required in many applications (e.g. in biochemistry).

This work presents several arguments which demonstrate that the traditional derivatization method used for the analysis of surfaces with nitrogen-containing functional groups is invalid and is based partially on myths. For decades, it has been thought that individual functional groups on plasma-modified polymer surfaces can be detected and quantified using selectively reacting derivatization reagents. For surfaces treated in nitrogen-containing plasmas it has traditionally been believed that amino groups can be analyzed selectively using electrophilic reagents such as benzaldehydes (much-used TFBA) or carboxylic acid anhydrides (e.g. TFAA). These two assumptions have been incorrectly accepted until now.

For the investigation of the plasma treatment a setup which allows *in situ* FTIR-ATR measurements of PE-coated ATR crystals was developed. *In situ* IR spectra of films treated in afterglows of DBDs in N_2 or in mixtures of N_2 with H_2 as well as after controlled exposure to various reagents, such as water vapor, oxygen, or derivatization reagents were taken. The plasma-treated surfaces generally showed a reaction with TFBA leading to the attachment of roughly two 4-trifluoromethyl-benzaldimine moieties per square nanometer. However, a search for a corresponding density of primary amino groups, using an isotope exchange technique was unsuccessful. Within the estimated limits of detection (about 0.3 nm^{-2}) no NH_2 groups of primary amines were present.

It was hypothesized that the aldehyde reactivity of such surfaces could be due to the presence of imino groups or, more generally, >N=C- moieties. In fact, an inspection of the chemical literature as well as own experiments showed that aliphatic imines are able to react with aromatic aldehydes. Besides nucleophilic reactivity, imines are also responsible for the electrophilic surface properties. Therefore, N, H-plasma treated surfaces were derivatized using three nucleophilic reagents, for the very first time. XPS and FTIR-ATR analyzes (both *ex situ*) proved a successful binding of significant amounts of reagents which corroborated our imino hypothesis. This was supported by near-edge X-ray absorption fine structure analyzes (NEXAFS) performed to confirm the presence of >C=N- groups.

It can be concluded that the chemical reactivity of our polyethylene surfaces after plasma treatment is largely, if not mainly, determined by the presence of imino groups instead of amino groups, as it had generally been assumed.

These results and also TFAA experiments show that neither the reaction with TFBA nor the derivatization with TFAA could be used to quantify concentrations or densities of primary and secondary amino groups. A derivatization of such surfaces just indicates how much of an electrophilic or a nucleophilic reaction partner can bind to the surface.

Contents

List of Figures

List of Tables

Acknowledgement

First and foremost, for giving me the opportunity to complete my thesis as a member of the Institute for surface technology, I would like to thank my supervisor Prof. Dr. Claus-Peter Klages. I would like to express my sincere gratitude to him for his encouragement, patience, motivation, never ending support, enthusiasm, and supervision throughout this study. Also, his deep expertise concerning the theoretical background of chemical science showed me the way in a difficult terrain.

Besides my supervisor, I am particularly thankful to Prof. Dr. Henning Menzel and Prof. Dr. Karl-Heinz Gericke for being the examiner of this work and their insightful comments.

I would like to extend the deepest thanks to my colleagues in the IOT group and Fraunhofer Institute for Surface Engineering and Thin Films (IST) for their cherished friendship and continuous support throughout my studies.

I would like to thank Mr. R. Schwetge from IOT for his technical help, Antje Jung from Fraunhofer IST for XPS measurements and helpful discussions as well as Kress Nagel for his valuable technical supervision on plasma equipment and his support during the entire course of this work. On a personal note, I wish to thank Dipl.-Ing. A. Hinze for her treasured partnership and enlightening me the first glance of research.

Furthermore I wish to thank Dr. W. Unger and Dipl.-Ing. A. Lippitz for NEXAFS measurements at the Federal Institute of Material Research and Testing (BAM) with BESSY facility in Berlin and their contributions to the analysis and fruitful discussions.

In particular, I owe a debt of gratitude to my lovely parents who encouraged and helped me at every stage of my personal and academic life, and longed to see this achievement come true. I am very much indebted to my family for the support they provided me through my entire life and in particular also their endless patience.

This work was supported by a grant from the Deutsche Forschungsgemeinschaft (DFG-No. Kl 1096/19). I kindly acknowledge the financial support of the DFG.

And my very special thanks go to my beloved husband, Benjamin, who supported me in every possible way with his continued and unfailing love to see the completion of this work. I thank you for all the things that you have done for me and your words that always help me.

The last but not least, I would like to extend my gratitude to my lovely brother and sister, Omid and Zahra for supporting me spiritually throughout my education and my life in general.

Above all, I owe it all to Almighty God for granting me the wisdom, health and strength to undertake this research task and enabling me to complete it.

1 Overview of dissertation

The plasma-based functionalization of polymer surfaces with nitrogen-containing groups has been studied by many authors [7–9], using gas discharges in N_2 [10, 11], NH_3 [10, 12, 13], $NH_3 + H_2$ [14], and $N_2 + H_2$ [10, 12]. Less focus has been given to nitrogenation using post-discharge plasmas at atmospheric pressure, although the use of this process may have advantages [15]. It is the aim of this work to contribute and to elucidate reaction mechanisms of remote-plasma-treatments. Knowledge of how reaction mechanisms operate in practice provides a good basis for the development and/or improvement of technical remote-plasma-based nitrogenation processes. Thus, investigations were carried out of the post-discharges of dielectric barrier discharge (DBD) in N_2-H_2 mixtures using polyethylene (PE) as a substrate.

Of key importance in this work was the determination of amino groups present on the treated surfaces with respect to their type and density. Nitrogen-containing functional groups can be introduced on polymer surfaces through plasma treatments using low- or ambient-pressure gas discharges in nitrogen or nitrogen-containing gases and gas mixtures [12, 16]. Chemical derivatization (CD), usually combined with X-ray photoelectron spectroscopy (XPS), has commonly been used for analytical studies of polymer surfaces treated with nitrogen plasmas to quantify the functional surface groups that are present [17]. For instance, in a large number of papers published over the last 30 years, derivatization of plasma-treated surfaces using an aromatic aldehyde, such as 4-(trifluoromethyl)benzaldehyde (TFBA), was accepted to be as a selective method for labelling and quantifying the primary amino groups -NH_2, as shown in Fig. 1.1.

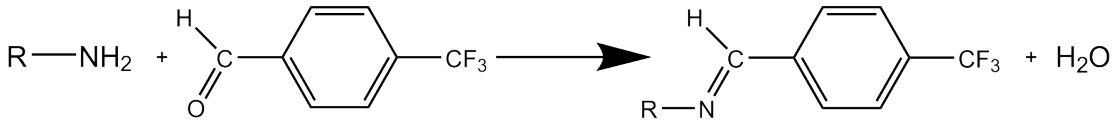

Figure 1.1: The derivatization reaction of primary amine (-NH_2) with 4-(trifluoromethyl) benzaldehyde (TFBA)

1.1 A short overview of the characterization of plasma-nitrogenated polymer surfaces

Since the 1960's, the formation of nitrogen-containing functional groups on polyethylene surfaces plasma-treated in nitrogen-containing gases has been studied [18, 19]. In a paper by Hollahan et al., it was reported that -NH_2 groups can be grafted on to various polymers by exposure to low-pressure gas discharges in ammonia or in nitrogen-hydrogen mixtures [12]. These researchers used several polymers, such as polypropylene, poly(vinyl chloride), polytetrafluoroethylene, polycarbonate, polyurethane, and poly(methyl methacrylate). Surface characterization was accomplished using an alkylation reaction in the solution. The procedure included immersing treated films for 24 hours in a methanol solution containing 10 % methyl iodide. Then, the obtained quaternary sites with positively charged nitrogen were able to form stable complexes with the negatively charged sulfate groups of heparin sulfate. The authors applied a heparin derivative tagged with ^{33}S to quantify the amount of heparin attached to the quaternary sites.

X-ray photoelectron spectroscopy (XPS) has been extensively applied to study organic, inorganic, and polymer systems [20–23]. In the 1970s, when plasma treatment of polymers gained significant interest [24], XPS played an important role in identifying formed species. XPS of plasma-treated polymer surfaces [20, 22] as well as plasma polymers [25–28] has been routinely applied.

In 1976, plasma-chemical modification of PE surfaces in nitrogen corona discharges at atmospheric pressure was performed by Courval et al. for the first time [16]. The authors referred to Hollahan et al.'s work [12] and also claimed the attachment of amino groups on the nitrogen-containing plasma-treated PE surfaces.

Applying different plasma parameters leads to varying results in the surface modification processes. Therefore, identification of functional groups requires an appropriate technique. However, due to the lack of energy resolution and specificity of the obtained spectra with respect to functional groups, XPS alone was not sufficient to gain detailed insight into chemical surface compositions. A new method was developed in order to clarify the different functional groups. This method combined XPS with a preceding chemical derivatization. The chemical derivatization method using a group of specific reagents containing XPS-detectable elements not contained in the original surface, was applied to radio-frequency (RF) nitrogen-plasma-treated polyethylene surfaces by Everhart and Reilley in 1981 [29]. As a derivatization reagent an aromatic aldehyde, pentafluorobenzaldehyde (PFB), was applied. The result of PFB derivatization of plasma-treated surfaces is the formation of a Schiff-base derivative via the reaction shown in Fig. 1.2. The authors claimed that "*pentafluorobenzaldehyde reacts with primary and secondary*

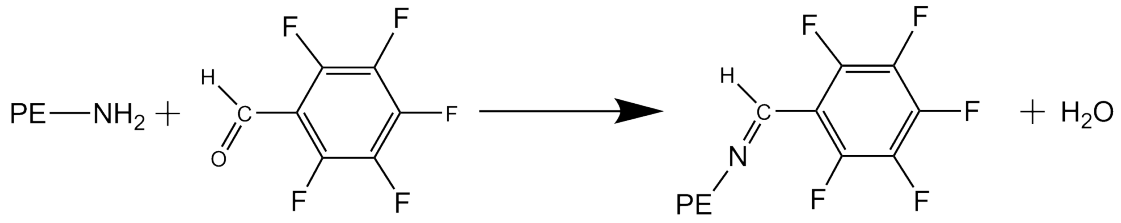

Figure 1.2: The reaction of plasma-treated PE surfaces with pentafluorobenzaldehyde (PFB)

amines and hydrazines but is not expected to react with amides, imines, nitriles, or nitrogen containing heterocyclics." [29]. However, in 1981, there was evidence already existed from other sources that did not support this statement. For instance, the reaction of aldehydes with imines had been reported by Ingold [30], Layer [31], and Patai [32].

In 1982, the chemical derivatization XPS on low-density polyethylene (LDPE) surfaces treated by air plasmas using several different derivatization reagents to quantify oxygen-containing functional groups, such as hydroperoxide, hydroxy, carbonyl, and carboxyl groups, was carried out [33]. Terlingen et al. were the first to use TFBA for derivatization. To analyze plasma-immobilized films prepared from preadsorbed amines; they assumed that the aldehyde is able to react with amines as well as hydrazines [34]. Since Everhart and Reilley made this statement more than 30 years ago, TFBA and other aromatic aldehydes have been considered to be derivatization reagents with selectivity for primary amino groups and have frequently been applied to determine the density of primary amino groups on the modified surfaces of polymers [28].

The assumed -NH_2 selective reaction with TFBA has never been conclusively proven. In regard to this assumption, the density of primary amino groups on plasma-treated polymer surfaces has been assumed to be proportional to the density of 4-trifluoromethyl-phenyl moieties (4-CF_3-C_6H_4-) chemically bonded to the surfaces. Chemical derivatization using another aromatic aldehyde, such as chlorobenzaldehyde, on N_2-H_2 plasma-treated polytetrafluoroethylene (PTFE) surfaces was performed to calculate the amount of grafted amine [35]. In another study, PFB was applied to quantify the functional groups on the surface of plasma polymers deposited by different amines [36].

Several other reagents have been used in the plasma polymer field. For instance, CD-XPS using trifluoroacetic anhydride (TFAA) has been assumed as a standard method for tagging primary amino, secondary amino, and hydroxyl groups [37]. These reactions between either primary or secondary amines with TFAA are illustrated in Fig. 1.3.

The assumption that aldehydes (and anhydrides) react selectively with primary amines (with primary and secondary amines and/or hydroxyl groups) in the presence of other nitrogen-containing

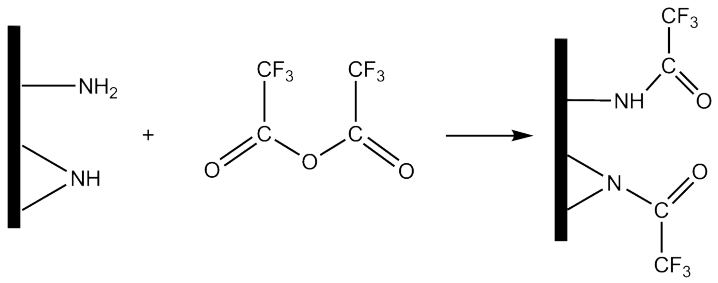

Figure 1.3: The reactions of primary and secondary amines, -NH_2 and -NH, with trifluoroacetic anhydride (TFAA)

species, is not supported by the results of this work. Functional groups containing >C=N structures, for example, can also react with aldehydes, such as TFBA, and anhydrides, such as TFAA. Imines have the general ability to exchange the carbonyl component with an aromatic aldehyde. Thus, surface reactivity of nitrogen plasma-treated polymers or amine-based plasma polymers with TFBA or similar reagents cannot be attributed to amine alone.

Plasma treatments may result in the formation of various functional groups on the substrate surface. Functionalization takes place during exposure of the substrate to the plasma but also during post-reactions. A hypothetic chain of PE after formation of nitrogenated functional groups by replacement of H and insertion reactions, respectively, in N_2-H_2 mixtures-plasma is shown in Fig. 1.4 top. Different nitrogen functional groups, such as amines -NH or -NH_2, aldimine -N=C, ketimine >C=NH, nitrile -C≡N, azine C=N-N=C, carbodiimide N=C=N, hydrazone -C=N-NH_2 or hydrazine -N-NH_2 may be expected on polymer surfaces that have been plasma-treated in nitrogen-containing gases. Supposing that primary-amino selectivity of TFBA is valid [13, 14, 38, 39], the TFBA molecule is able to bond to polymer surfaces exclusively via -NH_2, as shown in Fig. 1.4 bottom.

The hypothesis made in this work suggest that TFBA reaction with functional groups containing carbon-nitrogen double bonds must be taken into account, because all moieties containing carbon-nitrogen double bonds will react with TFBA. According to the results of this work, surface reactivity of treated polymers in nitrogen-containing plasmas with TFBA or other aldehydes cannot be attributed exclusively to primary amines.

1.2 Chapters contents

Chapter 1 gives the overview of the dissertation. A brief statement on N, H-treated polymer characterization, mainly the derivatization method is presented.

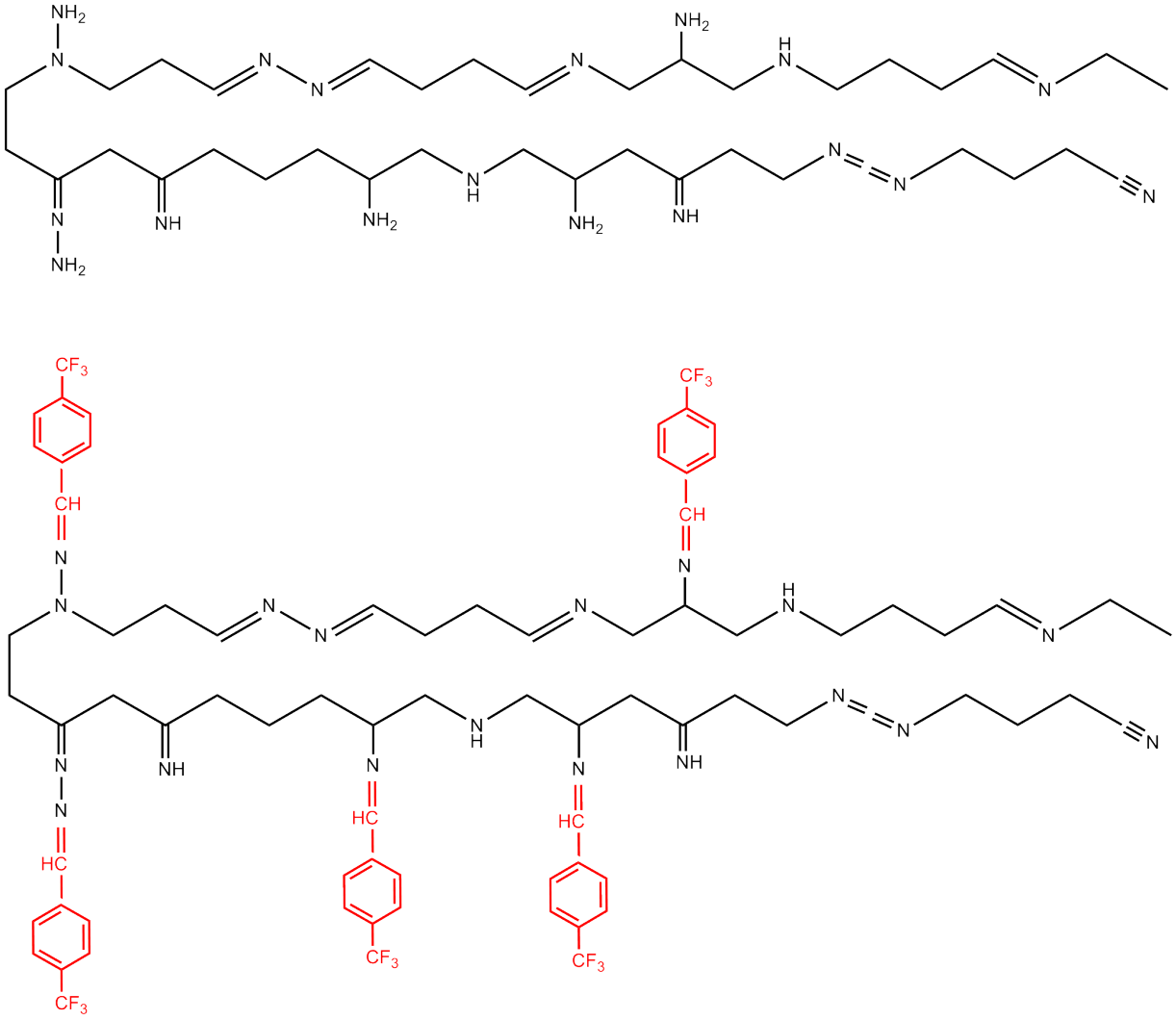

Figure 1.4: Top: PE chain with probable functional groups formed in N_2-H_2 mixtures plasma. Bottom: The assumed selective reaction of TFBA with -NH_2 groups on the plasma-treated polymer surface.

In chapter 2 a general introduction to plasmas and their various applications are given. Special consideration is given to plasmas for surface modification. Among various methods for plasma generation, dielectric barrier discharges (DBD) at atmospheric pressure are of special interest in this work. A short review on afterglow plasma, particularly nitrogen afterglow, is given.

Chapter 3 reviews the analytical methods applied to nitrogen-plasma-modified polymer surfaces in mixtures of nitrogen and hydrogen gases.

Chapter 4 describes the materials used, the experimental setups for derivatization and hydrogen-deuterium (H-D) exchange as well as the XPS procedure applied in this work.

In chapter 5, results and analyzes of PE surfaces plasma-treated in post-discharges of N_2-H_2 at ambient pressure are presented and discussed. This chapter includes results of afterglow plasma treatment of polymer surfaces for process gases with different concentrations of hydrogen into nitrogen as well as different treatment time. In addition, Fourier transform infrared (FTIR) measurements in attenuated total reflection (ATR) mode of plasma-treated surfaces after contact with water vapor and ambient atmosphere are evaluated. Finally, the H-D exchange experiment is discussed in detail. Result of chemical derivatization of plasma-treated surfaces with 4-(trifluoromethyl)benzaldehyde vapors is interpreted .

An "imine hypothesis" encouraged us to study the reaction of imines with several assumed amine selective derivatization reagents such as TFBA. These results are found in chapter 6. A review of available literature and several experiments; results of aldol reaction of TFBA with imine in the liquid phase, gas-phase reaction of TFBA with imines on solid surfaces, exchange reaction between aliphatic imine and TFBA in the liquid phase are investigated in this chapter.

In chapter 7, the main aim is to provide reasonable and logical arguments for evidence of C=N groups formed on plasma-treated surfaces by means of DBD setup fed by N_2-H_2-containing gas. For this purpose, the nucleophilic derivatization of plasma-treated surfaces using 4-(trifluoromethyl) phenylhydrazine (TFMPH) and 2-mercaptoethanol (ME) were checked by FTIR-ATR and XPS. Reaction of plasma-treated surfaces to 4-(trifluoromethyl)benzylamine (TFMBA) vapors is studied using FTIR-ATR. Additionally, near-edge X-ray absorption fine structure (NEXAFS) measurements of plasma-treated surfaces are studied.

The content of chapter 8 deals with optical emission spectroscopy of nitrogen and nitrogen-hydrogen-oxygen mixtures plasma in the post-discharge region. The nitrogen atom density in the post-discharge region, in which polymer films were treated, is determined.

In the chapter 9, results are summarized and outlooks on future works are presented.

A major part of the results presented here has already been published in three peer-reviewed papers [1–3]. References given in some of the chapter headings refer to own publications used as sources for the present thesis.

2 Introduction

2.1 Plasma general information

A plasma, often also referred to a fourth state of matter, is a partially ionized gas containing ions, electrons, atoms, and neutral species. It is characterized by free electrons, i.e., that are not bound to nuclei. The electron's energy required to have a plasma depends on the electron orbital configuration of the matter. In gases, the energy needed to free electrons is of the order of 10 eV. For plasma generation neutral atoms and molecules need to be ionized. This can be done by the collision of energetic particles, strong electric fields or ionising radiations. Plasma is characterized by certain parameters such as the mode of generation of the discharge (AC, DC, RF, HF, etc.), the pressure (low or ambient), etc. Atmospheric plasmas for the generation of ozone [40] have been used for a long time, since the Siemens process was presented in 1857 [41].

Plasma is also apply to polymerization [25, 28, 42, 43]. Plasma polymerization is a polymer-forming process under the influence of plasma. Monomer gas molecules are activated by plasma and cleaved into activated fragments. Two fragments then recombine into a larger molecule. Fragmentation and recombination are repeated until polymers are formed. Details for plasma polymerization can be found in Yasuda's book [44] and refs. [25–27, 42, 45].

Recently, biological and biomedical applications of plasma modifications have gained considerable interest [46]. Plasma is applied for bacterial inactivation [47], sterilization of medical instruments [48], and surface modification of implantable biomaterials [49]. The plasma conditions of a DBD device can be intended for use in medical applications, especially for skin treatment [50]. Different thermal plasma sources and non-thermal sources like plasma needle [51], plasma pencil [52], and miniature high-frequency (HF) plasma source [53] have been used in medical applications. Plasma sterilization is fast developing into a promising alternative to standard sterilizing techniques [54]. The spores which are basically composed of atoms like C, O, N, and H will form simple compounds like CO_2 after contact with UV photons and radicals of plasma. The CO_2 can be subsequently flushed out. Several examples in plasma applications can be found, for instance, in the recently published book by Thomas et al. [15].

2.2 Plasma applications for polymer surface treatment

Plasma treatment process provides a high grafting efficiency for the modified surface [55]. Creation of active species at low temperature and easily controllable electrical parameters of a plasma are two advantages of this method. Plasma treatment is an important technology for improving the surface wettability and adhesion [56]. The plasma treatment forms surface radicals [57], which promote different effects such as cross-linking, functionalization, and degradation. Utilizing plasma processes a wide variety of specific surface properties can be developed.

For decades, polymers which have suitable bulk physical and chemical properties, have been used in different fields such as packaging, electronics, and biomedical industries [58]. In many cases, good adhesion between two substrates is necessary. This requires polar groups on the surface of the polymer. Some polymer films have good adhesion properties, but in many cases the characterization of polymer surfaces reveals low surface tension, chemical inertness and a smooth surface. Therefore, the surface has quite weak adhesion properties. In order to enhance the bondability of surfaces, they need to be suitably treated. For instance, several attempts have been made to improve the adhesion property of PE with plasma treatment [59–61]. Plasma improves adhesion performance without altering the bulk properties. Hence, the plasma treatment of polymer surfaces is a widely used technique to enhance adhesion [62].

A great variety of plasma processing techniques have been developed to functionalize polymer surfaces [13, 63–65]. Plasma treatment of polymers leads to an activity of a polymeric surface by inserting active species (mainly polar groups), degradation, branching of the macromolecules, etching, and cross-linking processes [66]. These effects are dependant upon the gas used, energy of plasma ions, temperature during the treatment, discharge power, and general conditions. The treatment of surfaces by barrier discharges in air has already a long tradition [67]. Argon plasmas are suitable for cross-linking of polymer matrices which can improve the chemical resistance, optical density, hardness, and other surface properties. In addition, argon plasmas induce direct energy transfer to the surface due to vacuum-ultraviolet (VUV) radiation emitted by plasma glow [68]. By selecting the kind and nature of the gas applied, it is possible to choose the type of chemical modification of the polymer surface. A big advantage of plasma treatment is that due to the modification of only a very thin surface layer of polymer, the polymer bulk maintains its good mechanical properties. Several applications of plasma are presented shortly in the following.

Hydrophilic surface modification: The wettability enhancement is one of the apparent advantages of the plasma treatment. For hydrophilic surface modification of polymers, oxygen is one of the common gases used [69]. Active oxygen radicals oxidize (oxygen can be absorbed by the

upper most atomic layers) the polymer surface and increase the number of polar groups like carbonyl (>C=O) and carboxyl (-COOH) on the surface and therefore improves the wettability for water or other chemicals. As an example, polyethyleneterephthalate (PET) features a hydrophobic surface and thus poor adhesion. Before application PET must be modified to obtain hydrophilic properties. For this purpose, PET foils can be treated in a nitrogen plasma and its afterglow [70]. The effectiveness of the modification of polymers is closely related to the kind of plasma being used. PET polymers have been effectively changed to hydrophilic surfaces using oxygen, nitrogen, argon, hydrogen, and ammonia plasma [71].

Hydrophobic surface modification: Hydrophobic surface modification has applications in manufacturing industries such as micro inkjet printing, corrosion protection, self-cleaning surfaces, and as a bio-device to prevent protein coagulation, etc. To generate a hydrophobic surface, typically fluorocarbon compounds such as CF_4 is used for plasma-activated film deposition. Considering the toxicity of fluorine compounds, a precursor for film deposition like hexamethyldisiloxane (HMDSO) is often used [72].

Cleaning: Plasma treatment is a safe alternative to traditional cleaning methods. It can completely remove contaminant layers from surfaces which must be very clean. The active species in an oxygen plasma for example, combined with VUV energy, are able to create a chemical reaction with the surface contaminants. A wide variety of materials beyond polymers as well as complex surface geometries such as glass slides, substrates, optical fibers, semiconductor wafers, substrates (Si, Ge), and metal surfaces can be cleaned using plasma.

Sterilization: Plasma technology is useful for disinfection and sterilization of medical devices. One of the advantages of plasma technology is its ability to do both, surface modification and sterilization, simultaneously. This feature is more considerable in biomedical device fabrication and is suggested for medical implants and devices which are sensitive to temperature, chemicals and radiation.

Metallization: Polymer metallization is broadly used for electronic devices, packaging and reflective coatings. Because of the differences between physical and chemical properties of metallic film and substrates, a high-density of chemical bonds is needed. Normally, the surface is activated by generation of catalytically active palladium particles. A wet-chemical process is generally applied for catalytic activation of sites. Later, plasma treatment was applied as an alternative

Duration	1-10 ns	Total charge	0.1-1 nC
Filament radius	$\sim$ 0.1 mm	Electron density	10^{14}-10^{15} cm^{-3}
Peak current	0.1 A	Electron energy	1-10 eV
Current density	100-1000 A cm^{-2}	Gas temperature	$\sim$ average gap temperature

Table 2.1: Characteristic microdischarge properties [5]

reaction scheme, which is safer and low cost [73]. For metallization of certain areas, a new process, so-called "Plasma Printing" has been developed by Klages and Thomas [74–76]. In Plasma Printing, discharges are generated in volumes with linear dimensions of only a few microns.

2.3 Dielectric barrier discharge (DBD)

For several decades, ozone generation was the main industrial application of DBDs and was mainly applied in water treatment. Hence, the dielectric barrier discharge is sometimes also referred to as the "ozonizer discharge". DBD arrangements are usually comprised of two electrodes separated by a small distance (typically 0.2 to 5 mm) with at least one solid dielectric material in between [5]. Alumina, glass, quartz, and ceramics are typical materials for dielectric barriers.

The dielectric layer operates as a current limiter and avoids the formation of a spark or an arc discharge. The presence of the dielectric is essential for the proper functioning of the discharge. It limits the amount of charge and energy imparted to an individual microdischarge and spreads the microdischarges evenly over the whole electrode surface. In the discharge gap, the current is maintained by a large number of microdischarges which are of nanosecond duration and are uniformly distributed over the dielectric surface. Every microdischarge includes an almost cylindrical plasma channel of about 100 μm radius in the discharge gap, and spreads into a larger surface discharge on the dielectric. Current densities up to 1000 A/cm^2 can be reached in the current filaments. The typical operating frequency range for most technical DBD application is between 500 Hz and 500 kHz. Table 2.1 summarizes typical microdischarge properties (order of magnitude) for a 1 mm air gap at 1 bar [5]. In spite of high current densities, the transported charge (0.1-1 nc), and the energy density (10 mJ/cm^3) in the microdischarge channel are very small due to extremely short duration of the current flow (2-5 ns). Consequently, the gas temperature in the current filaments remains near to the average temperature in the discharge gap. In addition, the electron temperature reaches values of about 50000 K, which corresponds to a mean electron energy of about 5 eV.

The important characteristic of this type of electrical discharge is that non-equilibrium plasma conditions in atmospheric pressure gases can be provided in an economic and reliable way. This

feature has led to a number of industrial applications such as pollution control, excitation of excimer lamps, and more recently surface modification of various materials. One of the main potential application fields of non-thermal discharges is the treatment of living tissues without thermal damaging. Several applications of DBD with different electrode arrangements in surface treatment and porous materials are reported in refs. [77, 78]. DBD is also well known as an efficient source of active species like $^1O_2$, NO, N, O, and OH. These species play a significant role in plasma chemistry as well as organic and inorganic surface treatment due to their high reactivity.

Three different important regimes can be observed in DBDs including filamentary DBD (FDBD) and two types of uniform or diffuse DBD, namely glow DBD (GDBD), and Townsend DBD (TDBD). The volume discharge of a DBD normally operates in the filamentary discharge mode, and under special conditions a diffuse discharge or homogeneous discharge can be observed [79].

In the filamentary regime, due to a streamer breakdown, a multitude of microdischarges with almost 100 μm and 10-100 ns time duration exists. Electron and ion densities can reach values of 10^{14} to 10^{15} cm^3 for a current density of about 100-1000 A/cm^2, additionally the electron energy largely differs in time and space [80]. Homogeneous discharges are, due to a Townsend breakdown, easily achievable at lower pressure, while such a discharge in air or nitrogen at atmospheric pressure is not easy to obtain [81]. To get the homogeneous mode in atmospheric pressure the breakdown has to be a Townsend one and the ionization has to be slow enough to avoid a large avalanche development.

GDBD begins with a Townsend breakdown initiating a Townsend discharge, during which the discharge evenly covers the surface of electrodes at each moment of its development. The Townsend breakdown is defined by gas bulk ionisation (the 1^{st} Townsend coefficient, α) and secondary electron emission at cathode (2^{nd} Townsend coefficient, γ) needing slower ionization processes than the streamer mode. However, the overall volume is ionized and even longer than in a FDBD. The discharge duration of this breakdown is in the range of μs and the discharge area is equal to that of the electrodes. The empirical equation suggested by Townsend leads to the Paschen curve which demonstrates the existence of a minimum breakdown voltage at a certain pd-value (pressure distance product). Atmospheric pressure TDBD, similarly to GDBD, starts with a Townsend breakdown initiating a Townsend discharge but the formation of a cathode fall does not occur since the ionization level remains too low. Hence, the high electric field is achieved, which is in favor of streamer formation even after gas breakdown. Maximum electron density in GDBD and TDBD are 10^8 and 10^{11} cm^{-3}, respectively. The mechanism of homogeneous DBDs at atmospheric pressure was recently published in detail by Massines et al. [82]. A homogeneous discharge is more efficient for surface treatment where uniformity is the main issue [77]. Ho-

mogeneous DBDs at atmospheric pressure have been achieved using He [83], He-N_2 gas mixture [84], N_2 [85], Ne-N_2, Ar-N_2 [86], Ar [87], etc. More details on DBD operation can be obtained in refs. [79, 88].

2.4 Atmospheric-pressure nitrogen plasma

Functional groups containing nitrogen have generated considerable interest because they can improve the biocompatibility of artificial biomaterials or they can be used for covalent bonding of bioactive molecules [89]. Formation of such functional groups requires plasma treatment in nitrogen [18, 19, 90] or nitrogen-containing gas mixtures [1]. Upon contact of the polymer surface with such discharges or their afterglows many different chemical moieties may be expected to form on the polymer surface, as it was shown earlier in Fig. 1.4 top. Saturated C-C and C-H bonds in the polymers are inert. In contrast nitrogen can form polar covalent bonds with hydrocarbons which changes the chemical and physical properties of polymers. The recent interest in atmospheric-pressure plasma-based functionalization of polymers with nitrogen-bearing groups has kept growing [15].

2.4.1 Afterglow treatment

In the plasma afterglow (post-discharge) the external electric fields are either missing or not strong enough to maintain the discharge. In this region, the plasma-generated species de-excite and therefore secondary chemical reactions occur, which lead to the formation of stable species. Nitrogen afterglows are extensively used for many applications in surface treatment and chemical synthesis [1, 90]. Hence, more studies of chemical composition of the afterglow and gas temperature are required. It is known that species with long lifetimes, such as nitrogen atoms and excited metastable species, are responsible for chemical reactions with an added gas or a solid surface [91]. Recently, several investigations have been performed to find the rotational temperatures of N_2 and to identify and estimate the active species in the afterglow of N_2-discharges excited by microwave (2450 MHz) [92] and in DBDs [91, 93].

Nitrogen afterglow

Thanks to many experimental techniques, it is known that ground-state atomic nitrogen is the reactive component in active nitrogen (in the downstream region of discharge) [94–96]. The

lifetime of the afterglow depends on the pressure and the condition of the walls in the containing vessel. The first study of active nitrogen reactions with polymers was reported by Weininger [19]. The nitrogen atom reaction with carbon-carbon bond of polymer can result in nitrogen-containing groups or radicals as well as polymer cross-linking. Formation of hydrogen cyanide (HCN) and cyanogen $(CN)_2$ during treatment of polyethylene, polypropylene, and polyisobutylene were reported while for polyisobutylene ammonia formation is also seen [19]. More information, details in nature and the mechanism of nitrogen afterglow are reported in a review by Jennings et al. [95].

The emission bands in the nitrogen afterglow are related to a transition from a more highly-excited state (B $^3\Pi_g$) to a lower excited state (A $^3\Sigma^+{}_u$), so called first positive system (FPS) of nitrogen. Next, the molecules reach the ground state (X $^1\Sigma^+{}_g$) by losing additional energy in collisions with other molecules or walls. The green emission, due to the presence of NO, which can be detected at 557.7 nm, is because of a small quantity of oxygen or groups containing oxygen in the gas [95].

3 Theoretical background

Analytical methods applied to N, H-plasma-modified surfaces

Surface treatment requires the use of the appropriate methods to quantify the changes in the surface structure and composition. A very thin layer of a few nanometer thickness should be studied in which the density of atoms is of the order of 0.1 to 1 nm^{-2}. The analytic method should provide at least an elemental analysis of the near-surface layer or an identification of chemical groups.

In this work, plasma-modified polymer surfaces in nitrogen containing gases are of great interest. Reaction of active nitrogen with the polymer surface leads to the formation of nitrogen complexes, nitrogen-containing compounds or radicals as well as hydrogen abstraction from polymer chains [18, 19]. A nitrogen atom can be added at either end of the polymer chain or within the chain. The suitable surface analysis techniques applied in this work are:

- Fourier transform infrared spectroscopy (FTIR) equipped with diamond single reflection ATR crystal as well as a PIKE horizontal attenuated total reflectance (HATR) accessory with a multi-bounce ZnS ATR,

- X-ray photoelectron spectroscopy (XPS),

- chemical derivatization X-ray photoelectron spectroscopy (CD-XPS),

- chemical derivatization FTIR, and

- near-edge X-ray absorption fine structure (NEXAFS).

3.1 FTIR spectroscopy in the attenuated total reflection (ATR) mode

As an analytical tool, Fourier transform infrared (FTIR) spectroscopy in the attenuated total reflection (ATR) mode offers a possibility to study the films forming directly on the interface of an ATR crystal. For this purpose the crystal is coated with a thin and smooth layer of various materials for process studies [97]. As a significant advantage ultrathin films and surface coatings, especially polymers, can be investigated in a relatively undisturbed state [98]. Additionally, the chemistry of the coated surface can be directly monitored by collecting spectra in real time [1].

A summarized explanation of the ATR technique follows. A sample is placed in contact with an internal reflection element (IRE). Propagated radiation in the IRE with an optically dense medium of refractive index n_1 undergoes total internal reflection at an interface of an adjacent medium of lower optical density (refractive index $n_2 < n_1$) and creates an evanescent wave. The "evanescent" wave means to tend to vanish or pass away like a vapor. This phenomenon occurs when the angle of incidence exceeds a critical angle θ_c determined by:

$$sin\theta_c = \frac{n_2}{n_1} \tag{3.1}$$

The evanescent wave is a more informative probe of material because it is non-transverse and therefore has components in all spatial directions, which means vector components can interact with the dipoles in all directions.

There are some factors which influence the ATR analysis such as the wavelength of the infrared radiant, λ, refractive indices of sample and internal reflection element, (n_2, n_1 respectively) and the angle of incidence of the IR radiation θ. The penetration depth equation of the evanescent wave is seen below:

$$d_p = \frac{\lambda}{2\pi n_1[sin^2\theta - (n_2/n_1)^2]^{1/2}} \tag{3.2}$$

An ATR spectrum $S_{ATR}(\nu)$ will be proportional to a transmission spectrum of the same substance, $S_T(\nu)$, multiplied by ν^{-1}, i.e., bands at higher wavenumbers have relatively low absorbances.

For bulk material, the thickness of the rare medium is much larger than the penetration depth of the evanescent field. The electric field amplitudes in the rare medium are different for equal incident amplitudes of perpendicular and parallel polarization. Therefore, the effective thicknesses

for s and p polarization are different. In the case of parallel polarization, the electric vector is parallel to the plane of incidence [99]. The relative effective thicknesses for perpendicular (s) and parallel polarization (p) in bulk materials are shown in Eq. 3.3 and Eq. 3.4.

$$\frac{d_s}{\lambda_1} = \frac{n_{21}cos\theta}{\pi(1-n_{21}^2)(sin^2\theta - n_{21}^2)^{1/2}} \tag{3.3}$$

$$\frac{d_p}{\lambda_1} = \frac{n_{21}cos\theta(2sin^2\theta - n_{21}^2)}{\pi(1-n_{21}^2)[(1+n_{21}^2)sin^2\theta - n_{21}^2](sin^2\theta - n_{21}^2)^{1/2}} \tag{3.4}$$

Where λ_1 is the wavelength of radiation in denser medium ($\frac{\lambda}{n_1}$), λ wavelength in free space, θ incident angle, $n_{21} = \frac{n_2}{n_1}$.

The requirement for a thin film is fulfilled when the thickness of the film is thinner than the penetration depth. In this case we can assume that the electric field amplitude is constant over the film thickness. The effective thickness for both s and p polarization in the case of isotropic thin films are shown in Eq. 3.5 and 3.6.

$$d_s = [4n_{21}dcos\theta/(1-n_{31}^2)] \tag{3.5}$$

$$d_p = \frac{4n_{21}dcos\theta[(1+n_{32}^4)sin^2\theta - n_{31}^2]}{(1-n_{31}^2)[(1+n_{31}^2)sin^2\theta) - n_{31}^2]} \tag{3.6}$$

Where θ is incident angle $n_{31} = \frac{n_3}{n_1}$, $n_{32} = \frac{n_3}{n_2}$ and $n_{21} = \frac{n_2}{n_1}$. More information related to effective thickness are reported by Harrick [97]. The validity of the effective thickness equation used in internal reflection spectroscopy is proved by comparing it to exact computer calculations for different refractive indices, angles of incidence, extinction coefficients, and film thickness [99].

3.1.1 Quantitative evaluation of IR spectra to find the densities of chemically bonded reagents

In the following, we use the symbol ε for the decadic molar absorption coefficient as defined in Lambert-Beer's law, $A_T \equiv \log(I_0/I) = \varepsilon cl$, for the absorbance A_T of a sample with the path length l, containing the absorbing species at molar concentration c, measured in a transmission experiment with incident and transmitted intensities I_0 and I, respectively [100].

The absorption coefficient α is defined by the equation $\frac{I}{I_0} = exp(-\alpha l)$, which for low absorbance (αl$\ll$1) can be approximated by $\frac{I}{I_0} = 1 - \alpha l$. For ATR measurements Harrick by analogy defined an effective thickness d_e using the equation $R = \frac{I}{I_0} \equiv 1 - \alpha d_e$ for the reflectance R in a single-reflection configuration ($\alpha d_e \ll 1$). With N-fold reflections the resulting total reflectance is $R_N = R^N = (1-\alpha d_e)^N \approx 1 - N\alpha d_e$ [99]. As it is common practice, the results of ATR spectra are shown here as absorbance, $A = \log(\frac{1}{R_N})$ versus wavenumber ν in cm^{-1}.

$$A = \log \frac{1}{R_N} \cong \frac{N\alpha d_e}{ln(10)} \tag{3.7}$$

The integral of A over an absorption band b of a vibration is given by the equations

$$\int_b A d\nu = N d_e \int_b \alpha \frac{d\nu}{ln(10)} = N c d_e \int_b \varepsilon d\nu \tag{3.8}$$

The integral over ε on the right-hand side can be expressed using the integrated (or integral) absorption intensity [101]; we use the letter B for this quantity

$$\begin{aligned} \int_b A d\nu &= \frac{N d_e c B}{ln10} \\ B \equiv \frac{1}{cl} \int_b ln \frac{I_0}{I} d\nu &= ln10 \int_b \varepsilon d\nu \end{aligned} \tag{3.9}$$

For many infrared absorption bands, integrated intensities B can be found in the literature. It is important to pay attention to the units used: While the path length is generally given in cm and concentration in mol/L, the molar absorption coefficient may either be based on decadic logarithms like in the "practical units" used by Wexler [102] or on natural logarithms as, for example, in the papers by Ramsay as well as by Yagudaev et al. [103], and in this work.

Harrick's definition of an effective thickness is useful for samples which are either thick, compared to the penetration depth of the radiation d_p (bulk samples), or thin with respect to d_p (thin film samples). For a thin film of thickness d, the ratio $\frac{d_e}{d} \equiv f$ is a function of the refractive indices n_i of the three materials involved (i = 1: ATR element, i = 2: thin film, i = 3: third phase, usually air), the angle of incidence θ, and the state of polarization of the light with respect to the plane of incidence. Owing to the virtually constant electric field of the evanescent wave over a thin film sample of thickness d $\ll$ d_p the absorbance is independent of the distribution of absorbers over the thickness, as long as the concentration average c_{av} over d is the same. Therefore in the case

of a non-uniform distribution the product cd can be replaced by $c_{av}d$, which is the area density ρ of absorbers:

$$\int_b A d\nu = \frac{NcdfB}{ln10} = \frac{N\rho fB}{ln10} \tag{3.10}$$

Here the lhs is the band area measured in absorbance, N is the number of reflections in the ATR crystal (in our case N = 1) and ρ is the area density of absorbers. If B is known, equation 3.10 can be used to determine ρ from the measured vibrational band area and f as calculated from Harrick's formula [99]. (f is the ratio of the effective penetration depth to the thickness of the layer where IR absorption takes place, see above).

If literature data for B is unavailable, it can be determined from ATR measurements on solutions (index s) containing known concentrations c_s of suitable reference molecules featuring the oscillator: According to equation 3.10, B can be calculated from a plot of the integrated absorbance as a function of molar concentration: The slope of this plot equals the product $\frac{NdfB}{ln10}$. In the reference measurements, the sample solution thickness on the ATR element must exceed the penetration depth d_p by far and d_{es} is the effective thickness for a solution as a bulk sample.

3.2 Hydrogen-deuterium (H-D) exchange

Hydrogen atoms attached to nitrogen and oxygen in simple peptide groups in native proteins are immediately substituted by deuterium when dissolved in deuterium oxide solution [104]. Linderstrom-Lang and Hvidt accomplished a series of -XH exchange studies on a variety of proteins and polypeptides using their own designed and built equipment [105]. Lenormant and Blout showed that some of the amide hydrogens in two protein examples (bovine serum albumin and ovalbumin) are able to exchange rapidly with D_2O [106]. The rate of hydrogen-deuterium exchange of secondary amide hydrogens in polypeptides and proteins was later studied using infrared spectroscopy [107]. On studying the -NH stretching vibration of aminos and amides at 3300 cm^{-1}, the exchange of deuterium in some proteins and nucleoproteins was determined [108].

In general, hydrogen atoms bonded to heteroatoms such as O, N, S, or P atoms are chemically much more reactive than carbon-bonded hydrogen atoms. In contact with liquid or gaseous heavy water (D_2O) a rapid equilibration will take place furnishing a nearly statistical distribution of H and D over the compound carrying the heteroatom and water [108]. Spectroscopic observation

of H-D exchange between biomolecules and the surrounding water has become an important method for studying the structure of biomolecules [109].

3.3 X-ray photoelectron spectroscopy (XPS)

X-ray photoelectron spectroscopy (XPS) is a very powerful tool to study the outermost few tens of angstroms of the surface [110]. Investigations of binding energies and relative peak intensities corresponding to the direct photoionization of core levels gives information on polymer structures [23]. Structure and bonding in polymeric systems have been studied extensively using XPS at Durham university by Clark et al. [20, 21, 23]. XPS is frequently applied to distinguish the features formed on plasma-treated polymer [22, 111, 112]. Various plasma-treated polymers were investigated using XPS by Yasuda for the very first time [113]. Polyethylene and polystyrene treated in oxygen microwave plasma were found to be rich in peroxy features using XPS investigation [114]. Plasma treatment of polyethylene, polypropylene, and polystyrene modified by plasma treatment in pure oxygen and helium-oxygen mixtures were studied by means of XPS [111]. Argon, oxygen and nitrogen-plasma-treated PE surfaces were studied by Gerenser using XPS [115]. He concludes, the spectra for nitrogen plasma-treated PE suggest the formation of C-N-C species [115]. The scan for virgin PE consists of single intense peak centred at 284.6 eV due to the C1s electron. While the spectrum for the nitrogen-treated PE includes one additional peak centred at 399.0 eV due to 1Ns electrons. In order to get more information about the chemistry of the plasma-treated surfaces, high resolution scans of core level and valence band region are required. Nitrogen plasma treatments are often accompanied by uncontrollable oxidation phenomena. In order to avoid any air exposure of the polymer between plasma treatment and surface characterization, the plasma reactor can be coupled to the XPS spectrometer [116].

Using XPS, Forch et al. found that the incorporation of nitrogen into linear low-density polyethylene (LLDPE) occurs very rapidly under the influence of a nitrogen remote plasma and approximately 25 % of the nitrogen incorporates within one second. We can expect to observe groups such as amines (R-NH-R, R-NH_2) at binding energy shifts of 0.9 eV from the main hydrocarbon C1s peak [59, 115, 117]. A shift of 1.4-1.7 eV is normally observed for imines (C=N) which overlaps with hydroxyl and ether groups. A contribution of very small trace amounts of oxygen in any plasma treatment at atmospheric pressure is unavoidable. Hence, the presence of amides (O=C-NH_2) can be observed at binding energy shifts of approximately 3-3.5 eV and may overlap with C=O groups [90]. The amount of different surface groups is not easy to estimate, because

XPS can not differentiate between various nitrogen groups. Several corona-discharges treated-polymers such as PE, PP, and PET were studied by Briggs [118]. Many functional groups show similar energy shifts in the photoelectron spectrum. Derivatization reactions with group-specific reagents containing an XPS label is a technique used to distinguish between various functional groups. The chemical derivatization XPS technique is explained briefly in the section 3.4.1.

3.4 Chemical derivatization (CD)

Chemical derivatization (CD) techniques are based on specific reaction of sample functional groups with a derivatization reagent containing an element absent from the studied surface. This method allows one to identify reactive functional groups present on the surface [17, 29]. It was believed that by applying chemical derivatization, polymer surface functional groups of interest could be selectively labelled. However, selectivity and sensitivity for the labelling reagent reaction are required. These reactions can be carried out in gas phase or liquid phase. The results of a set of gas-phase derivatization reactions for primary amine, carboxylic, and hydroxyl groups using fluorine are interpreted by Nakayama et al. [8]. Derivatization procedure combined with several methods of analysis such as XPS and FTIR was recognized as an analytical method to determine the concentration(s) of certain functional groups. The concentration of the new element after the reaction is directly related to the concentration of the functional groups studied. Everhart and Reilley applied CD-XPS to a low-pressure radio-frequency plasma-treated polymer to identify certain species for the very first time [29]. They used pentafluorobenzaldehyde (PFB) as a reagent assuming it would undergo selective reaction with both primary and secondary amine groups. However, they did not explain how they arrived at their statement.

TFAA as an important derivatization reagent for hydroxyl [119–122] and amine groups [37, 121] has often been used for XPS analysis of oxygenated or nitrogenated polymer. In the case of the hydroxyl groups, TFAA reacts relatively fast to form ester groups (trifluoroacetates). Once the derivatization reaction has occurred, the TFAA molecule is bonded in place of a surface hydroxyl group. Therefore, It was supposed that the amount of surface-bonded hydroxyl groups can be quantified by measuring the fluorine concentration. However, it must be taken into account that TFAA can react with other nucleophilic functional groups, such as amines and thiols. If the sample contains both, -OH and -NH_x (x = 1 or 2) groups, it is not possible to distinguish these groups.

However, Chemical derivatization combined with XPS analysis (see following) has been used very frequently in the recent 35 years. For example, Choukourov and his co-workers determined the

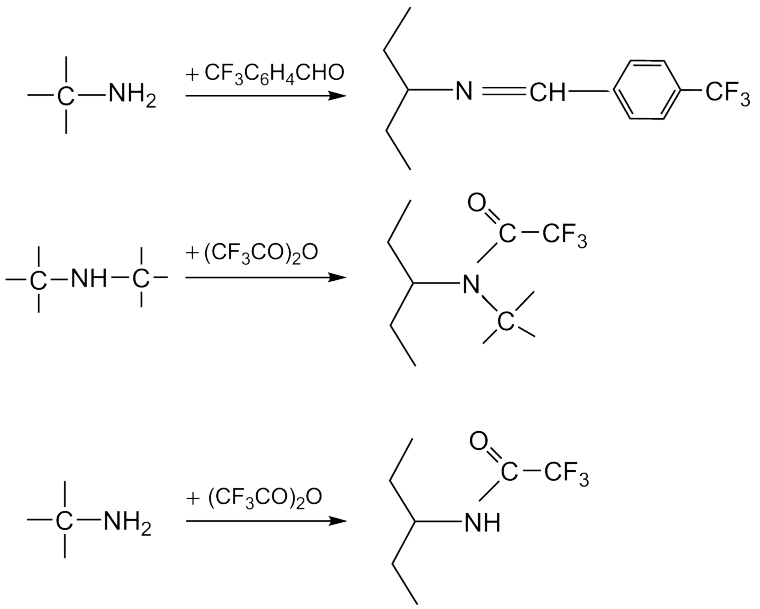

Figure 3.1: Derivatization of primary amine with TFBA, primary and secondary amine with TFAA

surface concentration of primary and secondary amine groups by the derivatization technique using TFBA and TFAA on plasma polymerized thin films. In Fig. 3.1, reaction of TFBA with primary amine and the reaction of TFAA with both primary and secondary amines are shown [37].

3.4.1 Chemical derivatization X-ray photoelectron spectroscopy (CD-XPS)

Due to the complexity of the structures formed on the plasma-treated surfaces, the spectra become challenging to interpret. XPS can be combined with the chemical derivatization technique in order to achieve a more precise identification of formed functional groups. For example, as mentioned above already, in absence of any nitrogen-bearing functionality, TFAA reaction with hydroxyl group leads to attachment of fluorine atoms to the surface via the very reactive trifluoroacetic anhydride. Thereby, in the XPS spectrum the fluorine peak appears, indicating the presence of -OH groups on the surface. In this manner, the concentration of fluorine atoms is directly attributed to the concentration of the studied functional groups e.g. -OH.

TFBA as a common electrophilic derivatization reagent has frequently been used for XPS analysis of nitrogenated polymer surfaces. It was commonly believed that amino groups can be analyzed selectively using TFBA reagent in regards to the reaction shown in Fig. 3.2. Referring to this

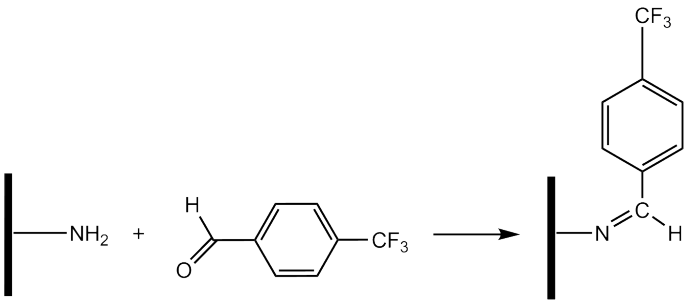

Figure 3.2: Reaction of -NH_2 group with TFBA

reaction, an NH_2 group will be substituted by a C=N group. The main characteristic feature is CF_3 which can be used to find the density of amines according to equation 3.11 [123].

$$[NH_2] = [\frac{\frac{[F]}{3}}{([C] - \frac{8[F]}{3})}] \times 100\% \tag{3.11}$$

[F] and [C] are the fluorine and carbon concentration determined by XPS after the reaction with TFBA.

The findings of this work reveal that applying TFAA or TFBA CD combined with XPS on plasma-modified surfaces it is practically impossible to detect and quantify amino groups on plasma-treated polymer surfaces.

3.4.2 Chemical derivatization Fourier transform infrared spectroscopy using TFBA (CD-FTIR)

TFBA as an aromatic compound with the reactive group -CH=O in para position of a -CF_3 group can be detected in the infrared spectrum by the strong C-CF_3 stretching vibration appearing near 1320 cm^{-1} (our measurement, liquid phase, diamond ATR). Assuming that TFBA reacts selectively with primary amines, the band area under ν(C-CF_3), appearing at 1324 cm^{-1}, is proportional to the amount of primary amine groups that underwent reaction with TFBA on the treated and derivatized sample [124]. The area density of the functional group (in this case -NH_2) reacting with TFBA can be found using equation 3.10. However, this work presents arguments indicating that traditionally applied TFBA derivatization of primary amine is partially based on myths.

3.5 The NEXAFS technique

X-ray absorption near-edge structure (XANES), also known as near-edge X-ray absorption fine structure (NEXAFS) is applied to so-called low-Z molecules, i.e. mostly organic molecules that consist of "light" atoms such as carbon, nitrogen, oxygen, and fluorine [125]. It has later been applied to many other molecules and materials [126]. The technique can identify and distinguish small molecules and macromolecules like polymers. Utilizing this method the partial density of the empty states of a molecule can be determined. It probes transitions from the K-edge of an atomic species into molecular orbitals of bonds to intra-molecular and extra-molecular neighbors. The surface X-ray absorption spectra of a core level of a surface atom can be divided into two parts, the X-ray absorption near-edge structures (XANES) and the extended X-ray absorption fine structure (EXAFS). Using the results from both techniques, structural information such as chemical bonding, site symmetry, interatomic distance, etc. can be extracted. The X-ray absorption spectra deal with the electronic transitions from atomic core levels to unoccupied final states. It is able to present strong (and distinctive) features typically in the energy region just below and up to about 50 eV above the absorption edge (e.g. K-edge). NEXAFS spectroscopy and XPS are known as complementary tools in surface analysis of polymers. Different molecular models have been used to interpret NEXAFS measurements of polymers [126]. Polymer NEXAFS spectra have previously been presented by Kikuma et al. [127], Unger et al. [128], and Ade [129].

3.5.1 Fluorescence yield NEXAFS

The sample is irradiated with monochromatic X-rays from an energy range around the ionization edge. The main process in the soft X-ray energy range (< 2000 eV) is photoabsorption. The result of the absorption process is a photoelectron and a core hole. The hole is subsequently filled by an electron either radiatively by the emission of a photon, or non-radiatively by the emission of an Auger electron. The core hole created by the X-ray absorption process can be studied either through the photon or the Auger electron. To detect the electrons an energy analyzer can be applied while radiative emission measurement needs a fluorescence detector. In addition the Auger electron yield (AEY) is much higher than the fluorescence yield for low-Z molecules [125]. Hence, the peak positions and spectral line shape in a NEXAFS spectrum are directly related to the nature of these unoccupied electronic states. Auger electrons arise from the top 10 nm while fluorescent photons originate from the top 200 nm of the film. This technique is both surface and bulk sensitive. One example is reported by Hemraj [130] in which they applied NEXAFS technique to probe both nanotube electronic structure as well as surface functional groups, simultaneously.

3.5.2 NEXAFS spectra

If the energy of the source photons corresponds exactly the energy difference between the initial state and an unoccupied (molecular) state, resonant transitions occur. According to the unfilled molecular orbitals symmetry, they are labelled as π*- or σ*-orbitals. Normally, the π*-orbital is the lowest unoccupied molecular orbital of a π-bonded diatomic subunit of a molecule, while σ*-orbitals are found at higher energies [131].

The X-ray photon will be absorbed by the target atom leading to a core electron emission, for example, from the K (1s) or L (2p) shell, exited to an unoccupied discrete level. As it was explained above, the created core may be filled by an electron from a higher energy shell releasing excess energy either by the radiation of fluorescence photons or by the emission of Auger electrons. NEXAFS measurements represent the electron yield or fluorescence yield as a function of incident photon energy. NEXAFS spectra are obtained by monitoring the absorption of X-rays as a function of energy close to a core level excitation energy.

We have demonstrated NEXAFS as a particularly useful and effective technique for probing the surface chemistry of plasma-treated LDPE foils. Results are reported and discussed in section 7.2.

3.6 Optical emission spectroscopy

Gas-phase plasma diagnostics combined with surface analyzes is a clue to providing an insight into the surface chemistry after treatment and development of effective plasma functionalization processes. The mechanism of surface functionalization required the identification of reactive species and plasma-surface interactions. Optical emission spectroscopy (OES) is known as a common diagnostic method to measure the relative densities of excited states. Since OES does not interfere with the plasma, undisturbed plasma species can be studied. The aim of investigations is to determine the absolute ground-state density of nitrogen reactive species in the post-discharges of a nitrogen discharge at ambient pressure. This requires a calibration and kinetics mechanisms information associated with the afterglow emission.

In the post-discharges of N_2 at ambient pressure ground-state atomic nitrogen N(^{4}S) are the dominant active intermediate [96, 132]. The excited nitrogen molecule A $^3\Sigma^+{}_u$ is the next dominant species in nitrogen afterglow which is populated by three-body recombination of nitrogen

atoms [96]. The nitrogen ground state atom density is monitored by measuring the emission intensities of the band heads of the FPS of nitrogen. One way to find the density of nitrogen atoms is to determine the absolute intensity of FPS of molecular nitrogen which is due to transitions between different vibrational levels of the B $^3\Pi_g$ and A $^3\Sigma^+{}_u$ electronic states [133].

Babayan et al. have shown how absolute nitrogen atom densities in an hydrogen-free post-discharge region can be calculated from the temporal or spatial decay of the emission intensity of N_2(B) [96].

4 Experimental

4.1 Materials

Decahydronaphthalene (decalin, mixture of cis and trans isomers, anhydrous, ≥99 %), isopropanol (ultrapure, 99.9 %), xylene (p-xylene, anhydrous, ≥99 %), hexadecane (99 %), 3-aminopentane, 1-aminohexane, 1-aminooctane, 4-(trifluoromethyl)benzaldehyde TFBA (98 %), heavy water (D_2O, deuterium oxide, 99.9 at % D), 2-mercaptoethanol (≥99.0 %), hexanal (98 %), hexenal (trans-2-hexen-1-al ≥98 %), 4-(trifluoromethyl)phenylhydrazine TFMPH (96 %), diethylene glycol dimethyl ether (diglyme) (99.5 %), 2-ethyl-1-hexylamine (≥98 %), isobutyraldehyde IB (≥99 %), trifluoroacetic anhydride TFAA (≥99 %), and 4-(trifluoromethyl)benzylamine TFMBA (98 %) were obtained from Sigma Aldrich Chemie GmbH (Schnelldorf, Germany), 2-aminooctane (99 %) from OMNILAB-LABORZENTRUM (Bremen, Germany). These chemicals were used without further purification. Sodium carbonate was from Merck (Darmstadt, Germany). Aminomethylated polystyrene beads (PS-AM-NH_2) were from Rapp Polymere GmbH (Tübingen, Germany).

Different low-density polyethylene (LDPE) foils have been used such as Goodfellow LDPE foils GmbH (Bad Nauheim, Germany), and foils produced by Sumitomo Chemical Co. in Japan using a peroxide initiator in a vessel reactor with a density of 919 kg/m^3, 2.0 g/10 min melt flow rate, and 76.4 branches with more than eight C atoms per molecule. N_2-H_2 gas mixtures obtained by adding pure N_2 (grade 6.0) to a premixture of 90 % N_2 (grade 4.3) with 10 % H_2 (grade 3.0) were used for the plasma treatment. In several experiments mixtures of N_2 and H_2 gas with 6.0 purity grade for both gases were used. Additional purification was done using gas cleaning systems from Messer Griesheim GmbH (Duisburg, Germany) and Spectron GmbH (Frankfurt am Main, Germany).

4.2 Processing

4.2.1 Thin film preparation and characterization

In situ FTIR investigations were performed on thin or ultrathin films coated onto the ATR crystals. In *ex situ* studies, PE in foil forms were generally used which had first been cleaned in isopropanol using an ultrasonic bath. Foils were then rinsed with isopropanol several times and dried in nitrogen gas. The cleaning and coating processes are explained in the following.

Polymer cleaning

Ultrathin LDPE films were prepared from a polymer produced by Sumitomo Chemical Co. in Japan which was cleaned by dissolution of foils in hot xylene and precipitation in isopropanol. Typically, 10 g of the polymer were dissolved in 200 ml xylene at a temperature of 80 °C and precipitated by slowly pouring the hot solution into 1 L of warm (40-50 °C) well-stirred isopropanol. The precipitate was collected on a 125 mm diameter filter paper using a Büchner funnel on a vacuum flask and washed thoroughly with small portions of warm isopropanol, 1 litre in total. The polymer was then dried in an oven at 60 °C overnight. This procedure was repeated twice. Purity checks of the obtained powder using *ex situ* FTIR-ATR (diamond, 51°) showed that the purified product was virtually free of fatty acid amides.

Spin coating of ATR crystal

To achieve the required surface sensitivity for the detection of the plasma-induced surface functionalization, a very thin PE layer was spin coated onto the ZnS internal reflection element. During the spin coating method the substrate rotates at a given angular velocity for a given period of time while an amount of polymer solution drops on the substrate. The film thickness is controlled by the concentration of the polymer in solution, polymer molecular weight, spinning velocity and solvent evaporation rate. Hot solutions of the purified LDPE in decalin were used to spin coat ultrathin polymer films with thicknesses of between 50 and 200 nm onto the preheated ZnS ATR crystal. In order to obtain a thickness of about 100 nm, 100 mg LDPE was dissolved in 10 ml decalin at 80-90 °C under continuous magnetic stirring. The ZnS crystal, covered by a glass cup, was preheated on a hotplate (150 °C). For film preparation the hot crystal was transferred to a spin coater (model WS-400E-6NPP, Laurell Technologies, North Wales, PA, USA) equipped with a suitable holder featuring a rectangular recess to accommodate the crystal. A

glass syringe was used to "flood" the ZnS crystal with the polymer solution prior to spinning. Substrate rotation was started and within a few seconds accelerated to a final spinning rate of 1100 revolutions per minute (rpm) which was held for 35 s.

Ellipsometric measurements on polymer thin film were made using a spectroscopic ellipsometer (SE 850 DUV, SENTECH Instruments GmbH, Berlin, Germany) at incident angles of 50°, 60° and 70° in the wavelength range from 380 to 900 nm using a dispersion model for the visible region. Thickness measurements were obtained by processing the data using the SpectraRay/3 software package (SENTECH) from a minimum of three different points on each layer

Thin films preparation and treatment for NEXAFS

For preparation of LDPE films polymer from Sumitomo was first dissolved in decahydronaphthalene solution at 80 °C. Droplets of the solution were then applied to the steel substrates and LDPE films with thicknesses of typically 20 nm were spin-coated using 3000 rpm for 90 seconds. LDPE thin films of about 20 nm were coated onto 10×20 mm^2 stainless steel substrates (304 grade stainless steel precision rolled shim, 0.25 mm thickness). These samples were plasma treated for 30 s in flowing DBD post-discharges of N_2 + y % H_2 mixtures (y = 0, 1, and 4) using a flow rate of 16 $Lmin^{-1}$ STP. For the N_2 + 4 % H_2 mixture, treatments with a duration of 10 and 60 s were also performed. Samples were stored in argon gas until they were measured one day later. In this work, NEXAFS measurements were carried out at the HE-SGM monochromator dipole magnet beam-line at the synchrotron radiation source BESSY II (Berlin, Germany). Time between plasma treatment and NEXAFS measurement was about 24 hours.

4.2.2 Preparation of solid-phase-bound imine from PS-AM-NH_2 beads and aldehyde vapor

Aminomethylated polystyrene beads (RAPP, PS-AM-NH_2, particle size: 200-400 mesh, capacity: 0.4-0.8 mmol/g) were exposed to isobutyraldehyde (IB) vapor for 60 min [134]. Infrared measurements of the beads after exposure to IB (Fig. 4.1 L (left)) exhibit a strong vibration at 1668 cm^{-1} which can be attributed to the newly formed isobutyraldimine, regarding the reaction shown in Fig. 4.2. The peak position at 1601 cm^{-1} related to ν(CC) from PS-AM is detectable. Additionally, the broad absorption at 1750-1700 cm^{-1} corresponds to the carbonyl group of physisorbed aldehyde. In order to get rid of physisorbed aldehyde on the beads, the sample remained in the natural atmosphere and the IR measurements were collected after 10, 30, 60, 90 min, 24 h, and 72 h. After one night, a significant amount of carbonyls are evaporated

while an absorption at 1702 cm^{-1} remain. Within 70 to 80 h the rest of physisorbed carbonyls are evaporated, while an imine vibration at 1668 cm^{-1} can still be seen. There are two peaks,

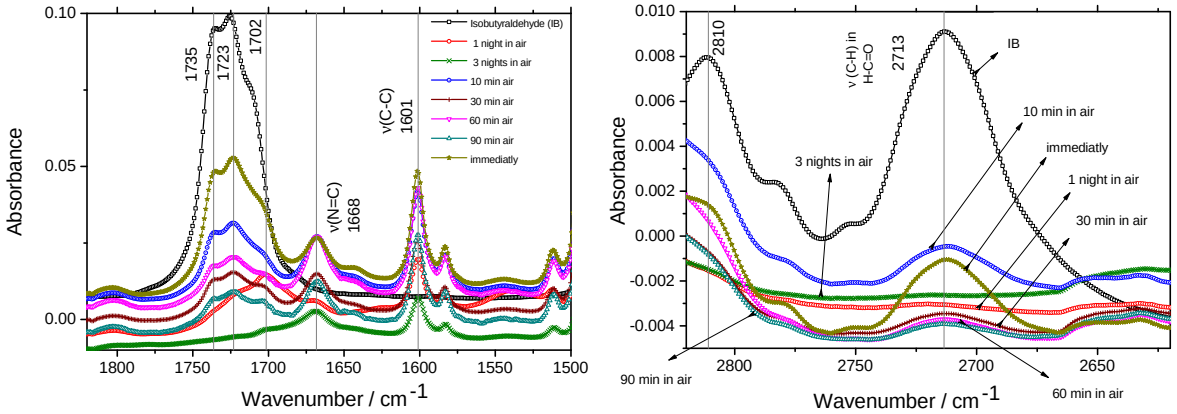

Figure 4.1: FTIR spectra of PS-AM-NH_2 beads after exposure to isobutyraldehyde (IB) vapor and subsequently to the natural atmosphere, measurements performed using diamond ATR 51°, non-polarized, 128 number of scans, res. 4 cm^{-1} (Arbitrary absorbance offsets).

both of moderate intensity, at 2810 and 2713 cm^{-1} related to the C-H stretching vibration in H-C=O from isobutyraldehyde. The intensity reduction of these vibrations after the reaction of primary amine and aldehyde is shown in Fig. 4.1 R (right). After three nights releasing the sample in the laboratory atmosphere almost no absorption at 2712 and 2810 cm^{-1} are seen.

The solid-phase-bound imine prepared from a reaction of aminomethylated polystyrene beads with adelhyde vapor is used to show the reaction of TFBA vapor with imines on solid phase in section 6.3.

4.2.3 Plasma treatment process

Thin layers, typically 80 nm, were *in situ* plasma-treated in flowing post-discharges of nitrogen-containing gas mixtures [135]. The change in the surface composition of the polymers during the plasma exposure time was analyzed by *in situ* ATR infrared spectroscopy, using a Nicolet 5700 spectrometer. The background was measured with the PE thin film. The coated crystal was then exposed to the downstream of afterglow plasma of N_2 + y % H_2 for different treatment durations. IR spectra were recorded repeatedly as the films were slowly etched away. The *in situ* FTIR setup used for the experiments in this work is shown in Fig. 4.3 .

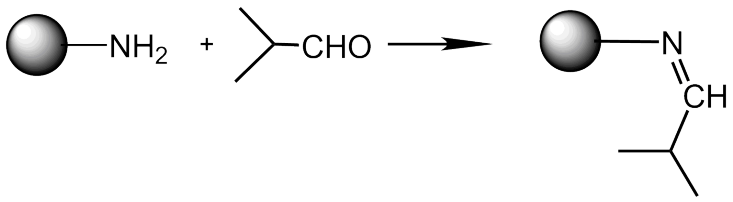

Figure 4.2: Primary amine and aldehyde reaction to imine

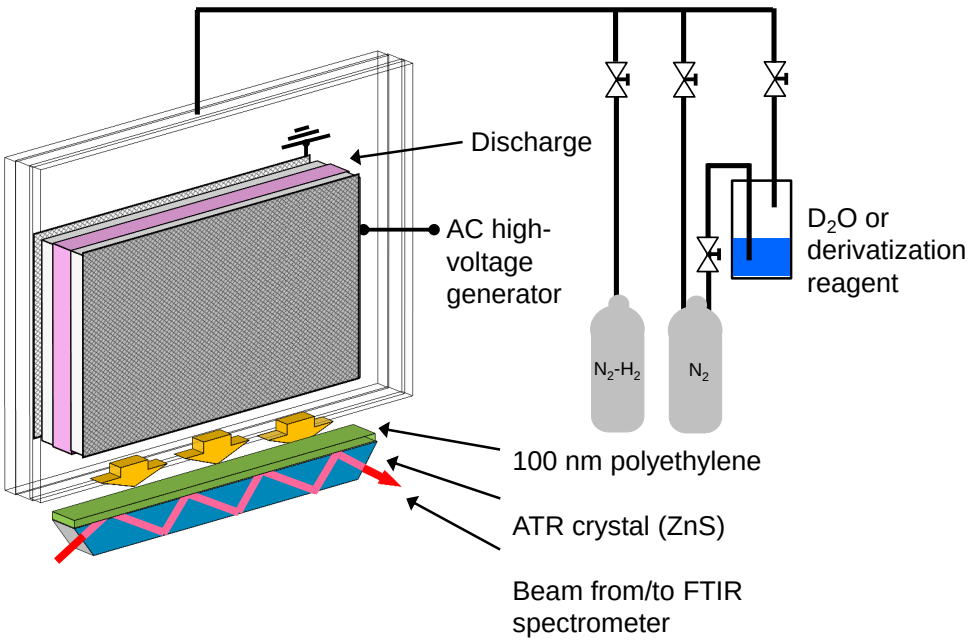

Figure 4.3: Scheme of setup used for plasma treatment, subsequent H-D exchange and chemical derivatization experiments [1]

4.2.4 *In situ* hydrogen-deuterium (H-D) exchange

The surface of LDPE was exposed in flowing post-discharges of N_2 + 4 % H_2 gas for 30 s. The surface was subsequetly exposed to vapors of D_2O, H_2O and D_2O, respectively by a bubbler flask via an N_2 stream of 1 $Lmin^{-1}$ STP for 30 minutes in every step. In preliminary experiments it was seen that spectral changes measured *in situ* during the contact of plasma-treated LDPE films with D_2O vapor came to an end within 30 min. It was found that spectra of a bare ZnS ATR crystal as well as an untreated LDPE thin film are dependent on the presence or absence of H_2O or D_2O. We ascribe these changes to the presence of several kinds of functional groups like thiol, sulfite, and sulfate moieties [136]. In order to exclude any influence of functional groups which contain active hydrogen present on either ZnS ATR or polymer thin film the following procedure

was applied. First, the LDPE film on ZnS was exposed for 30 min to a water atmosphere generated by a stream of H_2O vapor in N_2. Then the crystal was exposed for 30 min to dry N_2 to remove any physisorbed H_2O. The result was measured and collected in reference spectrum "Ref. H". The procedure was repeated with D_2O to obtain a reference spectrum of ZnS and LDPE with all active hydrogen atoms replaced by deuterium atoms, "Ref. D". The LDPE thin film was exposed to a stream of afterglow plasma of N_2 + 4 % H_2 for 30 s. While the surface was surrounded with inert nitrogen gas, heavy water vapor was transferred to the surface for 30 minutes and the spectra obtained after exposure to deuterium were called "D". In the next step, light water and heavy water were sent to the surface separately. The spectra obtained after exposure to vapor of H_2O and to vapor of D_2O were called "H" and "2D", respectively. Between every step the surface was overflown with 1 $Lmin^{-1}$ STP of dry N_2 in order to remove physisorbed water (for 30 min) [135].

4.2.5 *In situ* electrophilic derivatization

Thin polymer films coated on ZnS ATR crystals were exposed to the flowing post-discharges of N_2 + 4 % H_2 for 30 s. After that, 1 $Lmin^{-1}$ STP nitrogen was fed to the bubbler flask containing TFBA. TFBA vapor was transferred to the treated polymer surface for a certain time. The treated PE surface was kept constantly in an inert gas atmosphere to avoid reactions between active sites on the treated polymer and air. A series measurement was recorded before, during and after TFBA vapor contact with the polymer surface.

4.2.6 *Ex situ* nucleophilic derivatization

LDPE foils were firstly cleaned in an isopropanol ultrasonic bath for 10 minutes and rinsed with fresh isopropanol three times. Such cleaning process led to remove any low-molecular weight components which might have diffused to the surface. Then they were treated in the N_2 + 4% H_2 DBD afterglow for 30 s and kept in a stream of pure N_2 without plasma for another 30 min before removal from the reactor. Pieces of the treated foils were then immediately transformed to glass vessels to be exposed to the vapors of small amounts (typically 0.1 g) of 4-(trifluoromethyl)phenylhydrazine (TFMPH), 2-mercaptoethanol (ME) and 4-(trifluoromethyl)-benzylamine (TFMBA), respectively, then the evacuated glass vessels were kept at 50 °C for 24. In the next step, in order to remove physisorbed derivatization reagent, the samples were transferred to another vessel with continuous pumping off for another 24 h at 50 °C for the TFMPH samples and at room temperature for the ME and TFMBA samples. To obtain the reference

samples for XPS and FTIR measurements, non-plasma-treated PE samples were subjected to the same procedures. Sample exposure to laboratory air was normally shorter than 15 min between removal from the plasma reactor and XPS measurement or derivatization treatment [3]. Measurements were carried out at several positions on the treated foil pieces and averaged. *Ex situ* nucleophilic CD-XPS and FTIR-ATR analyzes of plasma-treated LDPE films are explained in section 7.1.

4.3 FTIR spectroscopy instrumentation

The FTIR spectra were registered with a Nicolet 5700 FTIR spectrometer (Thermo Fisher Scientific GmbH, Dreieich, Germany), equipped with an MCT detector and a DuraSamplIR ATR accessory with a single reflection diamond ATR crystal (average angle of incidence $\theta = 51$ °) for *ex situ* measurements on polymer foils. Zinc sulphide (ZnS) ATR crystal from Korth (Korth Kristalle GmbH, Hamburg, Germany) with a dimension of 80×10×4 mm^3 and an incident angle of 45° were applied using a horizontal attenuated total reflectance (HATR) accessory (PIKE Technologies) for *in situ* analyzes of plasma-treated thin films. The FTIR analyzes consisted of 64 scans in the range of 4000-1000 cm^{-1} for ZnS and 4000-650 cm^{-1} for the diamond ATR crystal. Normally a resolution of 4 cm^{-1} was chosen in our *in situ* studies.

For the *ex situ* FTIR measurement a single reflection diamond crystal was applied. In this case solid (polymer samples) or liquid were placed in intimate contact with the diamond ATR crystal and the infrared (IR) spectrum was collected. Series measurements were done using OMNIC software (version 7.3).

4.4 XPS

XPS spectra were acquired with a PHI ESCA 5500 system (Physical Electronics) with non-monochromatic Mg K_α radiation (100 W) and no charge compensation. The concentric hemispherical analyzer was operated in fixed analyzer transmission mode. The electron take-off-angle with respect to the surface plane was 47°, and the source-to-analyzer angle was 54.7°. Binding energies (BE) were charge shifted using the C1s component of hydrocarbons at a binding energy of 285.00 eV. The measured values of the C1s BE were in the range of 285.5 - 286.7 eV. The analyzed area was approximately 0.8 × 2 mm^2. The scan spectra, from which the atomic composition was computed using Multipak, were acquired in about 10 minutes using a pass energy

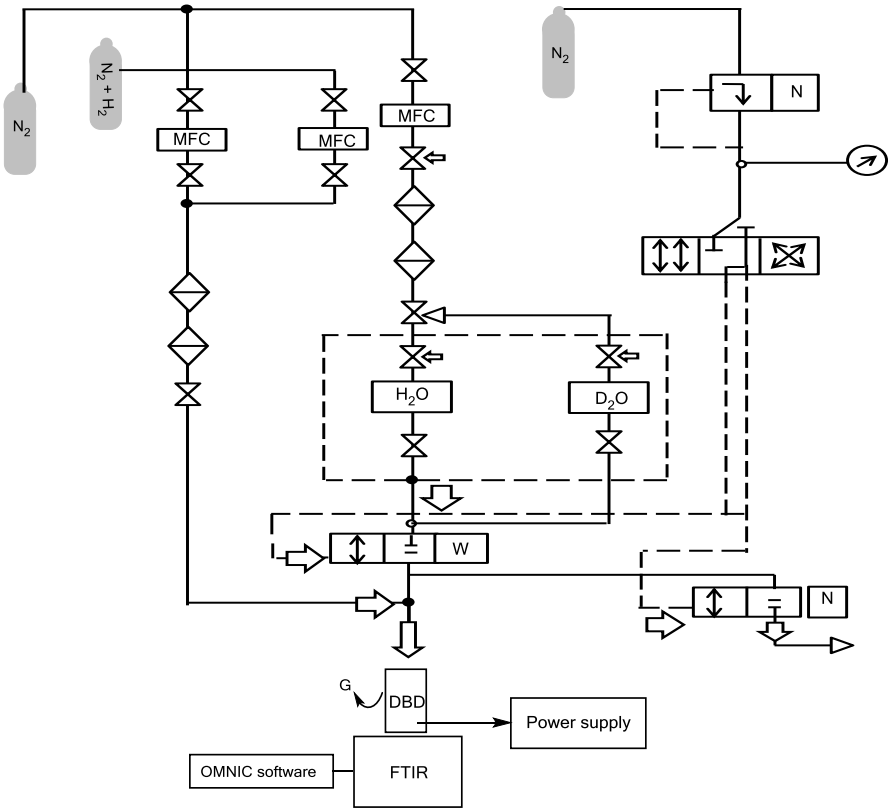

Figure 4.4: A general diagram of the apparatus and IR measurement setup for *in situ* treatment of PE film in the post-discharge region of a DBD reactor

of 117.4 eV and a 0.25 eV at each step. Atomic percentages (at%) of nitrogen, oxygen, fluorine, and sulfur were obtained under the implicit assumption of a compositional homogeneity of the sample throughout the sampling depth.

4.5 Experimental setup for plasma treatment of thin films

DBD reactor for thin films plasma treatment: The planar DBD flow reactor is made of two parallel borosilicate glasses of 10×15 cm^2 and 2 mm thickness. A wire mesh covers an area of 5×7 cm^2 on the outer surface of both glass dielectrics. The distance of 1 mm between the two glass pieces is achieved by placing two silicone spacers one on the right and one on the left hand side of each of glass. The electrodes were connected to earth and high voltage, respectively.

Gas supply: The schematic configuration of the *in situ* experimental setup is represented in Fig. 4.4. For the preparation of gas mixtures of N_2 + y % H_2 (y = 0 to 4), pure N_2 and N_2 + 10 % H_2 are mixed appropriately and fed into the discharge space.

The gas flow rate, adjusted by mass flow controllers, was normally 16 $Lmin^{-1}$ STP. For the hydrogen-deuterium exchange experiments two bubbler flasks filled with light and heavy water, respectively, were used. Generally 1 $Lmin^{-1}$ STP pure nitrogen (6.0) was fed through each bubbler flask for at least 30 min to transfer the removal of oxygen and other dissolved gases from the water to the air and to de-aerate the waters. Next, the pure nitrogen was fed through the bubbler flasks to transfer the water vapor onto the polymer surface. In the case of *in situ* derivatization with TFBA, a bubbler flask was filled with this compound and similar parameters for the gas flow were applied. The DBD reactor was mounted above the horizontal ATR accessory

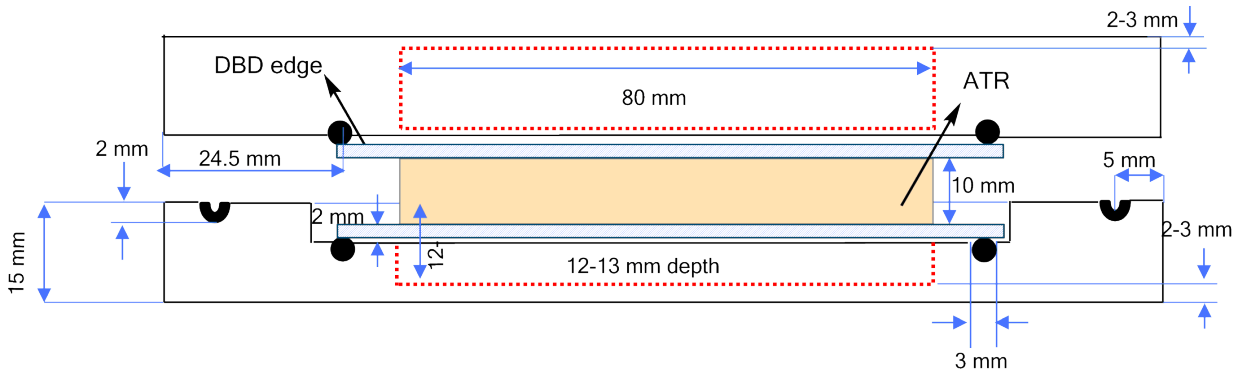

Figure 4.5: Top view of ATR crystal in horizontal attenuated total reflectance (HATR) accessory and down (bottom) edge of DBD

(Pike Technologies, Madison, WI, USA) in order to have the active volume located at the center of the ATR crystal with the LDPE film of a thickness between 80 and 200 nm on it, see Fig. 4.5. The surface is exposed to the flowing post-discharge of the DBD. The distance of 10 mm between the downstream edge of the discharge and the coated film, is equal to an afterglow delay time of 10 ms at a flow rate of 16 $Lmin^{-1}$ STP. The DBD was powered using a commercial generator (Model 7010 R, SOFTAL electronics GmbH, Hamburg, Germany). The peak voltage and frequency were typically 12 to 12.5 kV (ignition voltage 6.5 kV) and 20 kHz, respectively. In order to avoid electromagnetic interference between the high-voltage circuit powering the plasma and the electronics of the spectrometer, the DBD reactor was encased in a Faraday cage fabricated from a wire mesh. This shield and the ATR accessory were grounded.

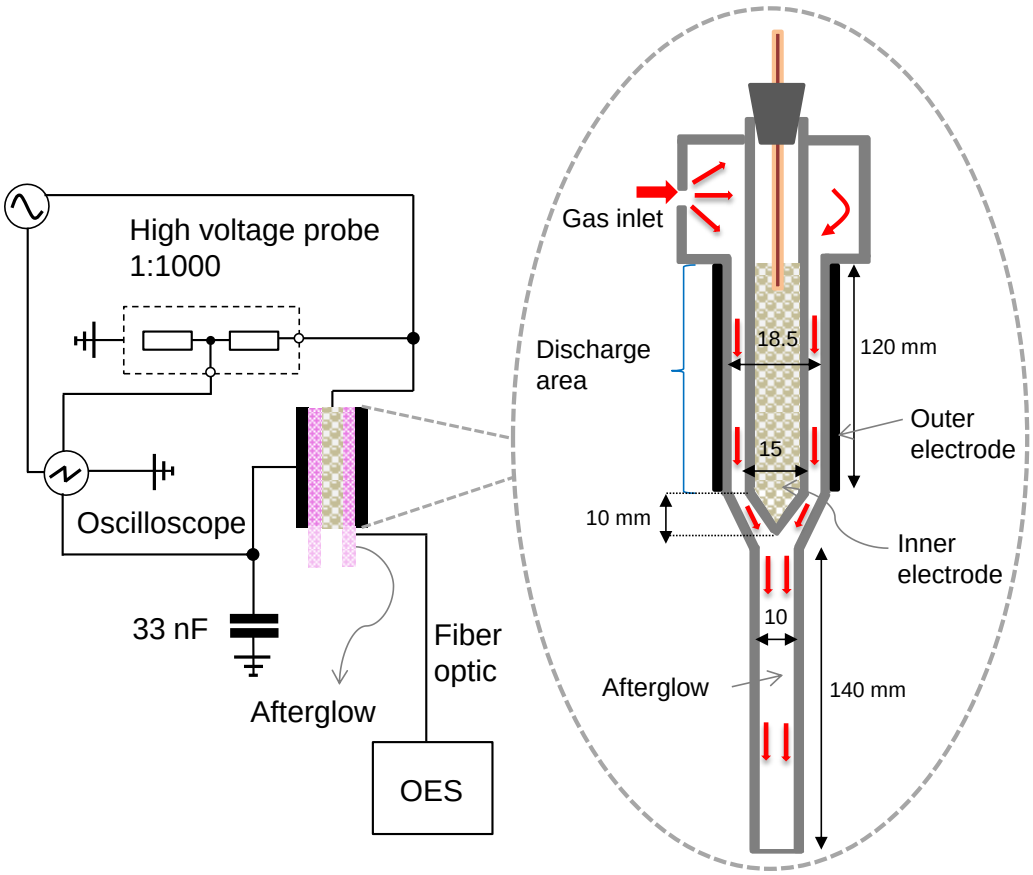

Figure 4.6: Schematic illustration of the experimental setup

4.6 Experimental setup for OES measurements

The coaxial home-made DBD reactor applied in this work is shown in Fig. 4.6. The discharge is sustained in the annular gap between two coaxial glass tubes of 1.75 mm wall thickness; the plasma zone has inner and outer diameters of 15 mm and 18.5 mm, respectively, and a length of 12 cm. The inner tube (one electrode) is filled with metal powder and the outer tube (other electrode) is covered by conductive mesh. One end of a piece of copper wire is located in the metallic powder and the other end is connected to the power source. The outer electrode is covered with silicone epoxy to prevent additional discharges. The power is applied to the top of the electrode through the isolated copper wire while the outer electrode is grounded. The experiments are carried out using nitrogen as the working gas (grade 6.0) and measurements are carried out in the afterglow region, usually used in our surface functionalization process. N_2-H_2 gas mixtures obtained by adding pure N_2 (grade 6.0) to a pre-mixture of 90 % N_2 (grade 6.0)

with 10 % H_2 (grade 6.0) were used for further investigations. Additional purification was done using gas cleaning systems from Messer Griesheim GmbH, (Duisburg, Germany) and Spectron GmbH (Frankfurt am Main, Germany). The flow of nitrogen or forming gas was monitored with mass flow controllers. The plasma is generated by a commercial generator (Model 7010 R, SOFTAL electronics GmbH, Hamburg, Germany). The power supply provides a sinusoidal voltage with adjustable voltage and frequency from 0 to 20 $kV_{pk/pk}$, and 1 to 20 kHz, respectively. The power is controlled using an oscilloscope to a constant value. Peak voltage and frequency were typically 19 kV and 20 kHz, respectively. Gas flow rate was maintained at 20 $Lmin^{-1}$ STP for all investigations.

UV-Vis and NIR light emitted by the plasma was collected by a collimator (74-UV-MP, UV-Vis Collimating Lens, 200-2000 nm) from different positions along the tube (1 cm in diameter) and transferred via an optical fiber attached to the collimator and to the spectrometer. The optical fiber moved along the discharge tube utilizing a home-made transferable fiber-holder. In this work, measurements were carried out using an Ocean Optics QE65000 Spectrometer (Ostfildern, Germany) to characterize the nitrogen plasma. The QE65000 equipped with a Hamamatsu back-thinned FFT-CCD detector with a 2-D arrangement of pixels (1044 horizontal $\times$ 64 vertical) is responsive from 200-1100 nm.

5 Results and discussions on PE surfaces plasma-treated in post-discharges of N_2-H_2 mixtures at ambient pressure

Analyzing the results of plasma treatment of polymer surfaces, two major group of effects can be distinguished. The first group of effects is due to the hydrogen abstraction, ablation process, and cross-linking. The second group of effects is characteristic for the formation of structures containing different functional groups. From the chemical point of view, plasma treatment is a radical-substitution reaction of C-H bonds in polymers. Hydrogen abstraction by the collision of ions, electrons or radicals leads to oxygen and nitrogen functionalities in the polymer chain. Therefore, hydrogen abstraction can be regarded as the starting point for the reactions and should lead to a successful plasma treatment [137].

Many highly reactive particles such as, radicals, ions, electrons, and reactive particles from the plasma interact with the polymer surface. Due to the complexity of these interactions, assignment of the mechanisms involved in the surface modification of polymers can be very difficult. The different functionalities which occur must be precisely analyzed.

The aim of the investigations in this chapter is to find out the effect of post-discharges plasma treatment on polyethylene surfaces using DBD in N_2-H_2 mixtures. Different parameters were varied e.g. the duration of plasma exposure and gas composition. Referring two early papers of Hollahan and Stafford [12] and Courval et al. [16] and previous results from Klages et al. [124], it was expected that based on CD-FTIR-ATR data obtained under the mentioned conditions, primary amine groups with densities in the order of at least 1 nm^{-2} would be found. Secondary amines show only one absorption band in the range of 3500-3300 cm^{-1} due to NH stretching vibration which is usually weak in solid and liquid phases. -NH deformation vibration of secondary amines occurs at 1580-1490 cm^{-1} with weak to medium intensity [6]. Primary aliphatic amines show two absorption bands at 3550-3260 cm^{-1} due to R-NH_2 and a medium-to-strong band at 1650-1580 cm^{-1} related to the bending deformation vibration [6]. FTIR-ATR investigations of treated samples will be interpreted in this Chapter.

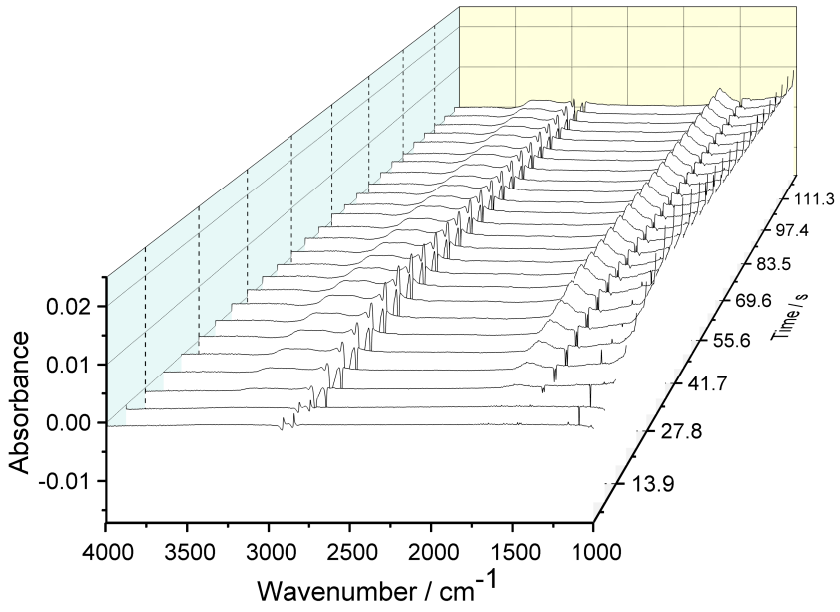

Figure 5.1: *In situ* FTIR measurement of LDPE thin film treated in post-discharges of N_2 + 4 % H_2 plasma for 30 s at ambient pressure, (2 min series measurement)

5.1 Plasma afterglow treatment of LDPE film surfaces

5.1.1 Plasma effect on PE thin film in afterglow of N_2 + 4 % H_2 for 30 s [1]

In Fig. 5.1, the *in situ* FTIR-ATR measurement of PE thin film on exposure to N_2 + 4 % H_2 plasma is shown (30 s plasma duration time).

A selection of FTIR spectra taken *in situ* at intervals of about 5 s during 30 s plasma treatment of a 80 nm LDPE film under standard conditions is shown in Fig. 5.2. One spectrum is taken before the plasma treatment as a background spectrum. The first spectrum (bottom) was taken before plasma ignition and the next one about 1 s after the plasma was ignited. The top solid-line spectrum corresponds to the situation directly following the end of the plasma treatment, and the dashed-line spectrum was obtained 1 s after the plasma treatment was finished. The spectra reveal effects of the plasma treatment on the ZnS crystal, the "bulk" of the PE film and on the PE surface. A shift in the baseline is not due to the offsetting spectra against each other, but they are the result of the exposure of the ZnS crystal to the plasma and also observed similarly in the absence of a PE film. Although the refractive index (n) of ZnS in the IR region is temperature dependent, the increase of n with temperature, $\frac{dn}{dT} = 2.9 \times 10^{-5}$ K^{-1} ($\lambda = 5.5$ μm) [138], is too small to explain the increase of baseline absorption during plasma exposure by an increase of the insertion loss due to enhanced IR reflections alone.

Baseline absorbance of untreated ZnS sample at 2000 cm^{-1} is between 0.001 and 0.007, depending on the individual crystals used. After the treatment, the absorbance slowly recovers with a relaxation time in the order of hours. The speculation is that the origin of these effects are caused by very weak UV-induced broadband IR absorptions due to electron traps which are populated by excited electrons, similar to UV-induced IR absorption bands observed by many orders of magnitude stronger in deliberately doped ZnS crystals [139]. The effect of plasma-induced etching of the LDPE film is seen in the regions of stretching vibrations of aliphatic C-H bonds ($\nu(CH_2)$, 2800-3000 cm^{-1}) and of deformation vibrations ($\delta(CH_2)$, scissoring, 1400-1500 cm^{-1}). But the effect of N_2-H_2 plasma is not restricted to the simple ablation (etching) process. The positive broad band at 1700-1500 cm^{-1} indicates the formation of new functional groups.

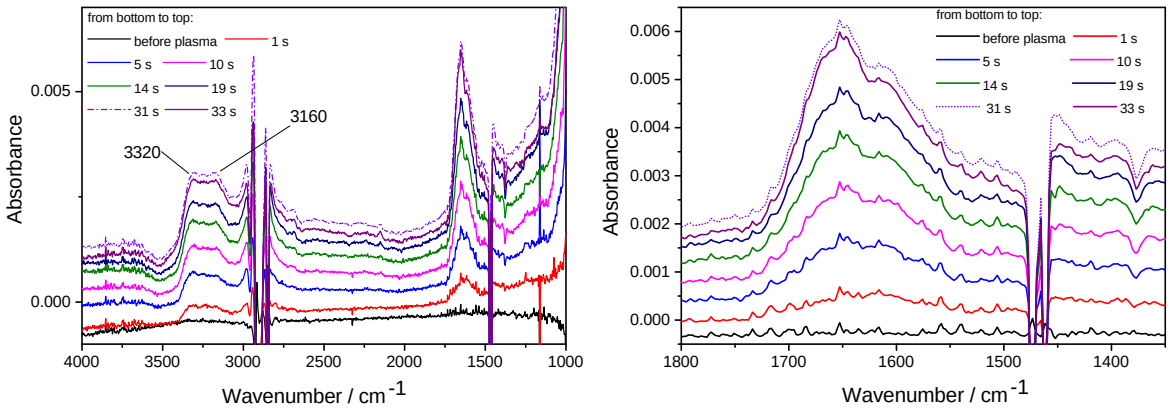

Figure 5.2: Left: FTIR spectra of 80 nm LDPE film on ZnS taken at different times (solid lines, see legend) during and after 30 s plasma treatment. Plasma was shut off after 30 s; the last FTIR spectrum (dashed-line) was taken 1 s after the end of the plasma exposure. Right: the expanded region of 1800-1350 cm^{-1}, showing vibrations of newly-formed functional groups.

A spectrum of the 80 nm LDPE film itself (with the uncoated crystal as background, in bold) and a difference spectrum representing the etched away material as a positive spectrum after multiplication of the original difference ("spectrum before" subtracted from "spectrum after plasma treatment") by a factor of 15 is shown in Fig. 5.3. Obviously, the spectrum of the etched material is not exactly a downsized copy of the original. The two peaks at 1461 and 1473 cm^{-1} are much better separated and quite similar in intensity, while in the spectrum of the film the 1463 cm^{-1} peak clearly dominates. Even more pronounced are differences in the 1330-1390 cm^{-1} range. Interestingly, the spectrum of the etched material shows only a peak at 1378 cm^{-1} attributed to the symmetric "umbrella" deformation vibration of methyl groups inside the chains of the polymer, while bands with maxima at 1363 and 1359 cm^{-1} of comparable

intensity, i.e. wagging vibrations of disordered polymethylene chain segments of the polymer, are also visible in the original film. In principle, three different possible reasons have to be considered in order to explain the observed differences: (i) A stratification of the original film with differences in structure between the bulk of the film and the etched-away surface region of typically about 3-6 nm thickness within 30 s plasma treatment due to segregation and crystallization processes during film formation or thereafter (ii) preferential etching of phases or crystallites with special orientations, and/or (iii) an effect of UV radiation from the plasma acting not only on the surface region, but more or less within the whole film. For a more detailed discussion of these issues, more systematic investigations with films of different thicknesses and varying etching depths are required, supported by other methods which are able to characterize the film structure. It has been reported that crystalline regions of polymers are less rapidly etched than amorphous regions [140]. The next treatment effect is the functionalization of the thin PE film. In Fig. 5.2

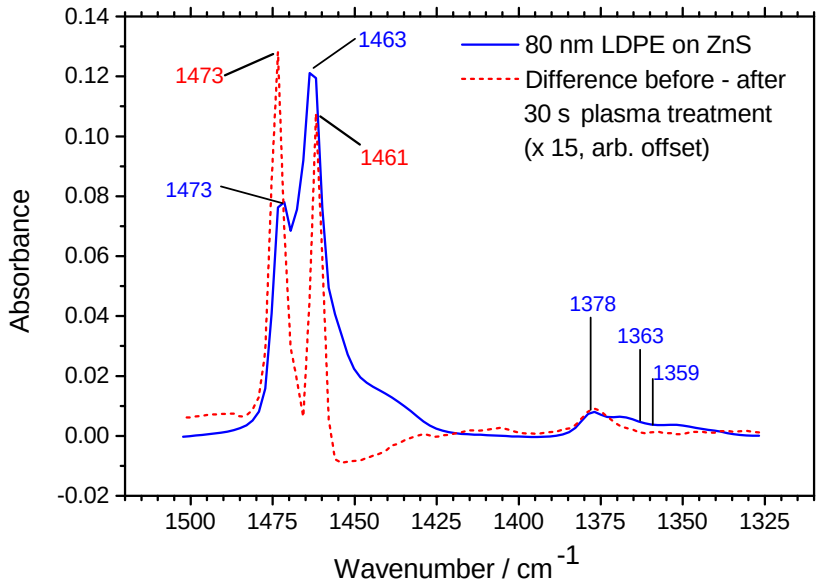

Figure 5.3: FTIR spectrum of 80 nm LDPE film on ZnS before plasma treatment and difference of spectra taken before and after 30 s plasma treatment in the region of bending deformation modes $\delta(CH_2)$ at 1463 and 1473 cm^{-1}, wagging deformation of CH_2 around 1363 and 1359 cm^{-1}, and the symmetric methyl ("umbrella") deformation of CH_3 at 1378 cm^{-1} [1].

(L), broad maxima at 3160 and 3320 cm^{-1} due to N-H and possibly O-H stretching vibrations are observed. The concentration is found to increase continuously with treatment time. In Fig. 5.2 (R) an interesting wavenumber region 1800-1350 cm^{-1} is shown which features stretching vibrations of C=O, C=N, and C=C, as well as bending vibration of XH_2 moieties like CH_2, NH_2 and OH_2. A group of at least four overlapping absorption bands appears between 1730-1540 cm^{-1}

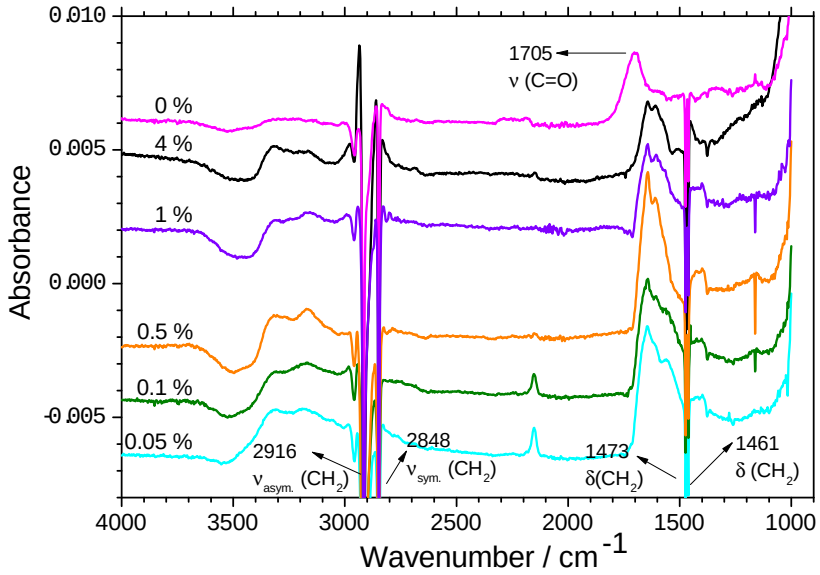

Figure 5.4: FTIR measurements of PE thin films treated in N_2 + y % H_2 (y = 0, 0.05, 0.1, 0.5, 1, and 4) plasma using flow rates of 16 Lmin^{-1} STP and 35 watts plasma power

during plasma exposure. It is worth noting that plasma treatment at atmospheric pressure can hardly get rid of any oxygen contribution. Even very pure gases may contain enough oxygen to form some oxygenated bonds. The presence of unsaturated carbon-carbon bonds, N-containing unsaturated functional groups mainly C=N, and possibly carbonyl makes it difficult to interpret this region. The results of our work showed that the imine groups may play a bigger role on polymer surfaces plasma-treated in nitrogen atmospheres than often expected [2]. Formation of imine as a result of plasma treatment on polymer surfaces has been reported several times [115, 141]. For example, Gerenser has studied new species formed on the PE surface after nitrogen plasma treatment by XPS investigation [115]. The line-shape analysis of the C1s spectrum of PE treated in nitrogen plasma shows two additional bands compared to oxygen treatment, which are assigned to C-N (amine type carbon) at 286.1 eV and C=N (imine type carbon) at 287.4 eV [115].

5.1.2 Plasma effect on PE thin films for different y in N_2 + y % H_2 in constant plasma power

A series of experiments was done where samples of LDPE thin films were exposed for 30 s in flowing post-discharges of N_2 + y % H_2 (y = 0, 0.05, 0.1, 0.5, and 4) plasma using flow rates of 16 Lmin^{-1} STP and 35 watts plasma power, see Fig. 5.4. The spectra of treated PE surfaces

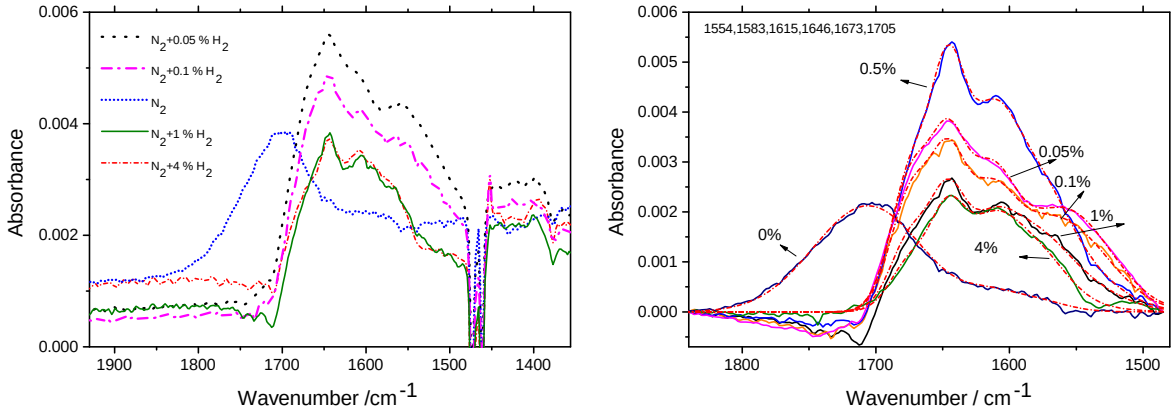

Figure 5.5: Left: intensity and peak position dependent on the behavior of a newly formed group in the range of 1800-1500 cm^{-1} after 30 s plasma treatment in flowing post-discharges of N_2 + y % H_2 (y = 0, 0.05, 0.1, 0.5, 1, and 4) as measured by means of an FTIR-ATR using a ZnS crystal and 45° angle of incidence. (*In situ* setup, 1 bar, t = 30 s, p = 35 W). Right: curve fitting of different FTIR spectra taken from treated sample shown in the left side. In IR spectrum of treated film in N_2 plasma absorption at 1705 cm^{-1} is dominant.

at interesting wavenumbers of 1840-1480 cm^{-1} for different gas compositions and their curve fitting results are shown in Fig. 5.5. A reasonable fit is found using a 6-component sum S(ν) of Gaussian functions with shared peak positions (i) and full width at half maximum (FWHM) w_i, see Eq. 5.1.

$$S(\nu) = \sum_{i=1}^{6} \frac{A_i}{w_i} \sqrt{\frac{ln4}{\pi}} exp[(-ln4(\frac{\nu - \nu_i}{w_i})^2] \tag{5.1}$$

The obtained parameters for the spectra of treated films in different gas compositions are shown in Table 5.1. It was expected that this region would be dominated by a band related to -NH_2 groups: primary aliphatic amines have scissoring deformation vibration $\delta(NH_2)$ band of medium to strong intensity in the range of 1650 to 1580 cm^{-1}, the most probable wavenumber range of appearance is from 1625 to 1620 cm^{-1} [142]. After treatment in pure nitrogen, three peaks at 1583, 1615, and 1705 cm^{-1} emerge. By adding just 0.05 % hydrogen to the gas stream, the peak at 1705 cm^{-1} is removed immediately, while the two other peaks at 1583 and 1615 cm^{-1} increase. Additionally, at least three new bands at 1554, 1646, and 1673 cm^{-1} develop. The N-H stretching vibration from primary amine and/or primary amide are expected to be located at 3340-3300 cm^{-1}. For secondary amine and secondary amide, the same stretching vibration with strong absorption occurs at 3500-3300 cm^{-1}. Hydrogen bonded -OH (intermolecular) has medium to strong infrared absorption at 3550-3230 cm^{-1} [6]. Therefore, the wide positive vibration at

Peak positions						
i	1	2	3	4	5	6
ν_i(cm^{-1})	1554	1583	1615	1646	1673	1705
A_i(cm^{-1}), y=0	0	0.0142	0.01072	0	0	0.21764
A_i(cm^{-1}), y=0.05	0.15202	0.01972	0.11477	0.0848	0.10401	0
A_i(cm^{-1}), y=0.1	0.12372	0.0333	0.09568	0.07773	0.09128	0
A_i(cm^{-1}), y=0.5	0.07014	0.1157	0.14459	0.12584	0.10643	0
A_i(cm^{-1}), y=1	0.04836	0.06387	0.06667	0.0626	0.05823	0
A_i(cm^{-1}), y=4	0.00887	0.06901	0.0666	0.05478	0.03943	0

Table 5.1: Peak positions ν_i and areas A_i of six Gaussian absorption bands used to fit the spectrum of PE thin films plasma-treated in N_2 + y % H_2 (y = 0, 0.05, 0.1, 0.5, 1, and 4. Treatment conditions: 1 bar, t = 30 s, p = 35 W).

3400-3040 cm^{-1} can be ascribed to -NH stretching vibration and possibly to -OH stretching.

A strong band in the region 1850-1550 cm^{-1} is possibly due to ν(C=O) from carbonyl compounds present on the surface [6]. The absorption at 1705 cm^{-1} can be attributed to carbonyl groups although oxygen incorporation was avoided as far as possible and very pure gases were used (nitrogen gas purity 6.0 and usage of purification systems). The plasma treatments were performed at atmospheric pressure and even very small amounts of oxygen are sufficient to form carbonyl groups on the treated surface. An additional source of oxygen is water vapor adsorbed at the reactor walls. Examples for carbonyl groups include different kinds of compounds like aldehydes, ketones, carboxylic acid, esters and amides. The vibration at 1705 cm^{-1} can be assigned to the α,β-unsaturated ketone (>C=C-C=O) which shows one very strong absorption in the range of 1705-1685 cm^{-1} [6, 143]. Other possible carbonyl compounds like α,β-unsaturated aliphatic aldehyde, esters or carboxylic acid seem unlikely because of the lack of other characteristic bands.

Secondary amides (-CO-NH-) in the solid phase have a characteristic absorption at 1570-1515 cm^{-1} related to the amide II band which is due to the motion combination of δ(N-H) and ν(C-N) [6]. Hence, absorption at 1554 cm^{-1} can be ascribed to amide II of secondary amides. The band at 1673 cm^{-1} is assigned to the amide I of secondary amides which absorbs strongly at 1680-1630 cm^{-1} [6]. The component at 1615 cm^{-1} can be ascribed to ν(C=C) of non-conjugated double bonds in alkenes (1680 to 1620 cm^{-1}) [6]. The absorption exhibited at 1646 cm^{-1} is due to ν(C=N) in monoconjugated aldimines (-CR=CR'-CH=N-).

Interestingly for x = 0.05 and 0.1, there is an absorption at 2150 cm^{-1}. Conversion of primary amine to imine (-CH=NH-, 1630 cm^{-1}) and a nitrile (-C≡N, 2190 cm^{-1}) in the plasma polymerization of allylamine is reported by Krishnamurthy et al. [144]. However, the absorption band at 2150 cm^{-1} for plasma-treated PE films in this work cannot be due to nitrile groups. In

fact, nitrile groups are stable and may not disappear after surface contact to water vapor. It can be speculated that this band may relate to carbodiimide (-N=C=N-). Generally, the -N=C=N- out-of-phase stretching of alkyl and aryl carbodiimides absorbs strongly in the 2152-2128 cm^{-1} region [145]. A systematic investigation of several carbodiimide showed that these compounds have characteristic peaks between 2150 and 2100 cm^{-1} [146]. The chemistry of carbodiimides can be found in detail in Mogul's thesis [147] and Ulrich's book [148]. Carbodiimides -N=C=N- could form from imines -CH=N- by hydrogen abstraction and addition of one nitrogen atom, providing an imidoylnitrene -C(-N:)=N- which could rearrange to -N=C=N- [149].

5.1.3 Plasma effect on PE thin films for different treatment times in N_2 + 4 % H_2

PE thin films were exposed to the downstream afterglow of N_2 + 4 % H_2 for different plasma treatment times of 10, 30, 50, 150, 200, 250, 600, and 925 seconds. The plasma was operated at 35 watts, using 16.0 $Lmin^{-1}$ STP ultra pure nitrogen and hydrogen. A 10 mm distance was kept from the exit edge of DBD to the substrate. *In situ* attenuated total reflection infrared spectroscopy of samples exhibited strong new bands around 1646 and 1605 cm^{-1}, as shown in Fig. 5.6 L. The integrated areas under the peak of the newly formed functional groups as a function of treatment time is displayed in Fig. 5.6 R. In the wavenumber region between 1740

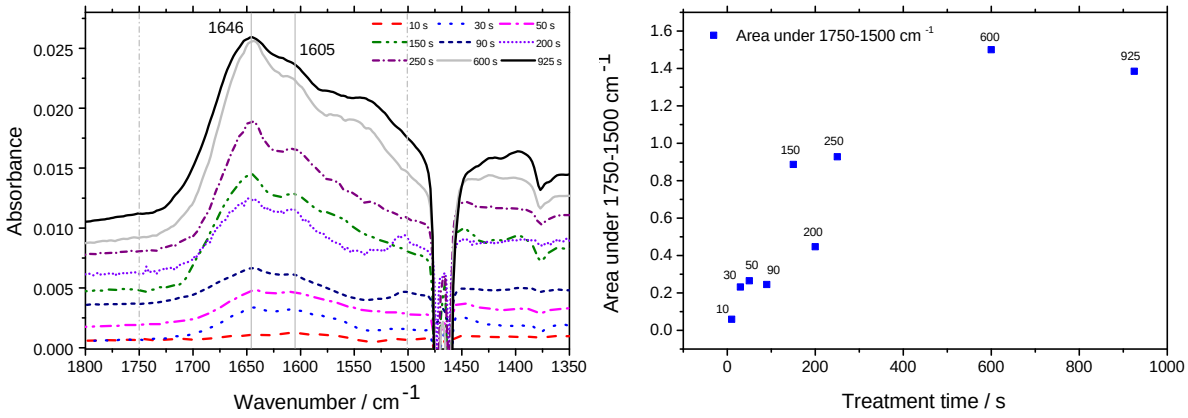

Figure 5.6: FTIR measurements of PE thin films treated in flowing post-discharges of nitrogen and 4 % hydrogen admixture at ambient pressure. Left: FTIR spectra taken from different films after different plasma exposure times, the two absorptions at 1646 and 1605 cm^{-1} are dominant. Right: peak area of newly absorption bands related to formed functional groups in the broad region of 1750-1500 cm^{-1} vs. treatment time.

Peak positions				
i	1	2	3	4
$\nu_i(\mathrm{cm}^{-1})$	1570	1601	1643	1675
$\mathrm{w}_i(\mathrm{cm}^{-1})$	31	37	51	50
$\mathrm{A}_i(\mathrm{cm}^{-1})$	0.03054	0.0606	0.10293	0.0264

Table 5.2: Peak positions ν_i, FWHM values w_i, and areas A_i of four Gaussian absorption bands used to fit the spectrum of plasma-treated PE thin films.

and 1540 cm^{-1}, a reasonable fit is obtained using a 4-component sum S(ν) of Gaussian functions (Eq. 5.1) with shared peak positions (i) and full width at half maximum (FWHM) w_i. The obtained parameters are shown in Table 5.2. Bands centered at 1675 and at 1643 cm^{-1} could be due to stretching vibration of C=N in non-conjugated and monoconjugated aldimines, -CH=N- and -CR=CR$'$-CH=N-, respectively. They are in good agreement with the C=N absorption in R-CH=N-R$'$ non-conjugated imine at 1674-1665 cm^{-1} and $\mathrm{C_6H_5}$-CH=NR' monoconjugated at 1656-1629 cm^{-1} reported by Patai [32]. According to Kosower's work, α,β-unsaturated imine absorbs between 1667-1653 cm^{-1} and α,β,γ,δ-unsaturated imines have absorptions in the range of 1630 to 1613 cm^{-1} [150]. Other literature sources for IR spectral data of α,β-unsaturated imine assign the 1640 and 1622 cm^{-1}: C=N (asym + sym), respectively [151].

For unsubstituted gaseous 2-azabutadiene (N-vinylimine, $\mathrm{H_2C}$=N-CH=$\mathrm{CH_2}$) values of 1618 and 1635 cm^{-1} were given by Amatatsu et al. [152], and 1610 (C=N) and 1628 cm^{-1} (C=C) by Guillemin et al. [153]. For an 1,4,4-trialkyl-2-azabutadiene values of 1626 and 1667 cm^{-1} can be found in the literature [154]. The range in which these vibrations appear coincides with the range of C=C stretching vibrations of non-conjugated double bonds in alkenes (1680 to 1620 cm^{-1}) [6]. Generally, however, C=C stretching vibrations are weak or too weak to be visible at all [102]. Conjugation may raise the intensity of these vibrations and in conjugated dienes without a center of symmetry the presence of a band near 1600 cm^{-1} (in addition to a weaker band at 1650 cm^{-1}) can be taken as an indication of conjugation [6]. It is therefore tempting to assign the component at 1601 cm^{-1} to conjugated double bonds.

A plot of a chemigram for the 1700-1500 cm^{-1} region as a function of different plasma duration time is shown in Fig. 5.7. For 30, 250, and 600 s plasma treatment no saturation can be seen. That means the surface of the thin polymer film is still subject to change due to the plasma effect and new functional groups are formed continuously. Finally, during a longer treatment time of 925 s, the curve shows a plateau due to the saturation of the film with newly formed compounds. The chemigram graphs for the region of 2960-2870 cm^{-1} (maximum absorption around 2917 cm^{-1}) reveal that the polymer surfaces are continuously etched during the plasma exposure time.

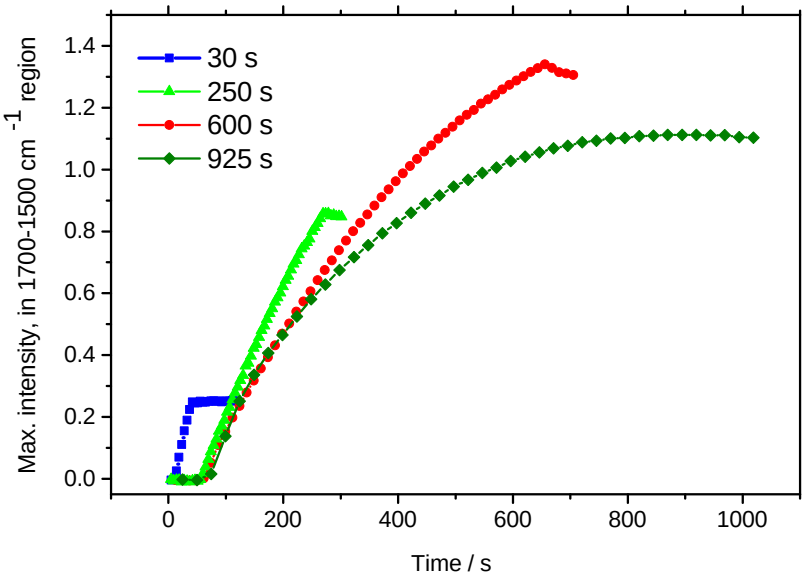

Figure 5.7: Chemigram for 1700-1500 cm^{-1} region as a function of different plasma duration times

5.1.4 Plasma treatment using N_2 + x % O_2 + y % H_2

FTIR spectra of LDPE thin films treated in DBD post-discharges from gas mixtures of general composition N_2 + x % O_2 + y % H_2 (x = 0, 0.01, 0.1; y = 0, 1, 4) are presented in Fig. 5.8. Curve fitting of the FTIR spectra of plasma-treated PE surfaces with x = 0, y > 0 requires five Gaussian peaks at 1673, 1646, 1615, 1583, and 1554 cm^{-1}. (Details of the curve fitting have been already presented in section 5.1.2.) Very pronounced changes are seen in the spectra upon adding 0.01 % or 0.1 % oxygen: The new absorption at 1710 to 1720 cm^{-1} is attributed to the formation of carbonyl groups (C=O). Even 4 % H_2 are not sufficient to prevent a strong carbonyl vibration (Fig. 5.8 R). A spectrum taken from a film treated using pure nitrogen exhibits a strong band at 1695 cm^{-1}, which is probably related to a carbonyl group, possibly in amide [6]. The addition of H_2 appears to suppress the formation of amides as observed in pure N_2, possibly from O-bearing contaminations in N_2 in the ppm range. However, the addition of hydrogen cannot prevent carbonyl formation even if only 0.01 % (or 100 ppm) O_2 is intentionally added.

5.1.5 The role of hydrogen in the plasma gas mixtures

The presence of imines as main functional groups was formerly discussed or inferred in several papers on plasma-based nitrogenation of polymers [14] as well as on plasma polymerization of

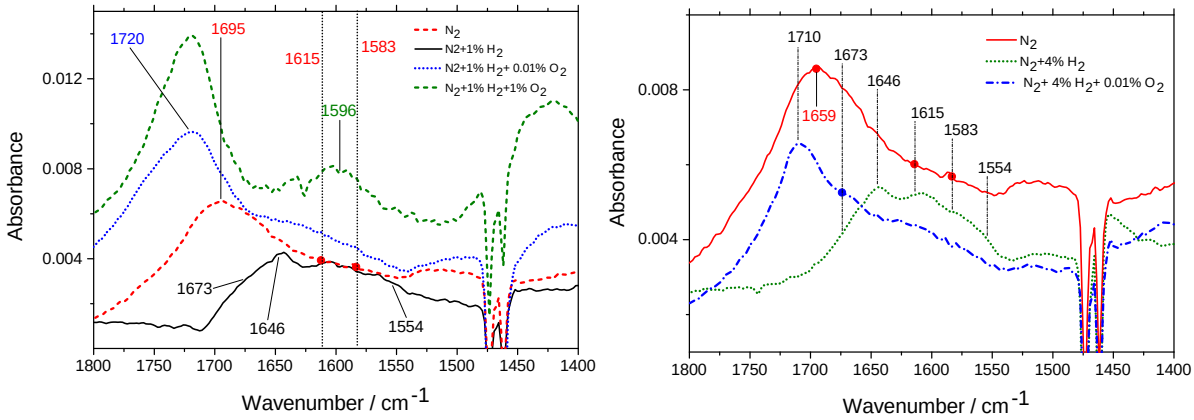

Figure 5.8: FTIR-ATR spectra obtained after 30 s post-discharges treatment using N_2 + y % H_2 + x % O_2 plasma introduced to LDPE thin films, measurement using ZnS crystal, resolution 4 cm^{-1}, 12 scans (Absorbances are offset arbitrary).

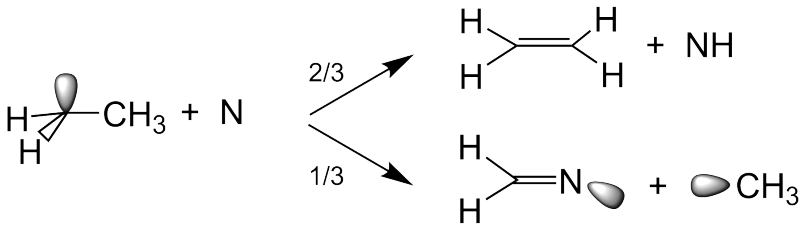

Figure 5.9: Reactions of ethyl radicals with nitrogen atoms in ground state, about 2/3 of the ethyl radicals forms ethylene, nearly 1/3 is converted to a pair of an iminyl radical and a methyl radical; regarding the results of ref. [4]

amines [36, 43, 155]. However, imine production is also imaginable via reactions of ethyl radicals and ground state nitrogen atoms in absence of NH_x [4], as shown in Fig 5.9.

Referring to the results obtained in this work, the main role of hydrogen admixtures in the plasma gas is hypothesized to passivate reactive oxygen-bearing species. Leading to the conclusion; adding a small amount of hydrogen to the nitrogen reduces the contribution of oxygen on the polymer functionalization, dramatically. The hydrogen addition leads to convert O_2 traces or reactive species derived from O_2 traces such as O_3, NO or NO_2 to a less reactive product (possibly water) which is not able to form amides as competitors for the desired amines or imines, see above.

For this speculation to be true, it would be necessary that nitrogen molecules in the first excited state, $N_2(A)$, and ground state nitrogen atoms $N(^4S)$ are still present in the post-discharge in the presence of a few percent hydrogen. Such long-lifetime species are most likely responsible for

surface-nitrogen functionalization. Optical emission spectra shall be taken from the nitrogen-hydrogen mixtures plasma in post-discharges region to get information about the main relevant species. Corresponding experiments and interpretations are given in Chapter 8.

Briefly, OES investigations from nitrogen-hydrogen mixtures plasma in post-discharges regions reveal that the nitrogen first positive state $N_2(A)$ and ground state nitrogen atoms $N(^4S)$ are still the main nitrogen species (see section 8.2).

5.1.6 Plasma effect on PE thin films treated in post-discharges of N_2 + 10 % NH_3

Here, we present results of an investigation on the PE thin film functionalization using mixture of nitrogen and ammonia plasmas. It is believed that amino groups provide an excellent basis for subsequent surface modification techniques since they allow to bond biomolecules with high selectivity [13]. Ammonia plasma treatment is known as a process which usually creates a number of different nitrogen-containing functionalities [8].

For example, radio-frequency plasma treatments of polymer surfaces at low pressure using NH_3 or N_2 + H_2 mixtures by Hollahan et al. [12] and using NH_3 + H_2 by Favia et al. [14] have been reported as a method to create amino functional groups on polymer surfaces. The applied technique to detect the presumed-formed amino groups by Hollahan et al. [12] has been previously explained in section 1.1. However, the experimental findings are not really convincing proofs that amino groups had actually been formed during plasma exposure of the investigated surfaces: Besides the possibility that, during exposure to acidic or basic dye solutions, any nitrogen functionalities had hydrolyzed under amine formation, the successful methylation or protonation of nitrogen atoms just indicates that there are nucleophilic or basic nitrogen atoms, but not necessarily that amino groups are present [156]. Favia et al. has applied chemical derivatization technique with electrophilic reagent TFBA which has been used very frequently in the recent 35 years [14]. However, there are several reasons presented in this work to conclude that TFBA derivatization applied to plasma-nitrogenated polymer surfaces is not having the amino-selectivity properties.

The experimental focus here is to examine the influence of ammonia and hydrogen mixtures plasma used for the nitrogen functionalization of polymer surfaces. Thereby, the surface chemical structures of PE thin film after exposure to N_2 + 10 % NH_3 mixtures are investigated using FTIR-ATR and subsequent H-D isotope exchange of active hydrogen atoms. Measurements of three different gas compositions including pure nitrogen (blue/dot), a mixture of nitrogen

and 4 % hydrogen (red/dash), and a mixture of nitrogen and 10 % ammonia (black/solid) are shown in Fig. 5.10. In all cases, the effect of plasma-induced etching of the LDPE thin film can be observed in the region of the stretching vibration of aliphatic C-H bonds, ($\nu(CH_2)$ peak position at 2918-2849 cm^{-1}) and deformation vibrations ($\delta(CH_2)$ peak position at 1473-1462 cm^{-1}). The effect of plasma is not restricted to the simple etching process. Several changes in the region, where different functional groups, such as X=Y stretching vibrations and X-H bending vibrations are expected to occur, is also seen. Curve fitting of the FTIR spectrum of nitrogen-plasma-treated PE surfaces requires three peaks at 1583, 1615, and 1705 cm^{-1}. The dominant absorption at 1705 cm^{-1}, which is related to the stretching vibration of ν(C=O), vanishes upon adding hydrogen or ammonia to the process gas. PE thin film treated in post-

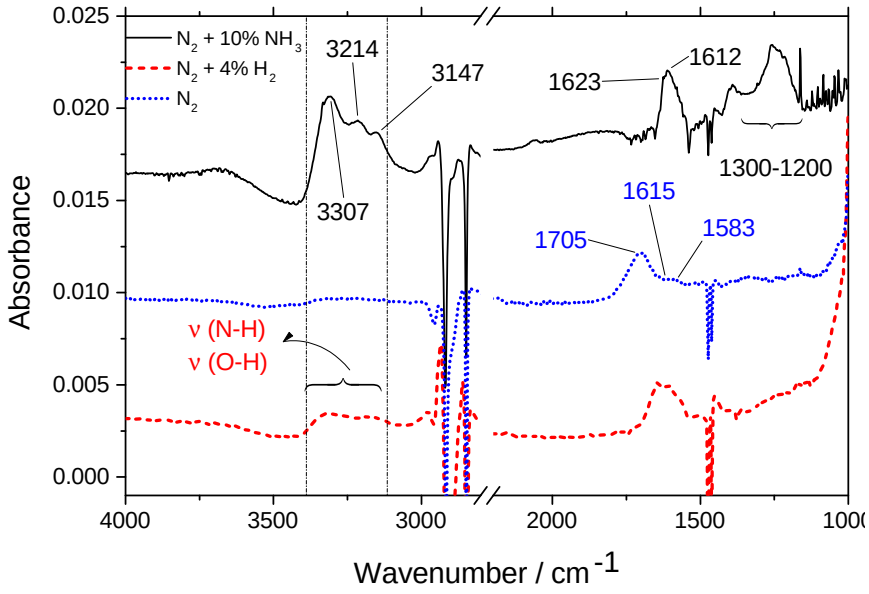

Figure 5.10: FTIR-ATR spectra of LDPE thin films after 30 s treatment in N_2, N_2 + 4 % H_2 and N_2 + 10 % NH_3 plasma. (Absorbance offsets are chosen arbitrary for the sake of clarity) [1].

discharges of 10 % ammonia in N_2 exhibits at least two absorptions at 1623 and 1612 cm^{-1}. The peak position at 1612 cm^{-1} may be attributed to bending deformation vibration of -NH_2. The band absorption at 1623 may be attributed to ν(C=C). The stretching vibrations at 3307 and 3214 cm^{-1} may be attributed to asymmetric and symmetric stretching vibrations of NH_2, respectively. Saturated primary amine absorbs at 1295-1145 cm^{-1} with weak intensity due to NH_2 rocking/twisting vibration [6]. The observed broad absorption at 1300-1200 cm^{-1} probably exhibits the rocking vibration of primary aliphatic amine. In order to confirm whether primary amines are formed on the treated surface, a hydrogen-deuterium exchange experiment was carried out *in situ* (the spectra are not shown here). The experimental findings of H-D exchange showed

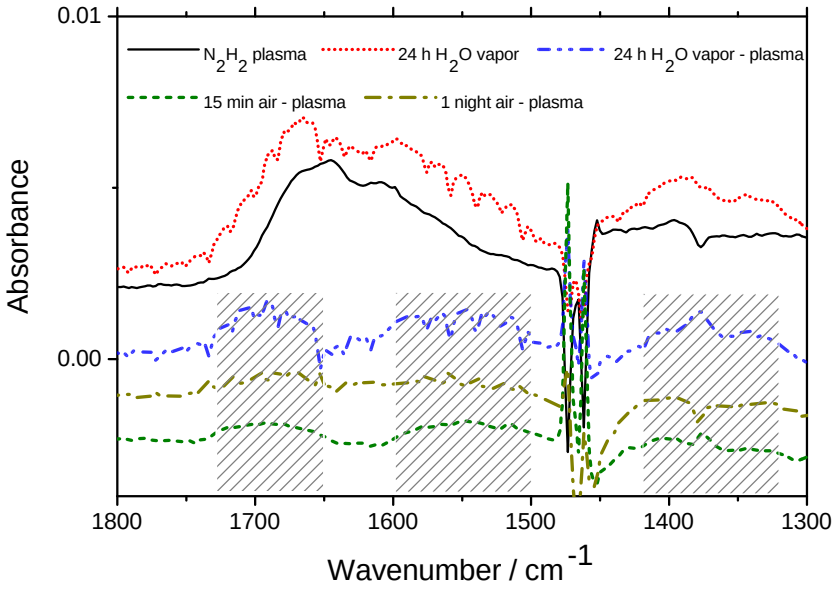

Figure 5.11: FTIR spectra of PE films plasma-treated under standard conditions before and after exposure to water vapor 24 hours and to air (15 min and 1 night). Spectra are arbitrarily offset against each other in vertical direction.

that there is no detectable vibration around 1200 cm^{-1} where -ND_2 groups should have their deformation vibration band. Consequently, amino groups had not been actually formed as a result of ammonia and nitrogen mixtures plasma treatment.

5.2 Effects of water vapor and ambient atmosphere on the plasma-treated PE surfaces

In Fig. 5.11 some of the relevant FTIR spectral results are assembled. The solid line represents the effect of plasma on the PE thin film. Subsequently, the treated polymer film was exposed to water vapor and ultra-pure N_2 for 24 h. One part of *in situ* series measurement of this experiment is shown in red/short dot. The measured spectrum was subtracted from the spectrum of unexposed, but treated thin film and the result is shown in blue/dash dot. The exposure of treated LDPE thin film to the water vapor and ambient atmosphere caused several new features to arise. Three bands of significantly increased absorbance can be recognized, extending from 1730 to 1650 cm^{-1}, from 1600 to 1500 cm^{-1}, and from 1420 to 1320 cm^{-1}. It is found that the quality of the spectra is reduced due to some water vapor entering the IR beam path. The green/short dash and dark yellow/dash dot curves were achieved after short (15 min) and long-term (1 night)

exposures of the freshly plasma-treated PE surface to the laboratory atmosphere and subtraction of the spectrum taken before air exposure. A comparison of the spectra shows that the chemical changes on the treated polymer surface with the ambient atmosphere is primarily a hydrolysis reaction, not an oxidation. Table 5.3 lists typical absorption band ranges from the available literature for amide I and amide II in secondary amide and ureas and compares them with the absorptions found for plasma-treated LDPE thin film exposed to water vapor.

The precursors for the formation of secondary amides by hydrolysis could be ketenimines CH=C=N- while ureas would be formed by hydrolysis of carbodiimides -N=C=N-. In fact, signs of the presence of functional groups with cumulated double bonds such as CH=C=N- or -N=C=N- have actually been detected [1]. Considering the reactivity of these moieties, it is not surprising that only very small densities were found. The corresponding groups could for example react with nucleophilic N-based centers (secondary amines, imines) on the surface and form more stable compounds such as amidines or guanidines which which then constitute the actual precursors to the observed hydrolysis products. It must be noted, however, that the assignment of the observed bands to secondary amide vibrations would not be satisfactorily in agreement with the results of the isotope exchange experiments, presented in the next section. According to previous research, upon deuteration of secondary amides the amide I vibration should shift by only 10 cm^{-1} to lower wavenumbers while the amide II vibration shifts by 100 cm^{-1} [107]. In our deuteration experiments, the short-wavelength band at 1690 cm^{-1} seems to downshift much stronger, probably by at least 50 cm^{-1}. To get more insight into the processes during hydrolysis and the products formed, it would probably be the best to prepare a few suitable model compounds (N,N'-dialkylurea and N-alkyl alkanoic acid amide) and investigate their IR spectra and spectral changes during H-D exchange in a hydrocarbon matrix.

5.3 Hydrogen-deuterium (H-D) exchange experiments [1]

Infrared spectra of treated LDPE thin film were investigated in the 4000-1000 cm^{-1} region. The interpretation of the spectra and the assignment of the bands was made on the basis of the frequency shift by deuteration however, there are some overlapping stretching vibrations of double bands in the 1750-1600 cm^{-1} region which are not easily distinguishable from each other. The *in situ* FTIR-ATR measurements of a treated LDPE surface after exposure to light and heavy water are presented in Fig. 5.12 L.

A visual detection of primary amine groups which are expected to appear at 1620 cm^{-1} is not trustworthy. Deuteration of primary aliphatic amines shifts the bending vibration of N-H from

	Amide I	Amide II	ν(C-N) or ν_{as}(N-C-N)
Bands in Fig. 5.11	1730-1650	1600-1500	1420-1320
Sec. amides (in solution)	1700-1665 s	1550-1510 s (trans)	1350-1310 w-m (cis)
Ureas (in solution)	1705-1660 s	1605-1515 m	1360-1300 s-m

Table 5.3: Comparison of absorption band ranges in Fig. 5.11 with typical regions of vibrations found in secondary amides and in ureas, according to reference [6] (s: strong, m: medium, w: weak).

1625-1620 cm^{-1} to 1240-1190 cm^{-1}, N-D form [142, 157, 158]. This is an effective way to detect primary amine groups in an IR region which is totally free of any vibration bands. The H-D exchange procedure was explained earlier, see section 4.2.4.

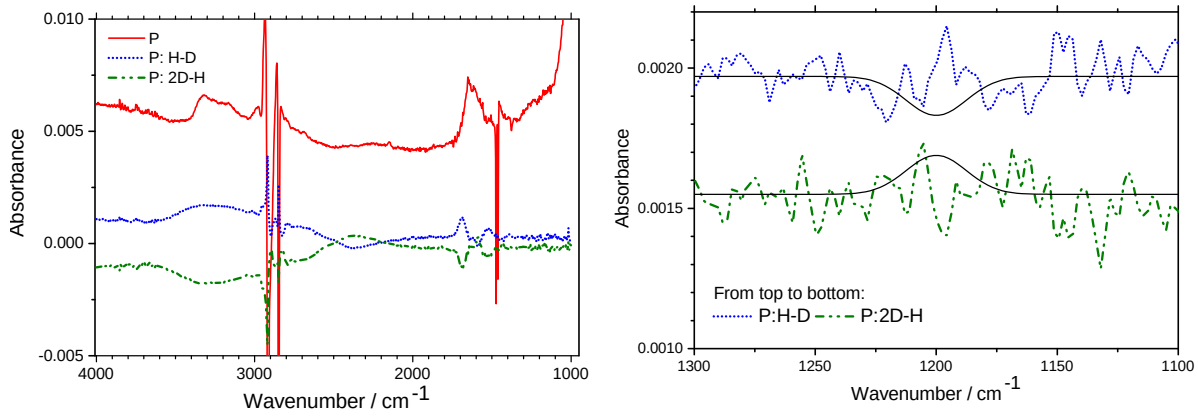

Figure 5.12: Left, FTIR spectra taken after 30 s afterglow exposure under standard conditions ("P") and pair of difference spectra during H-D exchange experiment after standard afterglow treatment: Spectrum after H_2O exposure minus spectrum after previous D_2O exposure (blue/short dot curve, "P:H-D") and vice versa after 2nd D_2O exposure (green/dot dash curve, "P:2D-H") (Arbitrary absorbance offsets). In graph on the right, wavenumber region around ND_2 deformation vibrations, expanded (Arbitrary absorbance offsets). On each spectrum, a Gaussian function centered at 1200 cm^{-1} is superimposed as a positive or negative theoretical spectral band, calculated under the assumption of an appeared or disappeared amino group -ND_2 density of 1 nm^{-2}, using experimental values B = 25 km/mol and FWHM = 30 cm^{-1}.

Three spectra in Fig. 5.12 L are related to the plasma-treated surface "P", spectra after H_2O exposure minus the spectra after previous D_2O exposure ("H-D") and vice versa after 2nd D_2O exposure ("2D-H"). The corresponding references (Ref. H or Ref. D) were subtracted. Repeating the exchange twice or more increases the sensitivity of the method. The mirror symmetry between the pairs of difference spectra shows that spectra D and H or spectra 2D and H differ only by

the reversible exchange of active hydrogen- any irreversible reaction with water is not visible within the time scale of the experiment. Aside from the replacement of N-H and possibly O-H stretching vibrations at $\nu > 3000$ cm^{-1} by N-D(O-D) bands between 2800 and 2000 cm^{-1}, a few exchange peaks in the region 1750-1300 cm^{-1} are observed.

Several vibrations related to exchangeable H at around 1690 and 1530 cm^{-1} in the spectrum "P: H-D" are seen. After deuteration, two vibrations related to moieties with exchangeable D at 1640 and 1588 cm^{-1} in the spectrum "P: 2D-H" are detectable. In order to achieve a precise identification of exchangeable functional groups with hydrogen and deuterium further investigations are required. IR spectra of several suitable model compounds and their spectral changes during H-D exchange can provide valuable information.

Primary amine groups should show a positive (negative) absorption band at 1625-1620 cm^{-1} for δ(N-H) in the H-D (2D-H) spectra and a negative (positive) band at 1240-1190 cm^{-1} for δ(N-D) in the H-D (2D-H) spectra. The expanded area at 1300-1100 cm^{-1} is shown in Fig. 5.12 R, where no obvious vibration related to $\delta(ND_2)$ is detectable. Theoretical bands calculated under the assumption of an -ND_2 density of 1 nm^{-2} appearing (disappearing) in the presence of D_2O (H_2O) vapor are superimposed as Gaussian functions. The comparison with measured results shows that the density of -ND_2 which would be detectable in these spectra is significantly below 1 nm^{-2}. We estimated that it is around 0.3 nm^{-2}.

5.3.1 Calculation of the integrated band intensity for ND_2 at 1201 cm^{-1} in a deuterated amine

In order to obtain quantitative values for the density of -NH_2 groups on the plasma-treated surface, an integrated band intensity around 1200 cm^{-1} for the ND_2 scissoring vibration is required. The integrated band intensity cannot be estimated from the result of the exchange on the surface without a reference measurement. Therefore, solutions of primary amines and deuterium oxide were prepared.

The primary amine used to determine the B integrated band intensity for ND_2 vibrations in a deuterated amine, it needs to meet certain conditions. Firstly, the amine should have relatively low volatility, which means that higher alkyls, e.g. hexylamine, heptylamine, 2-ethyl-hexylamine, etc. may be useful. Secondly, the amine should not take up too much water in the exchange process, which also holds true for the previous examples. Thirdly, the amine should be relatively pure (> 98 %), not containing too much CO_2. In order to get more reliable values, three different amines (1-aminooctane, 2-aminooctane and 2-ethyl-hexylamine) were used in our investigations.

Solutions of 1-aminooctane-d_2, 2-aminooctane-d_2, 2-ethyl-hexylamine-d_2 obtained from the amines by isotope exchange with heavy water, each in hexadecane, were used for the measurements. 5 ml of a 3.1 M solution of the corresponding amine (1-aminooctane, 2-aminooctane or 2-ethyl-hexylamine) in hexadecane was intensely shaken two times with 10 ml D_2O in a separating funnel, then the organic phase was thoroughly dried (Na_2CO_3). The measurements were performed in s-polarization with a single reflection diamond ATR at resolution of 4 cm^{-1}. The Smart DuraSamplIR accessory (SensIR Technologies, now part of Smith's Detection, Danbury, CT, USA) used provides an average incidence angle of 51°. In regard to Eq. 5.2, B can be found if the band area under the desired peak, the number of reflections (N) of the infrared beam on the sample, the concentration of the solution (c), and the effective thickness in certain polarizations (d × f) are known. The derivation of Eq. 5.2 was explained in section 3.1.1.

$$\int_b A \times d\nu = NcdBf(\frac{1}{ln10}) \tag{5.2}$$

The solvent hexadecane has a fairly similar refractive index in the visible region (n_D = 1.4345 at 20 °C) and in the far infrared (n[80cm^{-1}] = 1.428 at 20 °C). To calculate the effective thickness for ATR measurements with a diamond crystal (n_1 = 2.4; N = 1) we adopt n_2 = 1.43 for the hexadecane solution. Using an integral over the resulting ND_2 scissoring band (FWHM ≈ 30 cm^{-1}) from 1260 to 1160 cm^{-1} and with an effective depth d_e of 1.35 μm at 50° and 1200 cm^{-1}, the resulting average B is 25 km/mol.

As an example, an IR measurement of octylamine in hexadecane before and after deuteration is shown in Fig. 5.13. The absorption at 1618 cm^{-1} in the IR spectrum of the octylamine in hexadecane is ascribed to the NH scissoring mode in primary amine. It is seen that this vibration vanishes upon H-D isotope exchange of active hydrogen atoms, and a new absorption at 1201 cm^{-1} is formed which is attributed to the ND_2. The broad absorption seen at 2700-2100 cm^{-1} is attributed to N-D and/or O-D due to vibrations in moieties with deuterium bonded to oxygen or nitrogen atoms.

A collection of integrated band intensities B and typical peak positions ν_{max} of several important vibrational infrared absorption bands are listed in Table 5.4, which are expected to play a role for FTIR spectroscopy of nitrogen plasma-treated polymer surfaces. From reaction of imines with water or TFBA, unsaturated aldehyde and open chain ketones possibly form. Several examples are depicted in Table 5.4. Carboxylate ions may form on the polymer surface upon exposure of amine, imine, and other basic groups to the vapor of volatile organic acids.

Vibration, compound class	**B (km/mol)**	ν_{max}**(cm^{-1}) solvent**	**ref.**
$\delta(NH_2)$, amines	30	1620-1625 (heptan)	[103]
$\delta(ND_2)$, amines	18 (theor.)	1201(exp., Kr)	[142]
	25 (exp.)	1195-1205 (hexadecane)	[1]
$\nu_{asym}(NH_2)$, amines	5	3375	[102]
$\nu_{sym}(NH_2)$, amines	2	3310	[102]
ν(NH), sec. amines	1-2	3300	[102]
ν(C=N), alkyl-CH=N-alkyl	85	1670 (diglyme)	Unpubl.
	39	1671 ($CHCl_3$)	[159]
ν(C=N), aryl-CH=N-alkyl	58	1654 ($CHCl_3$)	[159]
ν(C-CF_3), 4-CF_3-benzaldimines	370	1324 (hexadecane)	[1]
Amide I+II, prim. amides	460	1690 ($CHCl_3$)	[102]
Amide I, sec. acetamides	230	1670 (KBr)	[102]
Amide II, sec. acetamides	210	1540 (KBr)	[102]
ν(C=O), CH_2=CH-CH=O	220	1696 ($CHCl_3$)	[143]
ν(C=O), satur. aliph.ketones	170	1715 (non-polar solvents)	[102]
ν(C=O), α,β-unsatur. ketones, trans	185	1690 (non-polar solvents)	[102]
ν(C=C), α,β-unsatur. ketones, trans	25	1660 (non-polar solvents)	[102]
ν(C=O), α,β-unsatur. ketones, cis	140	1680 (non-polar solvents)	[102]
ν(C=C), α,β-unsatur. ketones, cis	90	1630 (non-polar solvents)	[102]
$\nu_{asym}(CO_2)$, aliphat. carboxylates	830	1550-1600	[102]

Table 5.4: Integrated band intensities B and typical peak positions ν_{max} of characteristic vibrational infrared absorption bands of amines, imines, amides, acrolein CH_2=CH-CH=O as prototypic unsaturated aldehyde, ketones, and carboxylate ions.

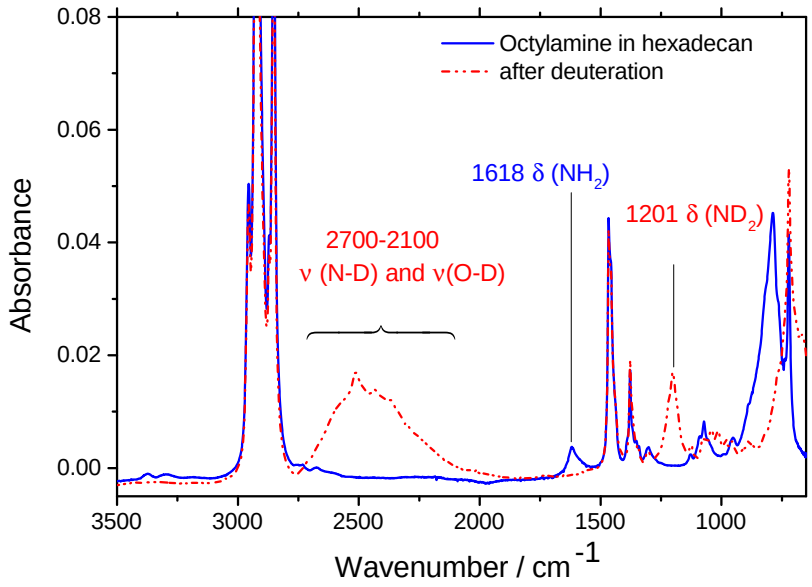

Figure 5.13: FTIR-ATR measurement of octylamine in hexadecane before and after deuteration. ATR crystal was diamond at 51° and resolution 4 cm^{-1}.

5.3.2 A long term series measurement from deuterated primary amine

In order to determine the difficulty of working with basic groups in the laboratory atmosphere, a solution of 2 ml of 2-aminooctane in 1 ml hexadecane (0.004 mol/cm^3) was mixed and placed on the diamond ATR crystal. A long term series measurement was carried out under natural atmospheric conditions for 30 min to monitor the reaction of amine with atmospheric CO_2. The infrared collection data consists of 120 scans, a sampling interval of about 4 minutes, a resolution of 4 cm^{-1} over a time period of 31 minutes utilizing a diamond ATR 51°. The result of the series measurement with a $\backsim$ 4 min time interval is shown in Fig. 5.14. The first measurement of the amine solution (2 min in the laboratory atmosphere, see legend) shows several absorption bands related to a typical primary amine. The two broad absorptions above 3000 cm^{-1} (3363 and 3286 cm^{-1}) are related to two ν(NH) stretching vibrations of NH_2. Two strong absorptions at 2980-2800 cm^{-1} are ascribed to asymmetric ν_{as}(CH) and symmetric stretching ν_s(CH) of C-H, respectively. An absorption band at 1618 cm^{-1} is related to the scissoring vibration of NH_2. With increasing exposure time to the laboratory atmosphere, a broad shoulder appears at 1600-1560 cm^{-1}. Two minutes time interval measurements of the 1700-1480 cm^{-1} region with more details are shown in Fig. 5.14. A new absorption band, having a pronounced peak at 1579 cm^{-1}, develop with time exposure in the laboratory atmosphere. This absorption band could be due to the NH_3^+ asymmetric deformation vibration from the reaction of amine with CO_2 in air [160]. Amine -NH_3^+ groups have medium-to-strong absorptions near 1600 and 1500 cm^{-1}

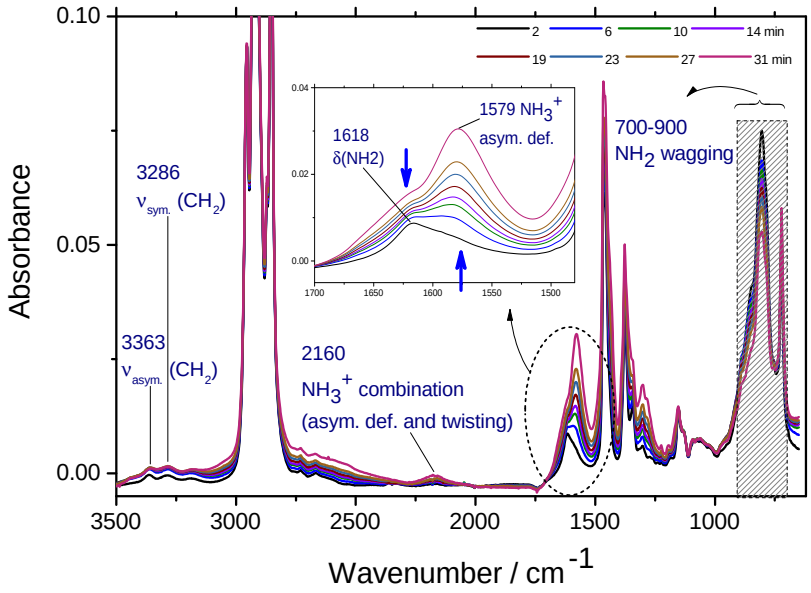

Figure 5.14: FTIR-ATR series measurement of 2-aminooctane in hexadecane at room temperature in contact with air, utilizing diamond 51° ATR single bounce, 128 number of scans, resolution 4 cm^{-1}.

due to asymmetric and symmetric deformation vibrations [6]. A weak absorption band around 2160 may be attributed to -NH_3^+ combination of asymmetric deformation and twisting vibration [160]. Moreover, the two absorptions at 1461 and 1378 cm^{-1} are related to bending deformation vibration of carbon-hydrogen bond δ(CH) and CH_3 umbrella in hydrocarbons, respectively. Additionally, NH_2 wagging vibration out of plane bending of NH_2 is seen with great intensity in the broad range of 900-700 cm^{-1}.

Next, the amine solution was mixed with deuterium oxide and the same parameters for series measurement was applied to determine the allowed measurement time interval in deuterated amine solution before changing to the hydrogen isotope. A long series measurement of this solution in air causes new features to appear in the absorbance spectrum as shown in Fig. 5.15. In the beginning of the measurement a very strong and broad absorption related to N-D and O-D at 2700-2000 cm^{-1} and a positive absorption at region 1266-1160 cm^{-1}, related to $\delta(ND_2)$ develop (maximum at 1205 cm^{-1}). While after about half an hour both intensities vanish and broad areas in two regions of 3500-3100 cm^{-1} and 1620-1520 cm^{-1} form, due to changing the ND_2 and D_2O to NH_2 and H_2O upon hydrogenation. Furthermore, the wagging vibration of amine appear again at 840-790 cm^{-1}.

A long series measurement of an amine compound reveals that amines are very sensitive to air. Even after a period of less than 6 min left standing in the laboratory atmosphere, CO_2 molecules

find a chance to react with the amine, thereby a strong broad region appears between 1600 and 1500 cm^{-1} with its maximum around 1577 cm^{-1}. The long IR measurement of the deuterated amine demonstrates that ν(ND) (at region 2700-2000 cm^{-1}) and $\delta(ND_2)$ (around 1205 cm^{-1}) rapidly change to ν(NH) (at 3500-3100 cm^{-1}) and $\delta(NH_2)$ (at $\backsim$ 1620 cm^{-1}) during exposure to the natural air, respectively. However, deuterated species in this compound rapidly change to hydrogenated form. Interestingly, IR spectra of both hydrogenated and deuterated amine in contact with the natural air exhibit an increased absorption at around 1577 or 1579 cm^{-1} due to NH_3^+ asymmetric deformation vibration. A note of caution needs to be added concerning infrared measurement of deuterated amine due to the time limitation, especially when B calculation is the main issue.

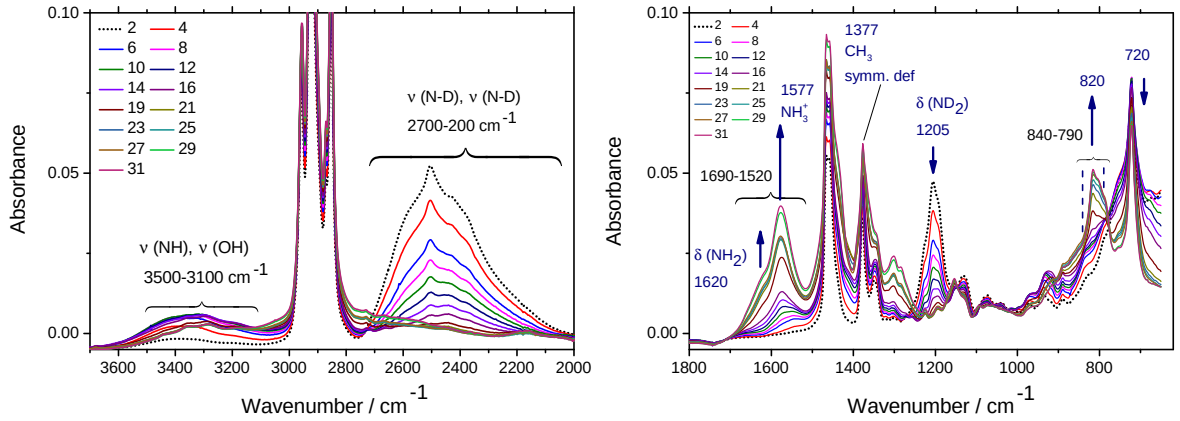

Figure 5.15: FTIR measurement of deuterated 2-aminooctane in hexadecane in contact with air utilizing diamond 51° ATR single bounce, 30 min series, 128 number of scans, resolution 4 cm^{-1}. ν(ND) at region 2700-2000 cm^{-1} and $\delta(ND_2)$ at around 1205 cm^{-1} are exchanged to ν(NH) at 3500-3100 cm^{-1} and $\delta(NH_2)$ at 1620 cm^{-1}.

5.3.3 Urea preparation and H-D exchange

As mentioned above already, H-D exchange spectra of polyethylene thin film treated in nitrogen-hydrogen mixtures plasma revealed a few exchange peaks in the region 1750-1300 cm^{-1} whose nature is so far unknown. It is, therefore, required to prepare several suitable model compounds which are taken into consideration as candidates for formed functional groups. Urea, for example, which can form by hydrolysis of carbodiimides -N=C=N- is considered to be a candidate. In the following, urea as a model substance is prepared and the effect of H→D and D→H isotope exchanges are investigated utilizing FTIR-ATR.

An attempt to produce urea from primary amine and hexyl isocyanate was successful. The same molarity of octylamine and isocyanate was mixed in dichloromethane medium. Hexyl isocyanate was slowly poured into octylamine while the solution was stirred strongly for one hour. It is known that the stretching vibration of the carbonyl group of urea, ν(C=O), in solution absorbs at 1705-1660 cm^{-1} while NH stretching and NH_2 deformation vibrations absorb with medium intensity at 3440-3200 cm^{-1} and 1605-1515 cm^{-1}, respectively [6]. The IR measurement of prepared solution exhibits a broad absorption at 3400-3260 cm^{-1} with a peak related to NH stretching at 3345 cm^{-1}, see Fig. 5.16 (red/solid). Two positive absorptions in the IR spectra of the formed urea at 1630 cm^{-1} and 1571 cm^{-1} can be attributed to characteristic bands in urea i.e. C=O stretching and NH deformation vibration (blue/dot). Subsequently, 2 ml of the prepared urea solution was shaken with 2 ml deuterium oxide. Two phases were formed minutes after releasing the sample in room atmosphere. The upper phase of the solution was separated and transferred to a small snap cap glass in which some molecular sieves were positioned to absorb the water. IR spectra of urea before and after reaction with deuterium oxide were recorded utilizing a diamond ATR crystal.

On subtracting the deuterated urea spectrum from the undeuterated significant changes are seen. These are depicted in Fig. 5.16 (blue/dot). The broad absorption at 3400-3250 cm^{-1}, related to NH stretching in urea, vanishes while a positive absorption at 2550-2400 cm^{-1} indicates ν(ND) and ν(OD) formation. The amide I band ν(C=O) (at 1630 cm^{-1}) is shifted by 20 cm^{-1} towards lower wavenumbers and appears at 1610 cm^{-1}. Blout et al. claimed that the amide I band does not change in intensity upon deuteration but shifts to lower frequency by about ten wavenumbers [107].

The NH_2 bending deformation at 1571 cm^{-1} shows larger changes by shifting to 1494 cm^{-1}. This is also comparable with the result of amid II deuteration in which a band at 1550 cm^{-1} is lost completely and deuterated amide II bands appear around 1450 cm^{-1} [107]. Additionally, the peak positions of amid I and amide II after urea deuteration compare well with the two sharp peak positions in IR spectrum of D_2NCOND_2 from Sigma Adrich data found at around 1600 and 1500 cm^{-1}, respectively. The comparison of the exchange results of urea and treated PE thin film (see section 5.3) reveal that urea alone cannot be the main functional group which is responsible for exchange peak positions on the treated film. We believe that there are a great variety of functional groups responsible for showing the exchangeable product formed on the plasma-treated polymer surfaces in contact with H_2O and D_2O, respectively.

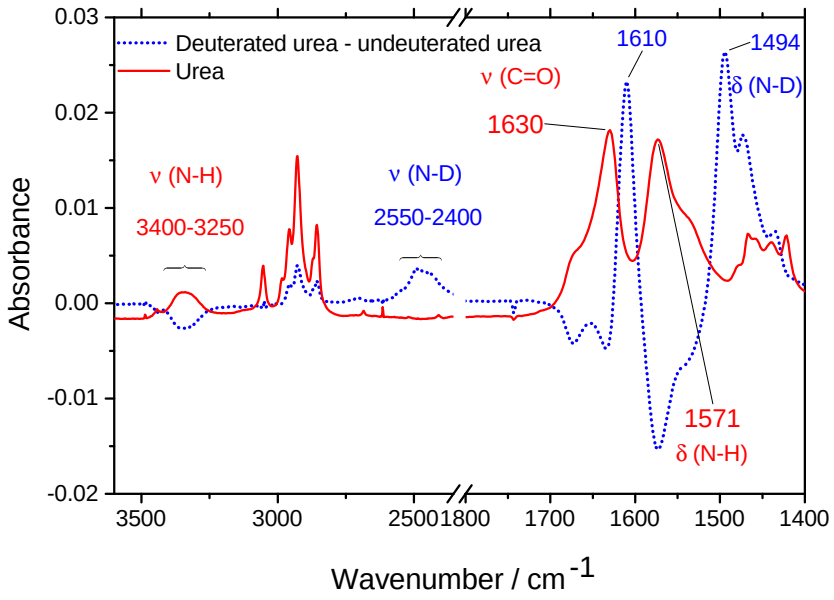

Figure 5.16: FTIR-ATR measurement of urea formed from octylamine and hexyl isocyanate (solid/red), spectrum of deuterated urea minus spectrum of urea (dots/blue)

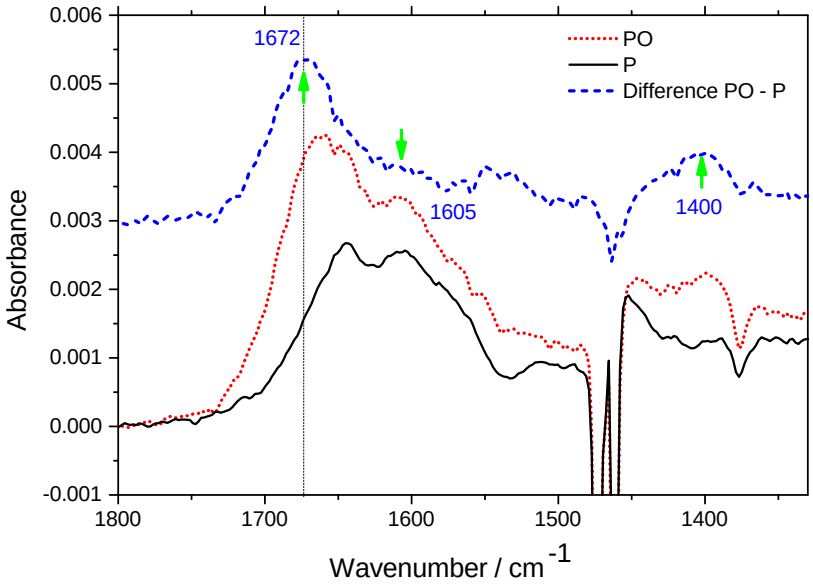

Figure 5.17: FTIR spectra taken after 30 s plasma treatment in post-discharges of N_2 + 4 % H_2 ("P") and with 5 ppm oxygen added ("PO"), respectively. The difference spectrum PO-P is dominated by peaks centered at 1672 and 1400 cm^{-1} [1].

5.3.4 Plasma afterglow treatment and subsequent H-D exchange of LDPE surfaces in the presence of 5 ppm oxygen [1]

Spectra shown in Figures 5.11 and 5.12 were obtained from nominally pure gas atmospheres containing well below 1 ppm oxygen. In the following experiment, 5 ppm oxygen was deliberately added to the process gas in order to investigate if any changes in the IR spectra might provide a hint towards oxygen-containing functional groups. The IR spectra from a mixture of 5 ppm oxygen in N_2-H_2 were collected. The final spectrum after 30 s of plasma afterglow treatment is shown in Fig. 5.17.

Curve fitting of the FTIR spectra using Gaussian functions was performed. In Table 5.2 the results of curve fitting of the IR spectra of plasma-treated PE films in the absence and presence, resp., of 5 ppm oxygen were shown. These results illustrated that the plasma treatment of films in N_2 + H_2 gas mixtures contained less than 5 ppm oxygen.

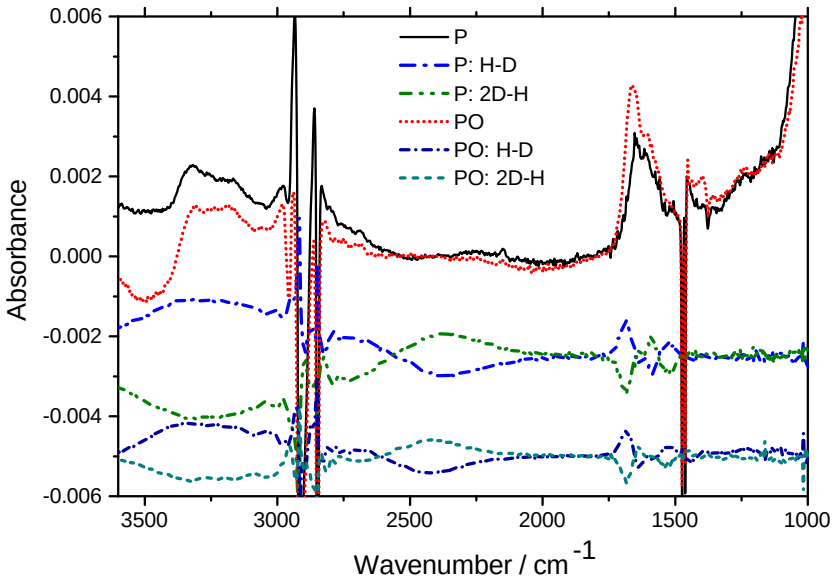

Figure 5.18: Top: FTIR spectra taken after 30 s afterglow exposure under standard conditions (top pair "P") and with 5 ppm oxygen added, respectively (top pair "PO"). Middle: Pair of difference spectra during H-D exchange experiment after standard afterglow treatment: Spectrum after H_2O exposure minus spectrum after previous D_2O exposure ("P:H-D") and vice versa after 2nd D_2O exposure ("P:2D-H"). Bottom: As before, but with 5 ppm oxygen added during afterglow exposure (Arbitrary absorbance offsets) [1].

The main effect of adding a small amount of oxygen to the process gas is increasing the absorption

at 1672 cm^{-1}, which might be related to amide groups. While, the band at 1605 cm^{-1} is reduced significantly. The latter absorption band was attributed to unsaturated carbon-carbon bonds in the PE chain. The hydrogen-deuterium exchange experiment was performed for plasma-treated thin film in the presence of 5 ppm oxygen, according to the experimental process explained in section 4.2.4. The result of the exchange reaction in the absence and presence of oxygen are similar, see Fig. 5.18.

5.4 CD of plasma-treated surfaces with 4-(trifluoromethyl)benzaldehyde vapors [1]

Further information can be achieved from the infrared spectra by chemical derivatization of the sample [161]. For the investigations carried out here, the gas phase derivatization of TFBA is applied to the plasma-exposed LDPE thin film. *In situ* FTIR measurements were accomplished to monitor the chemical labelling of particular functional groups. The experimental setup was shown earlier in Fig. 4.3. Fig 5.19 shows selected spectra measured during a TFBA derivatization experiment, which was extended over a period of nearly 5 h.

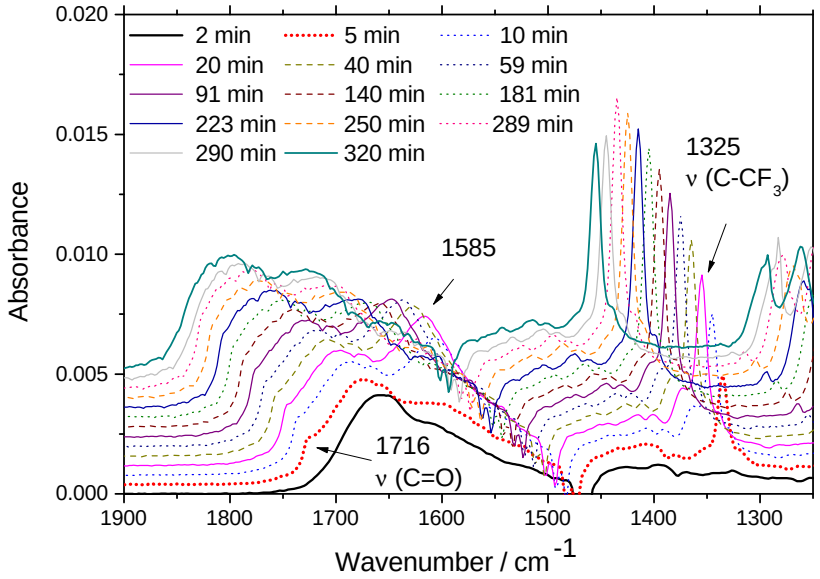

Figure 5.19: Selection of FTIR spectra taken during 287 min exposure of post-discharges treated LDPE surface to TFBA in an N_2 stream. Start of the TFBA exposure was at 2 min. After 289 min the TFBA-loaded N_2 stream was replaced by pure N_2. The spectra for t > 2 min are shifted vertically and horizontally for the sake of clarity [1].

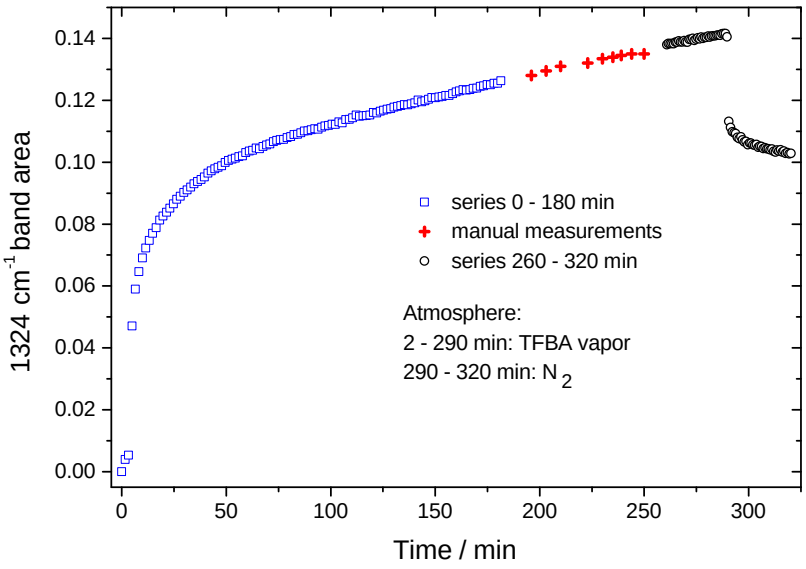

Figure 5.20: Area of C-CF_3 stretching band during 287 min exposure of afterglow-treated LDPE surface to TFBA in an N_2 stream. Start of TFBA exposure at 2 min. After 289 min the TFBA-loaded N_2 stream was replaced by pure N_2 [1].

Among the significant absorption bands are a strong C-CF_3 peak at 1325 cm^{-1}, a strong transient band at 1585 cm^{-1} reaching maximum intensity between 20 and 40 min, and a peak at 1716 cm^{-1} which is attributed to physisorbed TFBA on the treated surface. All of these features appear immediately in the first spectrum measured after starting TFBA exposure (5 min). The vibration band at 1716 cm^{-1} is immediately removed as soon as the TFBA-loaded N_2 stream is replaced by a pure N_2 stream after 289 min. This leads to the disappearance of the C=O peak from the spectrum collected at 290 min. The total density of chemically and physically bonded TFBA can be estimated from the band area of the C-CF_3 peak. The band area of the C-CF_3 stretching band in Fig. 5.20, representative of the total density of adsorbed plus chemically bonded TFBA, rises rapidly in the first 50 min and keeps growing even after nearly 5 h. (In a subsequent experiment there was a still weakly increasing signal even after 22 h of exposure to TFBA.) The removal of TFBA from the N_2 stream (289 min) leads to an immediate desorption of physisorbed and a slower vanish of some loosely bound TFBA.

The final band area obtained in this experiment (and also in the 22 hours run) was about 0.1 cm^{-1}. Integrated absorption intensity B for C-CF_3 is determined 370 km/mol. The calculation of the integrated band intensity can be found in section 5.4.1. Therefore, a density of 1.6 nm^{-2} is calculated for the 4-trifluoromethyl-phenyl moieties immobilized to the surface. This number is roughly a factor 5 above the primary amino group density ($\preceq$ 0.3 nm^{-2}) which

would be detectable by the deuteration experiments described above (see section 5.3). This is quantitative experimental evidence that TFBA is not or not only reacting with -NH_2 groups.

There is also qualitative evidence demonstrating that the derivatization reaction is proceeding different from the simple chemical reaction formulated in Fig. 1.1. If this equation would describe completely what happens upon exposure of the plasma-treated LDPE surface to TFBA, the only spectral changes observed would be a vanishing of the vibrations due to -NH_2 at around 1625 to 1620 cm^{-1} and an appearance of vibrations of an aromatic N-alkyl-aldimine Ar-CH=N-R (Ar = 4-CF_3-C_6H_4-, R = alkyl). In the 1800-1500 cm^{-1} region of difference spectra taken after and before derivatization one would correspondingly expect (i) a negative $\delta(NH_2)$ band at 1625-1605 cm^{-1} with about 8 % of the band area of the ν(C-CF_3) peak at 1325 cm^{-1} and (ii) a positive ν(aryl-CH=N-) band around 1655 cm^{-1}. (In our calibration experiments using TFBA and aliphatic amines in hexadecane, the corresponding C=N peak of N-alkyl-4-trifluoromethyl-benzaldimines appeared at 1652 cm^{-1}.)

The observations do not meet these expectations. The difference spectrum between the final spectrum after derivatization and the starting spectrum, shows that the strong characteristic C-CF_3 vibration at 1325 cm^{-1} is accompanied by a broad band in the region of 1710-1690 cm^{-1} probably- by reason of position and intensity- due to carbonyl groups (see Fig. 5.21). A peak due to 4-trifluoromethyl-benzaldimines near 1655 cm^{-1} is not visible. In addition, the intensity in the range of X-H stretching vibrations with wavenumbers beyond 3000 cm^{-1} is increased and two maxima appear at 3370 and 3210 cm^{-1}. Although this range is relatively low for O-H vibrations we tentatively attribute these bands to chelated O-H groups of β-hydroxycarbonyl compounds as they can be formed by aldol additions. Also, the relatively low carbonyl wavenumber could indicate aldol addition or aldol condensation products [2, 6].

On the other hand, 24 h exposure of a plasma-treated surface to water vapor also produces a carbonyl band of similar integrated intensity peaking in the 1710-1670 cm^{-1} region, Fig 5.22. Therefore we tentatively attribute the carbonyl band observed after TFBA exposure, located in a wavenumber range between the regions typical for saturated aldehydes or ketones on the one hand and saturated amides on the other, to structure elements containing a carbonyl group conjugated with a double bond. Moieties of this kind could be furnished by an exchange reaction of unsaturated imines on the plasma-treated surface with TFBA (see Fig. 5.23).

Similar to unsaturated ketones (R' = PE chain), α,β-unsaturated aldehydes (R' = H) are also characterized by very strong C=O stretching vibrations between 1705 and 1685 cm^{-1} [6].

Due to virtually same positions (about 1655 cm^{-1}) and comparable intensities of C=N vibrations in unsaturated imines and arylimines, contributions of the vanishing unsaturated imine on the

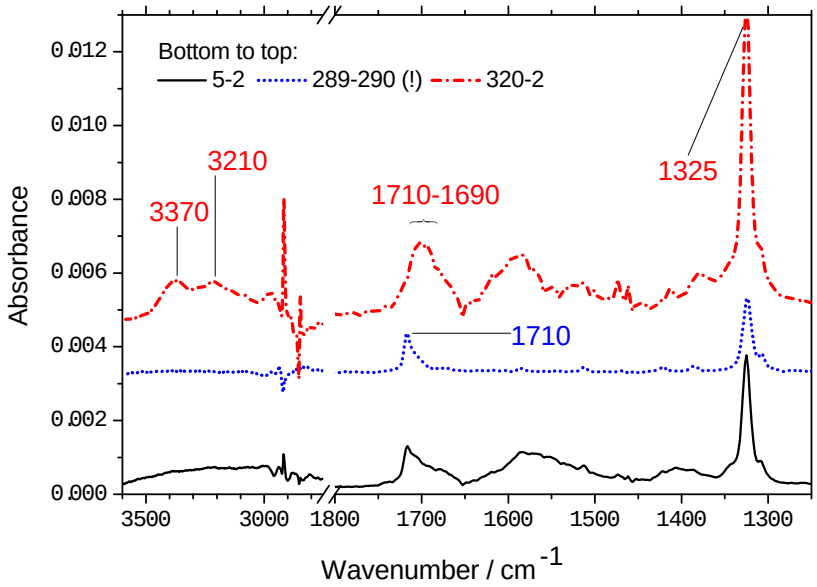

Figure 5.21: Selected difference FTIR spectra taken during TFBA exposure. A label "$m - n$" means that the spectrum at n min is subtracted from the spectrum at m min. From bottom to top these difference spectra demonstrate (i) physisorption and (ii) desorption of TFBA characterized by a narrow carbonyl peak at 1716 cm^{-1}, (iii) The top spectrum shows the overall difference between the final derivatization product spectrum and the starting spectrum before TFBA contact. A presumptive carbonyl peak is located at 1710 to 1656 cm^{-1}. In the ν(X-H) region, two peaks are visible at 3370 and 3210 cm^{-1} [1].

left hand side of Fig. 5.23 to the IR spectrum are cancelled by those of the newly formed benzaldimine on the right hand side. Therefore the region between 1655 and 1650 cm^{-1} is virtually devoid of a positive or negative absorbance. The scheme in Fig. 5.23 is not meant as a final description of the chemical nature of a nitrogen-plasma-treated PE surfaces and its TFBA derivatization but as a working hypothesis for future investigations. At least some aspects of the spectroscopic results obtained during TFBA exposure are interpretable in terms of Fig. 5.23, but not by the commonly assumed reaction shown in Fig. 1.1.

5.4.1 Calculation of the integrated band intensity for C-CF_3 stretching band in the aldimines at 1324 cm^{-1} [1]

If literature data for B are unavailable, it can be determined from ATR measurements on solutions (index s) containing known concentrations c_s of suitable reference molecules featuring the oscillator: Using Equation 3.10, B can be calculated from a plot of the integrated absorbance

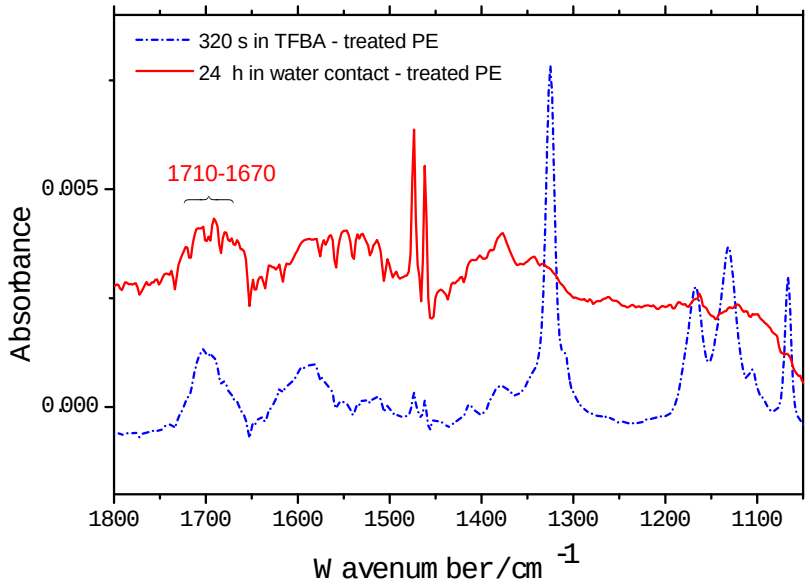

Figure 5.22: *In situ* FTIR measurement of treated LDPE surface; top) subsequently exposed to water vapor for 24 hours and subtracted from treated surface, bottom) subsequently exposed to TFBA vapor and subtracted from treated surface. ATR ZnS 45°, resolution 4 cm^{-1} [1].

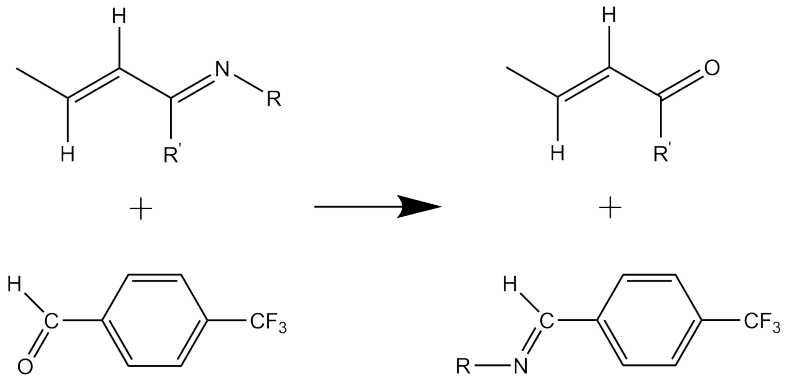

Figure 5.23: Exchange reaction of unsaturated imines (1-aza-butadienes) on the plasma-treated surface with TFBA

as a function of molar concentration: The slope of this plot equals the product N d_{es}B / ln(10). In the reference measurements the sample (solution) thickness on the ATR element must exceed the penetration depth d_p by far and d_{es} is the effective thickness for a solution as a bulk sample.

We used solutions of aldimines in hexadecane prepared *In situ* from TFBA and a 10-20% excess of 3-pentyl-amine or n-hexyl-amine in order to determine the area of the C-CF_3 stretching band at 1324 cm^{-1} by integration over a range of ± 25 cm^{-1}. Measurements were performed with s-

polarized light using a single-bounce diamond ATR crystal at a resolution of 1 cm^{-1}. To calculate the effective thickness for ATR measurements with a diamond crystal (n_1 = 2.4; N = 1) we adopt n = 1.43 for the hexadecane solutions to arrive at $d_{es} = 0.39\ \lambda\ /\ 2.4 = 1.23\ \mu$m at a wavenumber of $\nu = 1/\lambda = 1324\ cm^{-1}$. Regarding the Equation 3.10 a graph of $\int A d\nu$ via concentration (c) is provided. From the slope of the linear fit to the obtained data the integrated absorption intensity of the C-CF_3 stretching band in the aldimines can be calculated as B = 370 km/mol.

5.5 Imine hypothesis

The experimental results obtained in this work are clearly in contradiction to the generally assumed amino-selectivity of TFBA and also other aromatic aldehydes used for chemical derivatization. It is noteworthy that the chemical reactivity of the plasma-treated PE surfaces toward a derivatization reagent is not only due to primary amines. It is hypothesized in this work that such reactivity is largely, if not mainly, determined by the presence of carbon-nitrogen double bonds, i.e. imine groups.

Imino groups are chemical moieties which can also explain most of the experimental observations. Infrared peak positions, reaction of treated films with TFBA in the absence of -NH_2 groups, and lack of NH_2/ND_2 vibrations in the H-D exchange studies are all explainable by the presence of imino groups. However, formation of complex structures such as amidines >N-C=N- ("amino-imines") or guanidines $(>N-)_2C{=}N-$ ("diamino-imines") may not be excluded.

In contrast to amino groups, imino groups have not only nucleophilic but also electrophilic character. Therefore they should be able to undergo reactions with hydrazines, thiols, hydroxylamines, and other nucleophilic compounds. Several nucleophilic chemical derivatization experiments are suggested and studied in Chapter 6. Bonding of such reagents to the treated surfaces should not happen with a surface containing amines only. Several solid evidences to test the imine hypothesis are explained in the following chapters.

Additionally, imine formation on plasma-treated polymer surfaces after contact with nitrogen containing gases was reported previously [55, 162]. Essentially, there are some different possibilities to generate double bonds in structures including C and N. Some probable form of imines which can be formed on N, H-plasma-treated surfaces are listed in Table 5.5.

Functional group	**Name**	**Band Pos. cm^{-1}**	**ref.**
-N=C-C=N-	1,4-Diazabutadiene	1625 (KBr)	[163]
-N=C=N-	Carbodiimide	2138	[146]
-C=N-N=C-	2,3-Diazabutadiene (Aldazine)	1651 (KBr)	[164]
-C=N-C=N-	1,3-Diazabutadiene	1637, 1605 (KBr)	[165]
-C-C=N-C-	Aldimine	1665-1674	[159]
$-C^-=N^+=N-C-$	Nitrile imine	2000-2100	[149]
>C=C=N-R	Ketene imines	< 2050	[166]
$-C^-=N^+=C-$	Nitrile ylide	1926	[167]

Table 5.5: The characteristic C=N vibrations in potentially formed imines on N, H-plasma-treated surfaces

5.6 Arguments against -NH_2-selectivity of TFBA

Reactions of imines with aldehydes by an exchange of the carbonyl component, has been known since 1925 [30]. Later, in the following 90 years, several studies dealing with imine reactions with aromatic aldehydes were also carried out [31, 32].

On the other hand, formation of imines on plasma-treated polymer surfaces using nitrogen containing process gases has been reported many times [59, 141]. Imines are also formed through dehydrogenation processes in plasma polymerization using amine precursors, as suggested by Krishnamurthy et al. in 1989, based on FTIR spectroscopy studies [43]. The reactivity of these imines in evaluating chemical derivatization experiments should therefore be taken into account. Imines on the surface are expected to react with TFBA or PFB (R"=4-CF_3-C_6H_5 or C_6F_5) by liberating the aldehyde component (R-CH_2-CHO), as it is shown in Fig. 5.24. In this work a corresponding solution reaction was prepared by adding a primary alkylamine

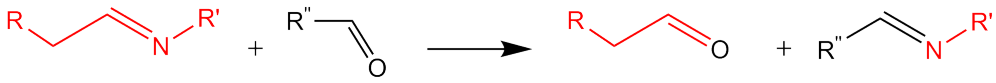

Figure 5.24: Reaction of imine with aldehyde by an exchange of the carbonyl component

(1-amino-2-ethylhexane) to an aliphatic aldehyde (hexanal) dissolved in an ether (diglyme) in the presence of molecular sieve as a drying agent. Upon adding TFBA solution, FTIR measurement shows that the carbonyl component of the imine is partly replaced by TFBA [1]. Consequently, the contribution of reactions of imines with TFBA (or other aromatic aldehydes in the derivatization process) should be considered.

Further arguments against -NH_2-selectivity of TFBA

In this work several reference experiments and model experiments were performed in order to specifically show the reaction of imine with TFBA. The results are shown and discussed in Chapter 6.

A considerable amount of TFBA can be attached to plasma-treated surfaces, although no trace of amino groups was detected [1]. It will be shown that PE surfaces which were plasma-treated in nitrogen containing gases exhibit unsaturated C=N imino groups. Electrophilic reactivity exhibited by such surfaces suggests that the treated surface contains nucleophilic groups. Nucleophilic derivatizations of plasma-treated PE films with various nucleophilic reagents and subsequent CD-FTIR and CD-XPS analysis of imino surface groups were performed. It was shown that a considerable amount of reagent was able to bond to the treated surface [3]. Details are discussed in Chapter 7.

Further arguments against the -NH_2-selectivity of TFBA from the following chapter are shortly summarized:

1. The review of available literature focussed the attention to reactivity of imine with aldehyde. Expected reactions of imines with common derivatization reagents and water vapor are demonstrated in section 6.1.

2. An imine model, N-isopropyl-propanaldimine, was shown to react with benzaldehyde uncatalyzed at room temperature [2]. Results are shown in section 6.2.

3. The gas-phase reaction of TFBA with imines on solid surfaces, (aminomethyl) polystyrene beads, was investigated by FTIR-ATR. Results are shown in section 6.3.

4. The gas-phase reaction of TFBA with thin unsaturated imines coated films onto the ATR crystal is discussed in section 6.4.

5. Exchange reaction between aliphatic imine and TFBA in the liquid-phase using FTIR spectroscopy was carried out. Results of investigations are shown in section 6.5.

5.7 Observational evidence against -NH_2, -NH, and -OH-selectivity of TFAA

In this work evidence from two different experiments listed below should clarify that TFAA is also able to undergo a reaction with functional groups other than amino and hydroxyl groups, e.g. imine groups:

1. A saturated imine was prepared from aliphatic aldehyde and primary amine. Its reaction with TFAA is studied in section 6.6.1.

2. Reaction of TFAA with imine on beads is shown in section 6.6.2.

6 Results of imine reactions with some assumed amine-selective derivatization reagents

6.1 Literature review [2]

A chemical reaction of an aromatic aldehyde with a plasma-nitrogenated polymer as a rule leads to a fixation of the aromatic moiety to the surface. The prevailing view today is that this is due to the presence of primary amine groups [168]. The general formular for an imine-forming reaction between a primary amine and a carbonyl compound (aldehyde or ketone) is shown in Fig. 6.1. In this equation R is used as a symbol for a polymer chain, R′ for an aryl radical such as 4-CF_3-C_6H_4- and R″ for a hydrogen atom or an organic residue. The product of this reaction is an aromatic aldimine being bound to the polymer surface. Imines are versatile building blocks or

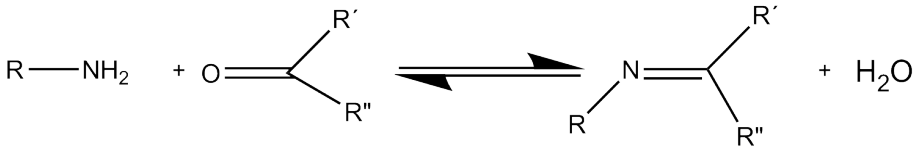

Figure 6.1: Imine-forming reaction between a primary amine and a carbonyl compound (aldehyde or ketone).

intermediates in organic chemistry since they can react like nucleophiles as well as electrophiles in different types of cycloaddition reactions. The chemistry of imine can be read in refs. [31, 32]. The reaction of imines with amines [169], with aromatic aldehydes [30], and with other imines are known since 1920 [170]. Further examples of carbonyl exchange are shown in the book by Patai (see pp. 82 and 265) [32] and the review by Layer [31].

The expected reactions of imines with common derivatization reagents and with water vapor are summarized in Fig. 6.2. The central structure is an enolizable secondary aldimine, i.e., an imine

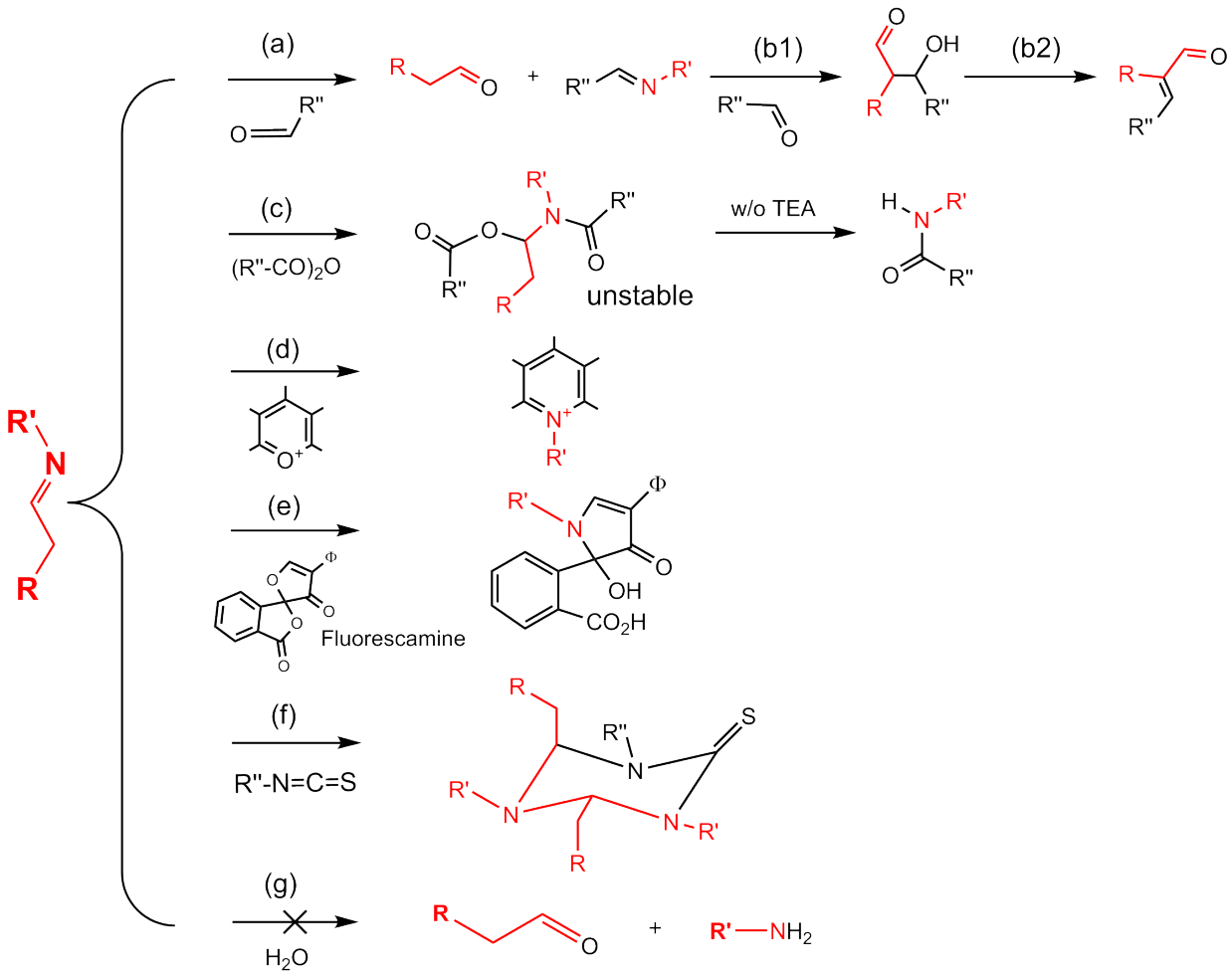

Figure 6.2: Collection of expected reactions of aldimine with common derivatization reagents and with water, a) C. K. Ingold, J. Chem. Soc. 1925, 127, 1141. b) R. Mahrwald, Aldol Reactions, Springer Netherlands, The Netherlands 2009. c) H. Breederveld, Recl. Trav. Chim. Pays-Bas 1960, 79, 401. d) D. E. Tosunyan, S. V. Verin, E. V. Kuznetsov, Chem. Heterocycl. Comp. 1994, 30, 1015. e) by analogy, no example found in the literature f) R. Huisgen, M. Morikawa, D. S. Breslow, R. Grashey, Chem. Ber. 1967, 100, 1602. g) S. Patai, "The chemistry of the carbon-nitrogen double bond", Interscience Publishers, London, UK 1960 [2].

derived from an aldehyde (R-CH_2-CHO) carrying at least one hydrogen atom in α-position to the C=N carbon atom and an organic substituent (R′) at the N atom. This imine structure with a skeleton -C-N-C- is chosen here because it formally represents the result of nitrogen insertion into the polymer chain, for example into the backbone of a polyolefine. In the following the expected reactions (a) to (f) with some important derivatization reagents as well as the reaction (g) with water vapor will be briefly commented on:

(a) The carbonyl exchange between aldehydes and imines has frequently been reported in the available literature, see above. Therefore, surface imines are expected to react with TFBA or PFB ($R^{"}$ = 4-CF_3-C_6H_5 or -C_6H_5) by liberating the aldehyde component (R-CH_2-CHO). The corresponding solution reaction can be easily demonstrated by adding a primary alkylamine to an aliphatic aldehyde dissolved in an ether in the presence of several molecular sieves which act as a drying agent: IR spectroscopy shows the appearance of the characteristic band due to C=N stretching vibration in the N-alkyl-aldimine. Upon addition of TFBA to the resulting imine solution the C=O vibration of the aliphatic aldehyde reappears together with the C=N vibration of the 4-trifluoromethyl-benzaldimine (1648 cm^{-1}) as the carbonyl component of the imine is partly replaced by TFBA [1]. The frequently observed increase of the oxygen content during derivatization with TFBA and PFB is explainable via reaction (a) [8, 36].

(b) The derivatization chemistry of imine-bearing surfaces is further complicated by aldol additions (b1) and aldol condensations (b2) between TFBA or PFB and the liberated aldehyde. Aldol reactions generally require catalysis by acids or bases, but the N-plasma-treated polymer surface itself is presumably a strongly basic environment owing to the presence of amines and imines.

(c) Breederveld showed that reaction (c) between N-alkylaldimines and acetanhydride (R=CH_3, C_2H_5, C_3H_7; $R^{'}$ = C_3H_7; $R^{"}$ = CH_3) proceeds below room temperature forming a labile intermediate compound which may react further to form two different acetamides, depending on the presence or absence of triethylamine (TEA) [171].

(d) This reaction was demonstrated by Tosunyan et al. [172].

(e) This is one example of reactions in which a nonfluorescent substance forms a fluorescent product upon reaction with the target moiety: primary amine groups [173].

(f) This reaction is expected, based on a paper of Huisgen et al., demonstrating that a 1:2 cycloaddition takes place between phenyl isothiocyanate and N-methyl-benzaldimine- without solvent at room temperature [174].

(g) Fast hydrolysis in humid air is not necessarily expected for N-alkyl-aldimines on the polymer surface after N-plasma treatment, because even in the presence of liquid water secondary aldimines are usually stable against hydrolysis, see the book by Patai, p. 64: [32] "*Aldehydes . . . can usually be condensed with amines without removing the water*". Therefore, it seems unlikely- from a practical point of view- that a freshly plasma-treated imine-bearing polymer surface is chemically equivalent to the completely hydrolyzed surface which exposes the formerly capped amine groups.

6.2 Aldol reaction of TFBA with imine in liquid phase

The course of the uncatalyzed reaction between TFBA and N-isopropyl-propanaldimine (1:1) without solvent at room temperature was studied in a model experiment in order to prove the possibility of aldol reactions under such conditions [175]. Work-up of the reaction mixture after 24 h yields two diastereomeric addition products between TFBA and propanal, the corresponding condensation product and the self-condensation product of propanol. The percentages are given in Fig. 6.3. This reaction at room temperature without using a catalyzer leads to the making of four different products. We are very grateful to Prof. Mahrwald, Humbold-Universität zu Berlin, for investigating the reaction and providing us with the results.

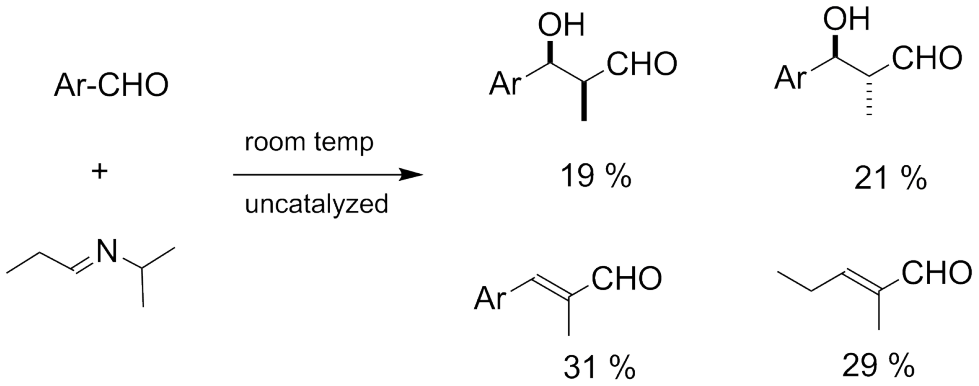

Figure 6.3: Aldol products obtained from TFBA (Ar=4-CF_3-C_6H_4-) and N-isopropyl-propanaldimine in an uncatalyzed reaction at room temperature.

6.3 Reaction of TFBA vapors with imines on solid surfaces

Preparation of imine from PS-AM-NH_2 beads and an aldehyde (isobutyraldehyde, IB) on beads has previously been explained in section 4.2.2. FTIR-ATR spectrum of the prepared imine on beads subtracted from the spectrum of aminomethylated polystyrene beads shows an absorption at 1668 cm^{-1} due to the C=N stretching mode, see Fig. 6.4 L, (middle). The beads were then exposed to the vapor of TFBA for 1 h. A spectrum of IB-reacted beads exposed to TFBA minus the spectrum of IB-reacted beads is shown in Fig. 6.4 L, (bottom). This spectrum exhibits a peak at 1710 cm^{-1} attributed to ν(C=O) of physisorbed TFBA. The weak negative absorption around 1668 cm^{-1} can be ascribed to vanished isobutyraldimine groups, while a weak positive absorption at 1647 cm^{-1} is due to the newly formed 4-trifluoromethylbenzaldimine. The band at 1324 cm^{-1} is related to ν(C-CF_3) stretching vibration in the newly formed imine compound

shown in Fig 6.4 R. Thus, the reaction of imine on solid surface with TFBA vapor was successfully demonstrated.

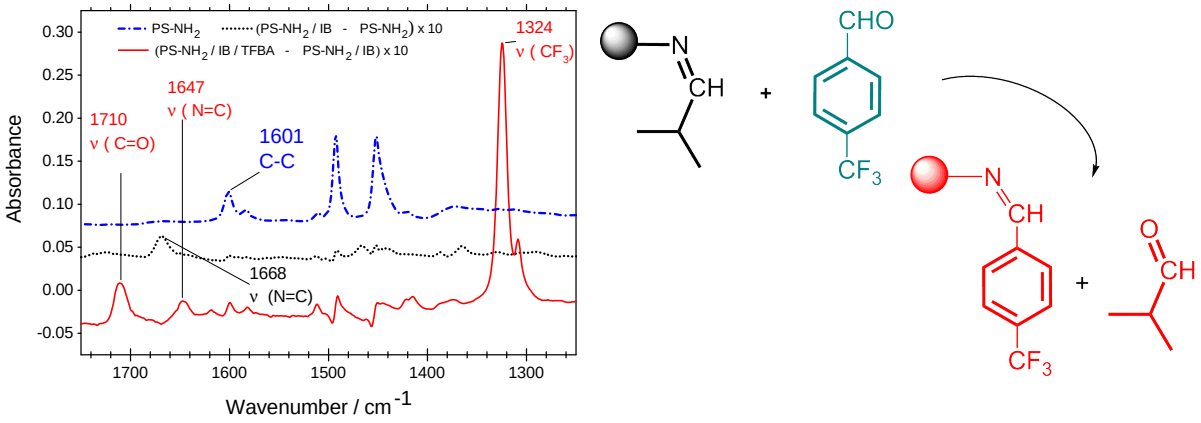

Figure 6.4: Left: FTIR-ATR spectra (diamond, 51°) of aminomethylated polystyrene beads (top, offset 0.1), beads after exposure to isobutyraldehyde (IB) subtracted from the spectrum of beads (middle, offset 0.05) and the IB-reacted beads after exposure to TFBA vapors minus spectrum of IB-exposed beads (bottom). Right: reaction between TFBA vapor and surface imines (from (PS-AM beads)

6.4 Reaction of TFBA vapors with a film of unsaturated imine

A model imine, from 2-ethyl-1-hexylamine and trans-2-hexen-1-al by mixing hexadecane solutions of equimolar amounts of these chemicals, adding molecular sieve and allowing the mixture to stand for 2 h at room temperature was prepared. The obtained imine solution was spin-coated onto a 1 cm × 8 cm rectangular surface area of a ZnS ATR crystal. The parameters for the spin-coating process were an acceleration speed of 1200 rpm, a spinning speed 2000 rpm, and a total spinning time of 60 seconds. The coated films were placed in a vacuum at room temperature for at least one night. The reaction of unsaturated ultra-thin imine film with TFBA was achieved by exposing the film to TFBA vapors for one, two, and three hours at 25 °C in a closed vessel. After reaction the film was dried some hours in a vacuum dessicator. The infrared measurements of a film of unsaturated imine before and after its exposing to the TFBA vapor are depicted in Fig. 6.5 L. A strong band assigned to the C=N stretching mode of imine is found at 1668 cm^{-1} regarding the equation shown in 6.5 R. (Surprisingly it is in the region of saturated imines, possibly due to a nonplanar structure of the C=C-C=N moiety.) It is seen that this vibration

vanishes upon exposing the film to TFBA vapor, and a new absorption at 1648 cm^{-1} is formed which may be attributed to the resulting aromatic imine. The band at 1324 cm^{-1} is related to C-CF_3 stretching vibration in the newly formed imine component shown in Fig. 6.5 R.

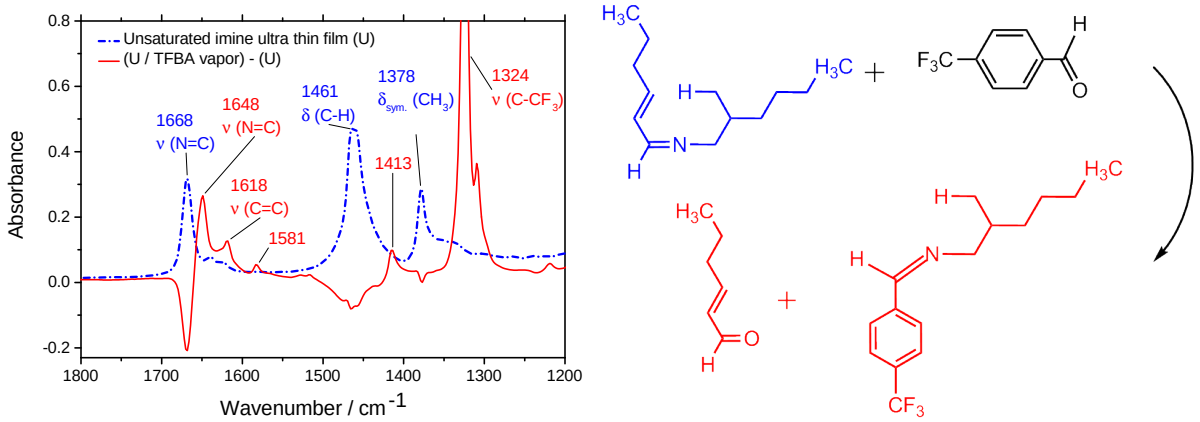

Figure 6.5: Left: FTIR-ATR spectra of unsaturated imine ultra-thin film: U(dash/blue). The spectrum of unsaturated imine film after contact with TFBA vapor minus the spectrum of film (solid/red) (ZnS, 45°, s-polarization), 1378 cm^{-1} is due to the umbrella mode of methyl groups which are attached to carbon atoms. (Absorbances are offset arbitrary). Right: reaction of unsaturated imine with TFBA

6.5 Exchange reaction of aliphatic imine and TFBA in the liquid phase

Another example of imine synthesis *in situ* and its reaction with TFBA was tested for a primary amine, e.g. 2-ethyl-1-hexylamine, with an N-H bond absorption at 1618 cm^{-1}. As an aldehyde component, hexanal with C=O stretching vibration at 1724 cm^{-1} was applied. A solution from 2-ethyl-1-hexylamine and hexanal in hexadecane was prepared; the product spectrum (R) is shown in Fig. 6.6. Infrared measurement of the solution (R) shows that a new absorption due to the imine formation at 1670 cm^{-1} occurs. After exposing the solution R to TFBA vapor a new spectrum is measured and subtracted from the product spectrum R, see Fig. 6.6, solid line. It is seen from this measurement that the imine vibration band vanishes after the reaction with TFBA, while a new absorption due to the aromatic imine forms at 1647 cm^{-1}. A broad absorption at 1740-1700 cm^{-1} corresponds to the C=O of TFBA with peak position at 1712 cm^{-1}. All the similarities of these findings and TFBA reaction with beads in the gas phase confirm the reaction

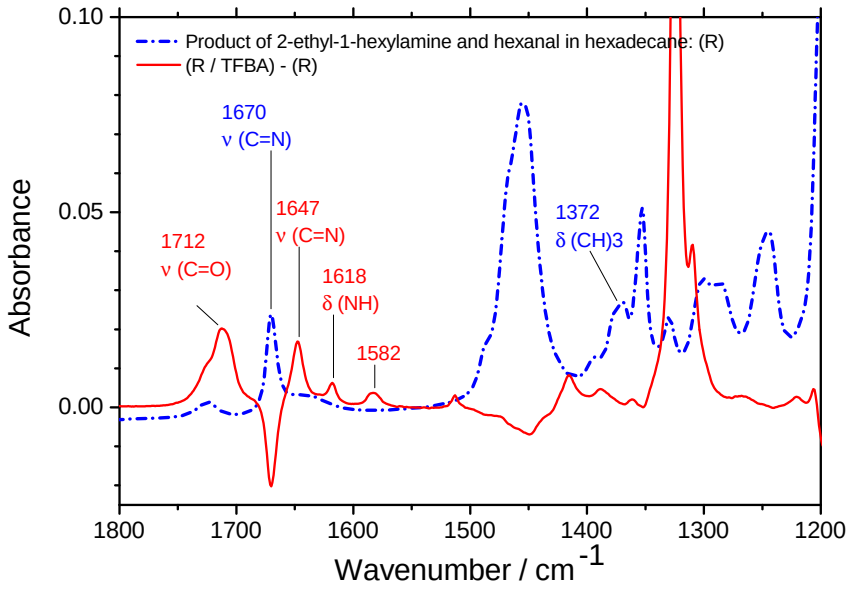

Figure 6.6: FTIR-ATR measurement of the solution from 2-ethyl-1-hexylamine and hexanal in hexadecane (R) (blue/dash) and the spectrum of product reaction R after exposure to TFBA vapor subtracted from the spectrum R (red/solid), diamond single bounce ATR 51°, 128 number of scans, res. 4 cm^{-1}

of the TFBA and aliphatic imines. The peak position at 1582 cm^{-1} is attributed to a transient species which was also observed in the IR measurement of treated PE surface after contact to TFBA vapor at around 1585 cm^{-1} shown earlier in Fig. 5.19.

6.6 Non-selectivity of TFAA for -OH, -NH, and -NH_2 groups

As already mentioned above (see section 3.4), CD-XPS using TFAA has become known as the standard method to tag the primary amine, secondary amine, and hydroxyl groups [8, 37, 120, 176, 177]. It is noteworthy that the hydroxyl and amino groups can not be easily distinguished by using TFAA derivatization technique if both are present in the medium [121]. In the absence of nitrogen-functional groups, TFAA is assumed to label hydroxyl groups selectively [17, 178], see Fig. 6.7. Although the presence of other nitrogen-bearing functionalities such as imines >C=N- on plasma-nitrogenated polymers and in plasma-polymerized films has been inferred several times, their reaction abilities during TFAA chemical derivatization have generally been ignored. Basically, carbon-nitrogen double bonds are also able to undergo reaction with anhydride, see Fig. 6.8. For instance, the reaction of N-alkylaldimines with acetic anhydride was reported in 1960 [171]. However, they are not the only possible reactions with trifluoroacetic anhydride. For

example, it is pointed out by Chilkoti and Ratner that TFAA is similarly as reactive towards epoxide groups as it is to hydroxyl groups [122]. It must be considered that the formation of epoxide groups on plasma-treated polymers has been frequently pointed out (seen, reported as occurring). Therefore its potential reaction with TFAA must be also taken into account [178].

In the following, two model experiments present the reaction of TFAA with (i) solution of a model aldimine formed *in situ* in a solvent and (ii) with aldimine moieties formed on aminomethylated polystyrene beads by reaction with aldehyde vapor.

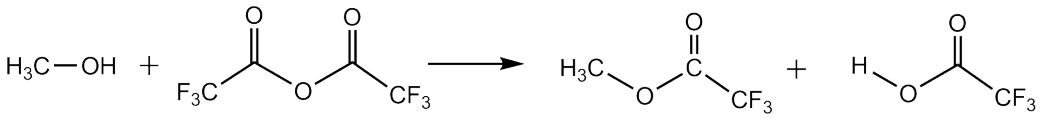

Figure 6.7: Derivatization reaction for hydroxyl group (-OH); analysis by XPS hydroxyl group detected by TFAA

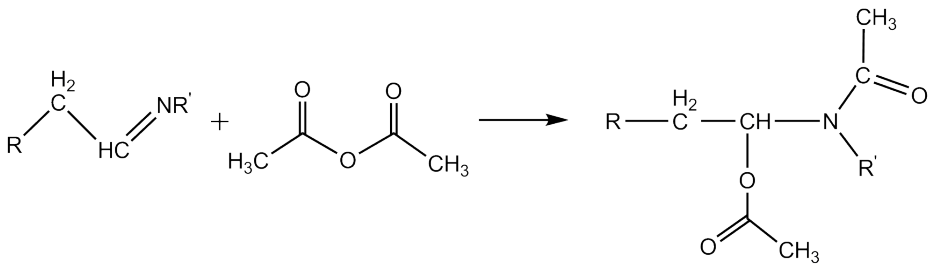

Figure 6.8: N-alkylaldimines reaction with acetic anhydride with the formation of the corresponding N-alkyl-N(1-acetoxyalkyl)-acetamides

6.6.1 Reaction of TFAA with imine in liquid phase

Saturated imine: A 0.06 M solution of a saturated imine was prepared from 2-ethyl-1-hexylamine and hexanal in hexadecane, the product spectrum is shown in Fig. 6.9 L (red/solid). The absorption at 1672 cm^{-1} is assigned to the C=N stretching mode. The spectrum of TFAA in hexadecane shows two absorptions at 1876 and 1808 cm^{-1} due to asymmetric and symmetric stretching vibrations of C=O groups in TFAA, see Fig. 6.9 L (blue/short dot). A strong absorption at the region of 1060-1020 cm^{-1} (peak position at 1041 cm^{-1}) in the infrared spectrum of

TFAA in hexadecane is related to C-O-C stretching vibration in acid anhydrides. This peak in the TFAA itself is broader and found at 1108-993 cm^{-1} in our measurements. This region of IR measurements is not shown here. Upon mixing identical volumes of 0.06 M solutions of imine and TFAA two new bands at 1791 and 1722 cm^{-1} are seen, attributable to an ester CF_3-CO-OR and a tertiary amide CF_3-CO-NR′R″, respectively. Spectra in the NIST Chemistry WebBook show ν(C=O) at 1722 cm^{-1} for gaseous N,N-dimethyltrifluoroacetamide and ν(C=O) near 1800 cm^{-1} for alkyltrifluoroacetates (alkyl esters). With this assignment the spectra are in accordance with the reaction scheme shown in Fig. 6.9 R.

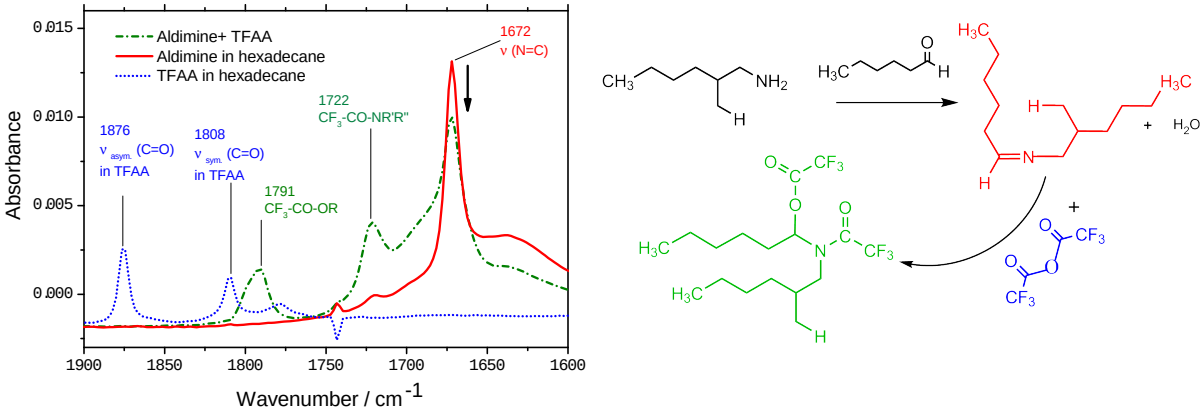

Figure 6.9: Left: FTIR-ATR measurement of aldimine before (red/solid) and after reaction with TFAA (green/dash). Imine was prepared from 2-ethyl-1-hexylamine and hexanal in hexadecane. An IR spectrum of TFAA in hexadecane is also shown (blue/dot). Right: 2-ethyl-1-hexylamine reaction with hexanal to form imine, subsequent imine reaction with TFAA molecule.

6.6.2 Reaction of TFAA with imine on beads

Aminobutylated polystyrene PS-C_4-NH_2 beads were exposed to IB and subsequently for 3 h to TFAA vapors. Spectrum of imine exposed to the vapor of TFAA is shown in Fig. 6.10 L. It is found that the absorption band at 1670 cm^{-1} (C=N) is removed while a broad absorption at around 1820-1720 cm^{-1} is formed. In addition, absorption at 1320 cm^{-1} related to C-CF_3 of TFAA is shifted to a broad and weak absorption area at 1290-1360 cm^{-1}. It must be noted that any unconverted amino groups will also undergo a reaction with TFAA (Fig. 6.10 R) but the vanishing of the imine vibration after exposure to the TFAA suggests that the imino group will be converted here, too - probably in the same way as in the solution.

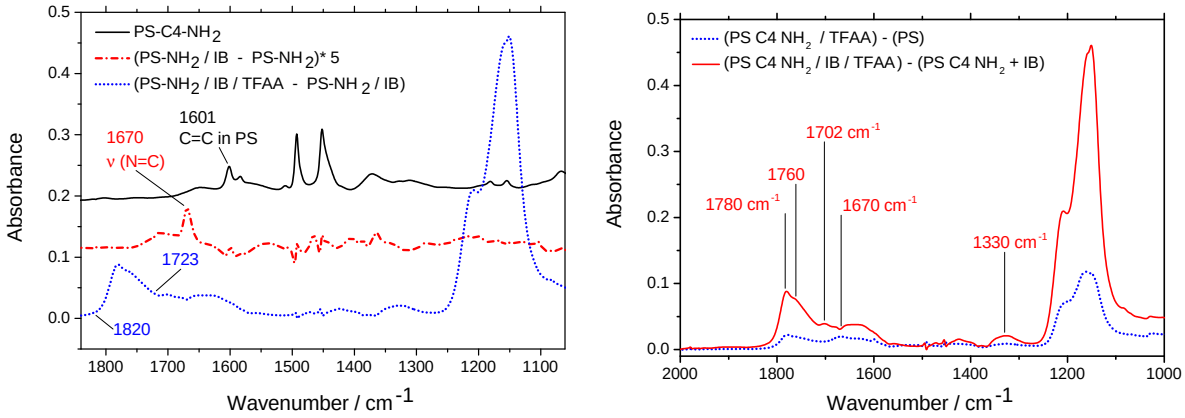

Figure 6.10: Left: FTIR-ATR spectra (diamond, 51°) of aminomethylated polystyrene beads (top, offset 0.2), beads after exposure to isobutyraldehyde (IB) subtracted from spectrum of beads (middle, offset 0.1) and IB-reacted beads after exposure to TFAA vapors minus spectrum of IB-exposed beads (bottom). Right: FTIR-ATR spectra (diamond, 51°) of aminomethylated polystyrene beads after exposure to TFAA subtracted from spectrum of beads compared with IB-exposed beads after contact with TFAA vapor.

From FTIR-ATR results of TFAA reaction with imine either formed in liquid phase or formed in solid phase (on beads), we could show that TFAA is also able to react with imines, in contrast to what had been assumed in a large number of publications.

From the several experiments outlined, we could show that imino groups are able to react with TFBA and TFAA, respectively. We conclude that the derivatization technique using electrophilic reagents e.g. TFBA, TFAA and PFB cannot be used as a standard analytical method as the reagents do not possess any certain functional group selectivity and cannot be used to quantify the density of functional groups that can undergo reaction with the derivatization reagents.

7 Evidence of C=N groups on polymer surfaces treated in N, H-DBDs

Electrophilic derivatization reagents such as carboxylic acid anhydrides or aldehydes have normally been applied for chemical analyzes of polymer surfaces plasma-treated in nitrogen or nitrogen-containing gases. Because, as mentioned already, the chemical reactivity of such surfaces has frequently been discussed in terms of amino groups formed by the exposure of the surface to reactive gas species formed in the plasma. However, regarding our findings in this work, we hypothesize that imino groups are present on the treated surfaces and they are also able to undergo reaction with electrophile reagents. Since imino groups have dual electrophile and nucleophile properties they can also react with nucleophilic reagents in contrast to amino groups. In this chapter, we will present results of derivatization experiments, using three different nucleophilic reagents, with subsequent analyzes by FTIR-ATR spectroscopy and/or XPS. Polyethylene surfaces were plasma-treated in the afterglow regions of dielectric barrier discharges in mixtures of nitrogen with 4 % hydrogen. 2-mercaptoethanol (ME) or 4-(trifluoromethyl)phenylhydrazine (TFMPH) or 4-(trifluoromethyl)benzylamine (TFMBA) were applied as nucleophilic reagents through the vapor phase. In addition, the nitrogen K-edge NEXAFS measurements of the plasma-treated LDPE thin films and imine model compounds were obtained.

7.1 Nucleophilic CD-XPS and FTIR-ATR of plasma-treated LDPE surfaces

Sample preparation, plasma treatment condition and derivatization procedure were explained in section 4.2.6.

7.1.1 Reaction of plasma-treated surfaces to 4-(trifluoromethyl)phenylhydrazine (TFMPH) vapors [3]

To obtain an estimate of the integrated absorption band intensity B of the ν(C-CF_3) vibration in the derivatization product of TFMPH, one reference solution needs to be provided. Therefore, a solution of 4-(trifluoromethyl)phenylhydrazone of hexanal was prepared *in situ* by reacting 1 equivalent of TFMPH with 1.1 equivalents of hexanal in hexadecane solution. Next, the band area of the corresponding vibrational band at 1323 cm^{-1} was found, utilizing the diamond ATR crystal. A spectrum of the resulting solution is shown below in Fig. 7.1 (blue/dot). The quantification procedure for B was explained in 5.3.1. The result is B = 467 km/mol, in reasonable agreement with the corresponding value for 4-(trifluoromethyl)benzaldimines (370 km/mol), see section 5.4.1). The accuracy of the resulting density of functional groups is probably no better than about ±10 %, due to the use of unpurified chemicals, the spread of the incident angle of ±7 in the ATR element, and the implicit assumption of the same "B" values for oscillators in the model compound and on the foil.

A difference spectrum obtained by subtracting the spectrum of an untreated foil from the spectrum obtained after plasma treatment and after subsequent derivatization in the hydrazine vapor are depicted in Fig. 7.1 (red/solid). The peaks at 1616 cm^{-1} in both spectra are ascribed to hydrazone vibration ν(C=N). In fact, this vibration can be predicted to occur at region of 1645 and 1610 cm^{-1} regarding my ref. being in the Socrates' book [6]. Strong absorption related to ν(C-CF_3) occurs at 1324 cm^{-1} and 1323 cm^{-1} in the foil and solution, respectively. Additionally, three absorption at 1162, 1116 and 1064 cm^{-1} are related to three stretching vibrations of carbon-fluorine at ν(C-CF_3) group. It should be mentioned here that the band area ratio of the presumed ν(C=N) and ν(C-CF_3) vibrations are the same, within the limits of accuracy of the measurements, in both spectra (0.31 in the solution and 0.32 in the foil spectrum). This is an indication that the 4-(trifluoromethyl)phenylhydrazo moiety (4-CF_3-C_6H_4-NH-N:) bonds in general as a hydrazone (4-CF_3-C_6H_4-NH-N=C<) and not as a hydrazide or hydrazine (4-CF_3-C_6H_4-NH-NH-), see below. From the band area of this vibration, the area density of 4-CF_3-C_6H_4- attached to the treated surface as hydrazones during derivatization can be found, (using the second term of equation 3.10). The B = 467 km/mol was already found from the solution measurement for vibration at 1323 cm^{-1}, see above. Effective thickness can be calculated with n_1 = 2.4 (diamond) and $n_2 = n_3$ = 1.5 for the polymer. The band area $\int_b$ A.dν of ν(C-CF_3) was found from integrated area over a range of ±25 cm^{-1} for 1324 cm^{-1}. Therefore, the absorber density ρ was found to be 5.6 nm^{-2} which is an indication for bonding considerable amount of hydrazine to the plasma-treated PE surfaces. This density is comparable to what we found in former studies with electrophilic (TFBA) derivatization of similarly treated LDPE foils [1].

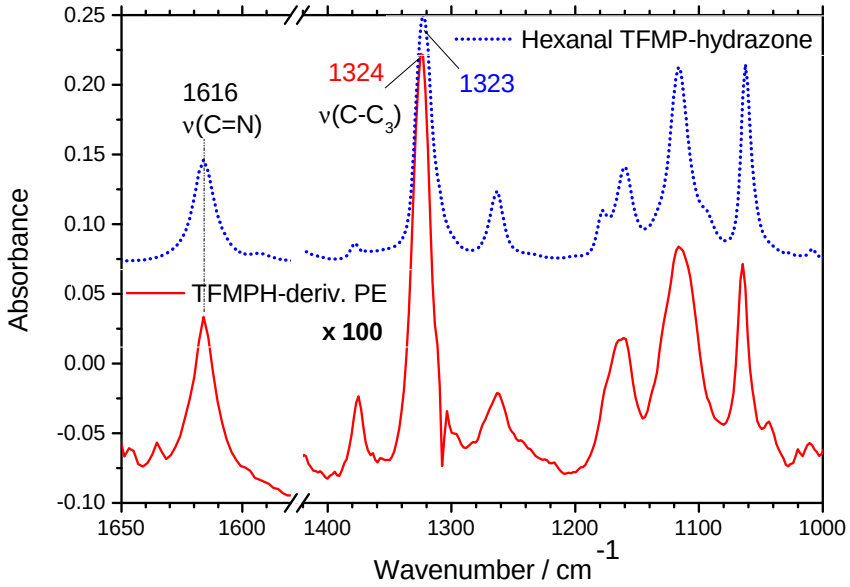

Figure 7.1: FTIR-ATR spectra of hexanal, 4-(trifluoromethyl)phenylhydrazone (solution in hexadecane, blue/dot), and of plasma-treated and then gas-phase TFMPH-derivatized LDPE surface after subtraction of a LDPE spectrum (multiplied by 100, red/solid). Important peak locations (in cm^{-1}) are 1616 in both spectra, 1324 (foil) 1323 (hydrazone) (Absorbances are offset arbitrarily) [3]

In addition, B has been obtained for 1616 cm^{-1} related to C=N stretching vibration in hydrazone for 179 km/mol which is relatively large and should normally be of week to medium intensity [6]. Based on this vibration, a density of 4.6 nm^{-2} has been found.

In view of the appreciable content of oxygen, which is present on the surface after plasma treatment see Table 7.1, it can be speculated that some surface carbonyl groups of ketone or aldehyde moieties, formed either during the plasma treatment or thereafter by oxidation or hydrolysis, might be responsible, see Fig. 7.2 ($\Phi \equiv$ 4-CF_3-C_6H_4). However, due to the formation of volatile water, this reaction should decrease the oxygen content of the derivatized foil and it should increase the nitrogen atom concentration by two thirds of the fluorine percentage present after derivatization. An inspection of the corresponding XPS results in Table 7.1 shows that the opposite is the case: There is a further increase of the oxygen concentration but the nitrogen percentage is nearly unchanged although an appreciable amount of F is present. This result is quite surprising, because with about 10.8 at.% fluorine in hydrazone groups 7.2 % nitrogen are associated unless one would question the integrity of the =N-NH-C_6H_4-CF_3 moiety under the conditions of the derivatization reaction. From an organic-chemical point of view, however, this is improbable because cleavage of the N-N bond, for example, requires more drastic conditions. Hence, a further hypothetical reaction is shown in Fig. 7.3 ($\Phi \equiv$ 4-CF_3-C_6H_4).

	C(1s)	N(1s)	O(1s)	S(2p)	F(1s)	traces
LDPE	99.33		0.67			
LDPE / plasma	88.07	7.45	4.48			
LDPE / plasma / TFMPH	72.6	7.85	8.79		10.76	S, Si
LDPE / TFMPH	98.43		1.07		0.51	Si
LDPE / plasma / ME	83.63	5.07	8.66	2.64		Si
LDPE / ME	99.39		0.61			Si

Table 7.1: XPS analyzes of untreated PE foils, plasma-treated foils, plasma-treated and derivatized foils as well as reference samples. Reference samples are untreated PE foils which were derivatized in the same procedure

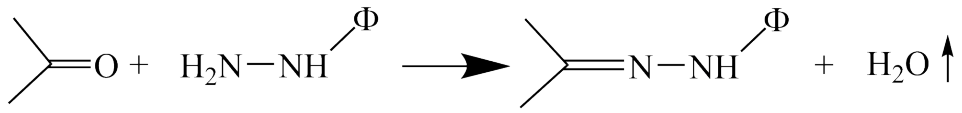

Figure 7.2: Reaction of surface carbonyl groups of ketone or aldehyde moieties with hydrazine

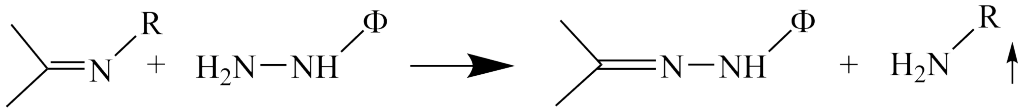

Figure 7.3: Reaction of imine with hydrazine

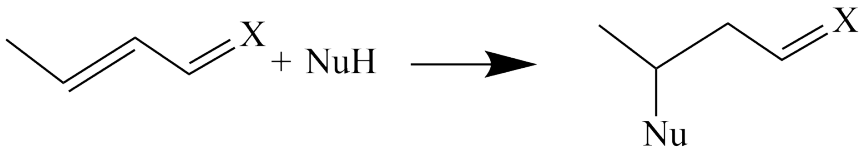

Figure 7.4: Reaction of unsaturated imine or carbonyl with hydrazine, (Nu=NH-NH-R″)

In relation to Fig. 7.3, this reaction could account for a derivatization result with a ratio of the percentages of F and N of approximately 3/2 in the XPS analysis result. In addition no oxygen would be involved- the oxygen percentage would left unchanged. The derivatization after Fig. 7.3 with R=H corresponds to the addition of a "molecule" with 1 N, 7 C, and 3 F atom(s) (H not counted) per functional group >C=N-H. In order to achieve an F atom percentage of 10.8 on the derivatized sample, starting with a surface containing 88 C, 7.5 N and 4.5 O, one would need 6.0 of these molecules and arrive at a surface with $(6.0 + 7.5)/(100 + 6 \times 11) = 8.1$ % N- an almost unchanged N percentage in close agreement with the experimental result obtained. A complicated reaction shown in Fig. 7.4 in the presence of unsaturated imine or carbonyl group is also imaginable.

Imine (X=N-R) or hydrazone (X=N-NH-R′) or carbonyl compound (X=O) are able to react with

a nucleophilic compound such as a hydrazine (Nu=NH-NH-R″) in the sense of a conjugate nucleophilic addition or 1,4-addition. The products including hydrazine and the carbonyl (or imine) component in the ratio of 2:1 or 3:2 may thus be formed [179]. From our IR measurements of derivatized PE foils the -CF_3-C_4H_4- groups detected on the surface are actually belong to hydrazones. As otherwise the ratio of the band area of ν(C=N) and ν(C-CF_3) vibrations measured on the foil should be significantly smaller than in the model hydrazone. The presence of a relatively high oxygen content after the plasma treatment is not explainable at present. Although very pure gases and an additional gas cleaning system were applied, the presence of some amount of oxygen can be justified. However, there is not any indication of ketone, aldehyde, carboxylic acid or ester groups in our *in situ* FTIR measurements because the expected C=O stretching band is absent. Additionally, significant absorptions in the range of C-O stretching bands related to formation of alcohol or ether moieties, is also missing. Nevertheless, it cannot exclude that some primary or secondary amide groups are formed during plasma treatment. This conclusion is derived from exposing the plasma-treated surface to deuterium oxide, in which absorption band at 1690 cm^{-1} vanished. This band can be attributed to amide I in -CO-NH- groups. Other explanations of these bands are also imaginable, such as primary imines or oximes. A certain amount of oxygen might be generated from reaction of the freshly plasma-treated sample with the humid air from both oxidation and hydrolysis. In this case we do not expect to have a big change because the experiment setup provides an oxygen free environment.

Additionally, treated thin film remains under the inert nitrogen flowing gas immediately after the plasma treatment for some minutes in order to allow residual radical centres to decay as far as possible before exposing the sample to humid air. IR spectra taken *in situ* during exposure of such surfaces to laboratory air normally do not show relative intensity changes of bands in the range between 1500 and 1700 cm^{-1} beyond an average 15 % during an exposure of 60 min. Certainly, due to the reaction shown in Fig. 7.3 no additional oxygen should be seen after TFMPH derivatization. We can speculate that some oxygen-containing impurities of the foil may migrate to the surface during derivatization and the following vacuum treatment. The oxygen percentage in the reference PE foil (neat) which was exposed to TFMPH vapor did not show a similar increase in the oxygen amount. The difference can be attributed to the reactive surface after plasma treatment. The higher reactivity of the derivatized surfaces towards CO_2 or water from the laboratory atmosphere could also be an imaginable reason. Therefore, *in situ* FTIR-ATIR investigations of derivatized thin film (such as that done for TFBA) will provide more information [1].

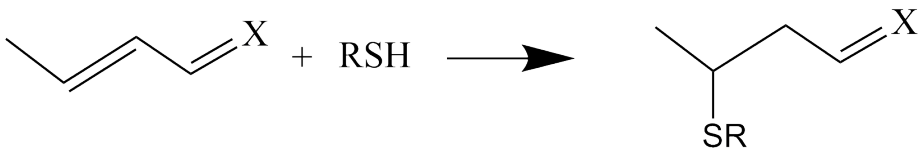

Figure 7.5: Unsaturated imines and thiol reaction

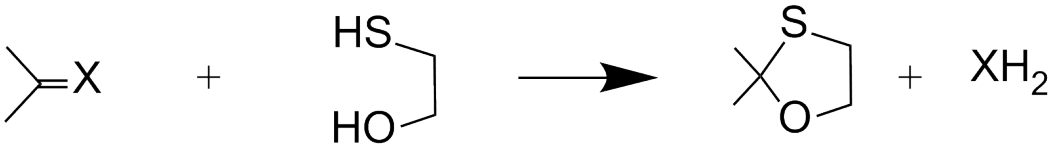

Figure 7.6: Formation of a five-membered heterocyclic compound from thiol and imine

7.1.2 Reaction of plasma-treated surfaces to mercaptoethanol (ME) vapors [3]

Treated foil was derivatized using 2-mercaptoethanol in a vapor phase. XPS results in Table 7.1 show the changes in the chemical structure after derivatization. It is seen that nitrogen percentage clearly decreased. The amount of nitrogen lost is about one third of the originally present nitrogen. The reason for nitrogen content reducing is due to the some nucleophilic replacement of nitrogen by the mercaptan. In addition, nitrogen is reduced by volatilization.

From the chemistry of organic material it is known that aliphatic imine may not form a stable addition product with thiols [31], but unsaturated imines can be bonded to thiol following the scheme of Fig. 7.5 [180]. In addition unsaturated imines can also react to form a a five-membered heterocyclic compound (1,3-oxathiolane), equation shown in Fig. 7.6, because of -OH in 2-mercaptoethanol.

In order to identify more clearly the chemical groups formed on the derivatized plasma-treated surface the samples were analyzed using FTIR. At present it is not clear to what extent the broad band peaking at 1076 cm^{-1} in the IR spectrum obtained from an ME-derivatized plasma-treated foil (see Fig. 7.7) is due to the characteristic, strong CCO stretching vibration in primary alcohols, normally observed at 1090 to 1000 cm^{-1} because oxidation products of sulfides characterized by the -SO- structure usually have strong bands in the same region [6]. In Fig. 7.7 IR spectrum of ME is seen which shows a characteristic absorption of ν(SH) at 2555 cm^{-1} missing in the ME-derivatized plasma-treated foil. It is therefore clear that, *in situ* experimental set-up for ME derivaization will provide more understanding of chemical changes under typical derivatization conditions.

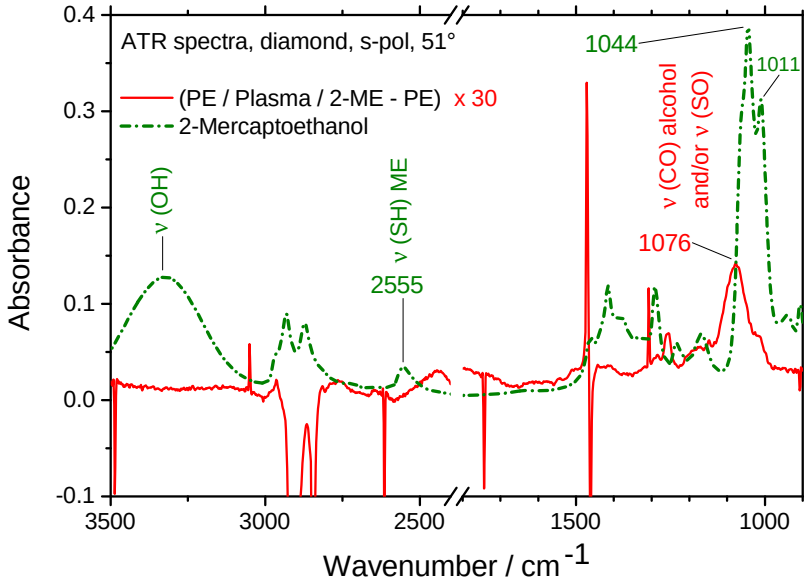

Figure 7.7: FTIR-ATR spectra of 2-mercaptoethanol (pure liquid) (green/dash), plasma-treated and then gas-phase ME derivatized LDPE surface after subtraction of an LDPE spectrum, then multiplied by 30 (red/solid). Peaks positions (cm^{-1}) are 1076 for the foil sample, probably ν(C-O) and/or ν(S-O), 1044 and 1011 for ME [3].

7.1.3 Reaction of plasma-treated surfaces to 4-(trifluoromethyl)benzylamine (TFMBA) vapors

To confirm the electrophilic reactivity of N, H-plasma-treated polymer surfaces, LDPE foils are derivatized using, instead of mercaptane or hydrazine employed previously, another nucleophilic reagent, 4-(trifluoromethyl)benzylamine (TFMBA), after treatment in either DBD afterglow (in this project) or direct DBD plasma [76]. LDPE thin films treated in flowing post-discharges of N_2 or mixtures of N_2 and H_2 were subsequently derivatized *ex situ*, i.e., after exposure to air, for 3 h in the vapor of TFMBA. Results are shown in Fig. 7.8 L. The broad region at 1780-1600 cm^{-1} in the film treated by pure nitrogen can be attributed to absorption by carbonyl groups and groups containing C=N. Although very pure gases were applied (nitrogen gas purity 6.0 and usage of purification systems), the presence of a very small quantity of oxygen is sufficient to form substantial amounts of carbonyl groups. Adding 0.5 % of hydrogen into the nitrogen gas leads to disappearance of the carbonyl group while a broad band at 1720-1500 cm^{-1} is seen and a new absorption at 1580-1520 cm^{-1} emerged.

Signature of TFMBA bonding is an absorption at 1326 cm^{-1} due to ν(C-CF_3) showing that the amine group of TFMBA has chemically reacted with electrophilic moieties on the plasma-treated

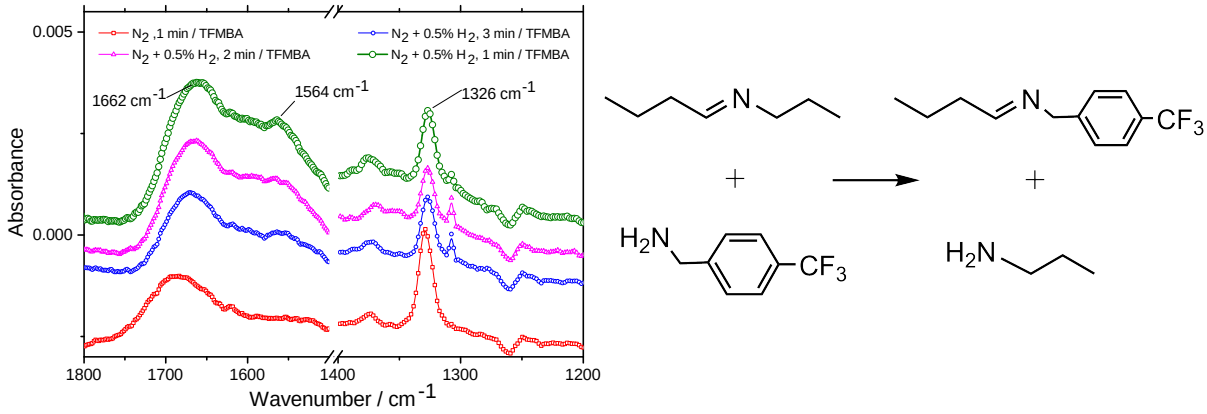

Figure 7.8: Left: FTIR-ATR spectra of LDPE treated in post-discharge of pure nitrogen or N_2 + 0.5 % H_2 mixtures (for 1, 2, and 3 min) and subsequently gas-phase-derivatized TFMBA. Spectrum of untreated LDPE foil was subtracted. Right: Proposed reaction of imine with TFMBA

surface. The absorption at 1680-1630 cm^{-1} may be due to resulting ν(C=N). C=N stretching vibrations in R-CH=N-Ar which are expected to appear with medium to strong intensity at 1660-1630 cm^{-1} [6]. A probable reaction between the treated surface and TFMBA is shown in Fig. 7.8 R. LDPE foils treated in direct plasma and derivatized with TFMBA showed an absorption at 1324 cm^{-1}, (The spectra are not shown here) [76, 181]. In addition, a negative vibration at 1581 cm^{-1} is observed due to the functional group reacting with the amine. The presence of H_2 in the N_2 plasma on electrophilic properties of the surface was also studied. A maximum of electrophilic reactivity was observed for 0.5 % H_2 content. Evidently, the N-treated surfaces show nucleophilic as well as electrophilic character for both treatment methods, flowing post-discharges and direct DBD plasma. An investigation of the question whether the electrophilic reactivity is due to carbonyl groups showed that the electrophilic character of the N, H-plasma-treated surface is not due to C=O containing groups, but due to other, most probably nitrogen-based functionalities [181, 182].

We have demonstrated, however, that substantial amounts of nucleophilic derivatization reagents, 4-(trifluoromethyl)hydrazine, 2-mercaptoethanol, and 4-(trifluoromethyl)benzylamine (TFMBA) may also react with the surface of polyethylene foils plasma-treated in the flowing post discharge region of DBDs in nitrogen-hydrogen mixtures. The successful binding of significant amounts of these chemicals corroborates our hypothesis that chemical functional groups containing electrophilic C=N double bonds are present on such treated surfaces and they are mainly responsible for the chemical reactivity of the obtained surfaces.

No.	Photon energy / eV	Assignment	References
A	398.9	π^*(N=C)	399.1 [155], 397.8 [183]
B	399.9	π^*(N≡C)	399.7 [155, 183]
C	400.8	σ^*(N-H)	400.6 [183], 401.3 [155]
D	401.3	π^*(NHC=O)	401.0-405.1 [183]

Table 7.2: Nitrogen K-edge NEXAFS data for LDPE thin film plasma-treated in flowing DBD post-discharges of N_2 + H_2 with peak assignments from different literature sources

7.2 Experimental NEXAFS observations of plasma-treated PE surfaces

In order to help further elucidate types of chemical functionalities in the plasma-treated nitrogen-functionalized surfaces, NEXAFS spectroscopy was used. Sample preparation and plasma treatment condition were explained earlier in section 4.2.1. Nitrogen K-edge NEXAFS spectra of

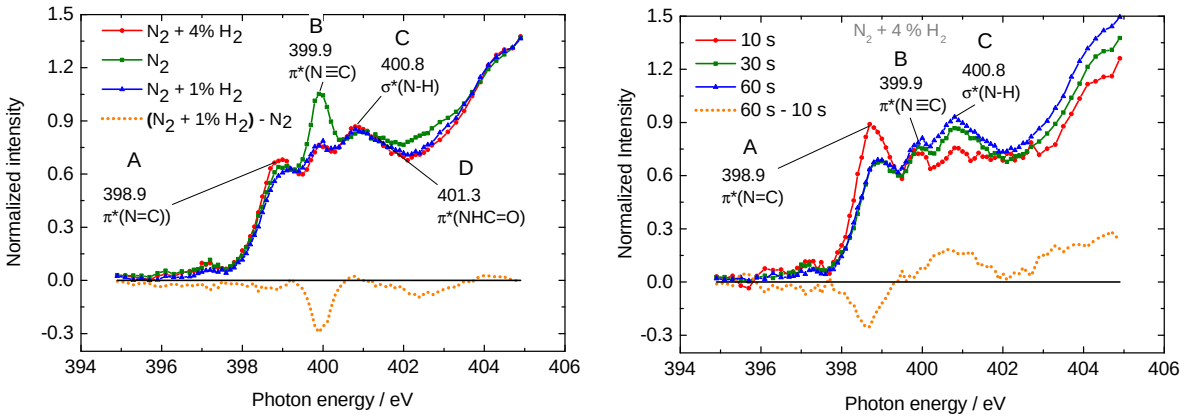

Figure 7.9: Nitrogen K-edge NEXAFS spectra obtained from LDPE ultra-thin films post-discharge-treated in different nitrogen gas mixtures (N_2 + y % H_2, y = 0, 1, or 4) left, and in N_2 + 4 % H_2 for different durations (10, 30, and 60 s) right.

the PE surfaces treated in afterglows of DBDs in N_2 + H_2 gas mixtures which are depicted in Fig. 7.9 show four main peaks: Peak A at 398.9 eV, B at 399.9 eV, C at 400.8 eV, and D at 401.3 eV. Tentative assignments are given in Table 7.2, based on papers by Beck et al. [183] and Shard et al. [155]. The "A" peak near 399 eV may be attributed to π^*(C=N) in imines [155]. These results suggest that imines or other moieties with C=N bonds are actually present on the plasma-treated surfaces, in addition to other N-containing functionalities such as amides, which are in agreement with FTIR spectra. The second absorption peak "B" appears at 399.9 eV and

shows presence of nitrogen in triple bonds (π^*(C≡N)), i.e. nitriles which was surprising because no evidence of nitrile groups was seen in the FTIR spectra. Another absorption peak "C" is located at 400.8 eV and can be accounted to σ^*(N-H) which was expected to appear on a polymer surface treated with nitrogen-hydrogen plasma and might originate from various functional groups, e.g. amines, amides, hydrazines, etc. Also one absorption peak ("D") is appearing at 401.3 eV that originates from π^*(NHC=O) resonances which is more pronounce in the case of treatment in pure nitrogen due to oxygen-containing impurities. The subtraction spectrum of LDPE films treated in pure nitrogen plasma and the spectrum of film treated in N_2 + H_2 (1 %) plasma is also shown in Fig. 7.9 L (short dot). The negative peaks in this spectrum illustrate that (i) more N≡C is present on the nitrogen-treated surface than on nitrogen-hydrogen-treated surface and (ii) more NHC=O appears on the surface treated in "pure" nitrogen. This information is corroborated by the hypothesis regarding the role of hydrogen in the used gas mixture. It was shown that the main role of hydrogen addition is to passivate oxygen (see section 5.1.5).

In figure Fig. 7.9 R, NEXAFS spectra of LDPE treated in N_2 + H_2 (4%) plasma for different treatment times (10, 30, and 60 s) are depicted. It can be seen that treatment for 10 s leads to the highest intensity of π^*(N=C) indicating the highest imine content on the surface. Longer treatment times lead to decrease of π^*(N=C) and at the same time increase of σ^*(N-H). The spectrum in the bottom of Fig. 7.9 R (short dot) is obtained by subtracting a spectrum measured after treating the LDPE sample for 60 s from a spectrum measured after treating the sample for 10 s. It is seen that double bonds are removed over longer periods of plasma exposition while N-H single bonds get more pronounced.

However, as far as our literature inspection, there is a lack of suitable reference NEXAFS data for C=N bonds in aliphatic saturated or unsaturated imines because unrepresentative compounds with heterocyclic rings or aromatic imines (Schiff bases) have exclusively been studied. For this reason, we decided to prepare saturated and unsaturated ultra-thin imine films to measure their NEXAFS data.

Preparation and NEXAFS of reference compounds Solutions of a saturated and an unsaturated imine were prepared by reacting 2-ethyl-1-hexylamine with hexanal and trans-2-hexen-al, respectively, in p-xylene in the presence of molecular sieves. Ultrathin films, less than 20 nm thick, were coated onto the preheated Si by spin coating at 2000 rpm and a total spinning time of 90 seconds. Infrared measurement of the products in solution show a strong band at 1656 and 1670 cm^{-1}, assigned to the C=N stretching mode of unsaturated and saturated imine, respectively. The unsaturated imine exhibits an additional band at 1628 cm^{-1} due to ν(C=C). An ultrathin film of a polyamidine with the moiety -(R_1-N=C(R_2)-NH)$_n$-, R_1 = -(CH_2)$_{10}$-, R_2 =

CH_3, poly(decamethylene-acetamidine, received by courtesy of F. Boehme, Institute of Polymer Research Dresden) was prepared similarly.

The reference model's structures are shown in Fig. 7.10 R. NEXAFS spectra are shown in Fig. 7.10 L. Common features in all three compounds are peaks near 399 eV and 401 eV. The lowest resonance may be assigned to π^*(C=N), which is in accordance with the assignment made by Shard et al., confirming the presence of C=N groups in the plasma-treated samples [155]. The reason(s) for the existence of the resonances appearing at around 401 is (are) still unclear. They cannot be attributed neither to σ^*(N-H) [155] nor to π^*(NHC=O) [183], regarding the structure of model compounds shown in Fig. 7.10 R.

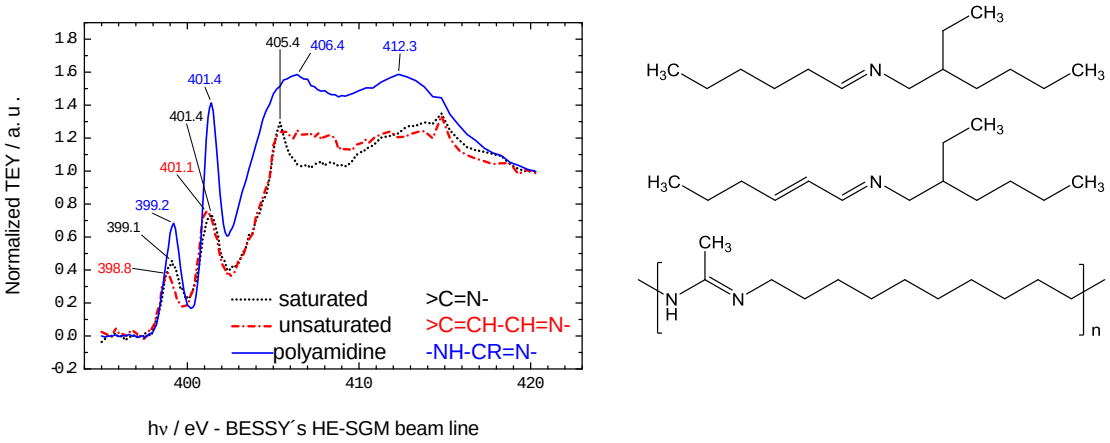

Figure 7.10: Left: NEXAFS measurement of probes shown in right side, top: N-(2-ethylhexyl)-hexanaldimine, middle: N-(2-ethylhexyl)-(E)-2-hexenaldimine, bottom: poly(decamethylene-acetamidine). Right: Molecular structures of the model compounds in the same ordering.

The hypothesis that imino groups are actually present on our plasma-treated surfaces is supported by nucleophilic derivatization of treated surfaces using nucleophilic reagents. Furthermore, NEXAFS measurements confirmed that imine or other moieties with carbon-nitrogen double bonds are indeed present on such plasma-treated surfaces.

8 OES investigation

The purpose of this chapter is the acquisition and interpretation of experimental data about the influence of hydrogen addition in gas mixtures "y" on the optical emission spectra of the flowing post discharge in N_2 + y % H_2. Of most interest are the intensities of components of the first positive system (FPS) of N_2 due to transitions between different vibrational levels of the B $^3\Pi_g$ and A $^3\Sigma_u^+$ electronic states [184]. The concentration of N atoms in the post-discharge of a DBD in N_2 can be determined using the emission of the first positive system of N_2. We expect that the intensity of this emission from the afterglow will decline with increasing H_2 content in the discharge. In the following experiments the dependence of the intensity of a selected component of the first positive system will be shown as a function of hydrogen content "y" and the distance "z" from the outlet of the DBD reactor.

8.1 Determination of N atom concentrations in the post-discharge region

In an N_2 post-discharge or afterglow, vibrational levels with v = 10 to 12 of the B $^3\Pi_g$ state are populated by three-body recombinations of nitrogen atoms via an intervening $^5\Sigma_g{}^+$ state, while levels B $^3\Pi_g$ v = 0 to 2 originate via higher vibrational levels of A $^3\Sigma_u^+$ (v = 7 to 9) [184]. Fig. 8.1 shows spectra of various bands belonging to the FPS of N_2 for Δv = 1 to 4 which appear between 550 and 900 nm, taken at distance z = 20 mm from the end of the discharge. The experimental setup for OES measurements can be found in section 4.6. The band observed at 557.6 nm in the green coloured region ("Aurora" band, 557.7 nm) is generated by emission of an excited complex formed by collisions between O(^{1}S) and ground-state N_2 [185]. Generation and excitation of O atoms in our post-discharge is probably driven by reaction of O-bearing species with ground-state N_2 [186].

It is known that the intensity of lines from high vibrational levels v = 6 to 12 in the FPS is accurately proportional to $[N]^2$ [184]. Thanks to the low wall reactivity of N atoms, surface

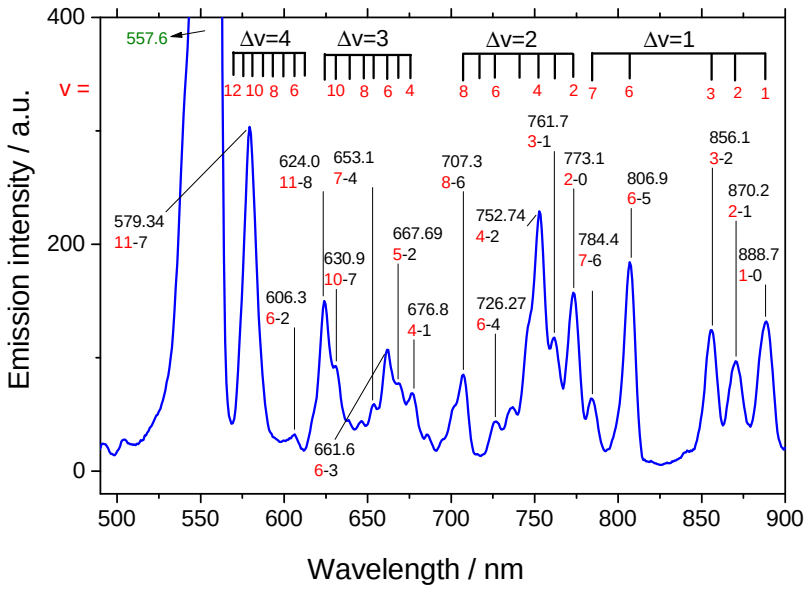

Figure 8.1: Emission spectrum between 500 and 900 nm measured at z = 20 mm in the N_2 flowing post-discharge region. Changes of vibrational quantum number are Δv = 4, 3, 2, and 1. The "green band" at 557.6 nm is due to emission from an excited complex $O(^1S).N_2$

recombinations can be neglected in our case and a simple analytical expression may be given for the shape of the [N](z) profile, involving the well-known recombination constant k_3 implicitly defined by the kinetic equation d[N]/dt = -2k_3[N_2][N][N], with $k_3 = 7.39 \times 10^{-33}$ cm^6s, at an estimated post-discharge gas temperature of 300 K [187].

It follows the below equation, according to which the unknown value of α, relating the intensity and the square of [N] can be determined by plotting of the square root of the intensity vs. kz/v_{av} with the average gas velocity v_{av}, in our case 420 cm/s. [N_2] at 300 K and 1 bar is 2.41×10^{19} cm^{-3}.

$$\frac{1}{\sqrt{(I(z)}} = \frac{1}{\sqrt{(I(0)}} + \sqrt{\alpha} kz/v_{av}, \quad \alpha \equiv [N]^2/I, \quad k \equiv 2k_3[N_2] = 3.56 \times 10^{-13} cm^3/s \qquad (8.1)$$

Once the value of α has been determined from measurements using pure N_2, band intensities can easily be converted into N atom concentrations by the equation [N] = $(\alpha\ I)^{1/2}$ - even for mixtures of N_2 with other gases, as long as the same optical arrangement is used. The transition N_2 (B, $v' = 11$) $\rightarrow$ N_2 (A, $v'' = 7$) at 579.34 nm was used for determining α.

The absolute nitrogen atom concentration [N] as a function of the distance z from the discharge end (= begin of post-discharge region), at a given discharge power (50 watts, 4.5 W/cm^3) and

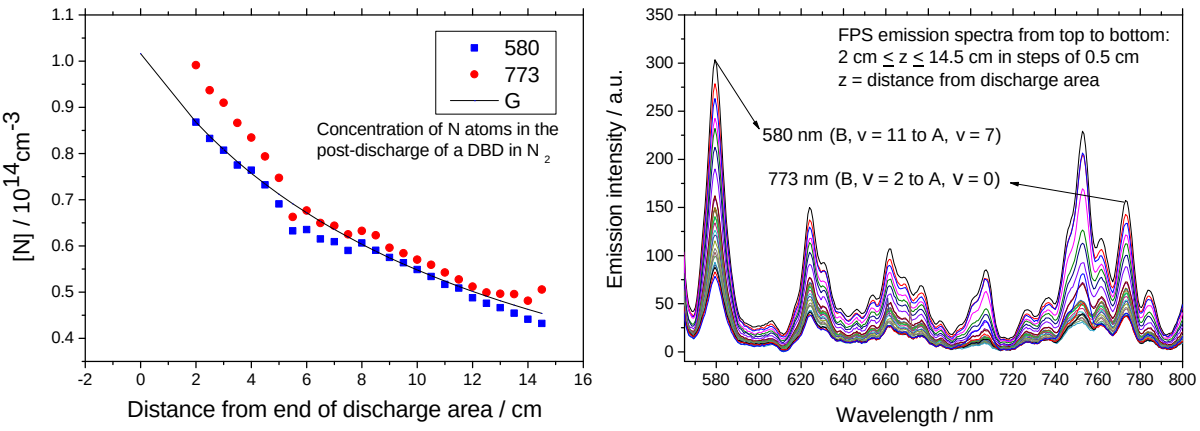

Figure 8.2: Left: The z-dependence of nitrogen atom concentration in flowing post-discharge of a DBD in pure nitrogen determined independently from two N_2 FPS bands. Right: Emission spectra in the z region 2 cm $\leq$ z $\leq$ 14.5 cm; z = distance to the end of the active discharge region. Gas velocity 420 cm/s; integration time 2 s.

20 $Lmin^{-1}$ STP gas flow is shown in Fig. 8.2 L. A graph of the analytical dependence of [N] vs. z is achieved using the following relation and substituting the k = 3.56 $\times$ 10^{-13} cm^3s^{-1}, the known N(0) from data measured at 580 nm, and v_{av} = 420 cms^{-1}, see curve G in Fig. 8.2 L.

$$N(z) = \frac{1}{\frac{1}{N(0)} + \frac{k}{v_{av}} z} \tag{8.2}$$

OES spectra are shown in Fig. 8.2 R. In addition to the concentration measurement based on the line near 580 nm, the same procedure was applied to the 2-0 band at 773.1, although the assumption of a proportionality between I and $[N]^2$ was not justified *a priori*. However, the data points in red/sphere in Fig. 8.2 L demonstrate that empirically this proportionality holds, too, as far as the precision of the measurements allows to conclude. Not surprisingly, the degree of dissociation [N](z = 0)/ $[N^2]$ achieved in these experiments, about 10^{-5}, is in order of magnitude smaller than what can be achieved in low-pressure discharges, see, e.g., a paper by Ricard et al. [188].

8.2 OES at post-discharges of N_2 + y % H_2 mixtures

With the calibration of the measurement of nitrogen atom concentrations [N] from measurements of the emission from post-discharges in pure N_2, the effect of small quantities (0.1 to

4.0 %) of H_2 introduced into the N_2 gas on [N] can be investigated using the same optical arrangement. Using the same α for measurements with and without H_2 requires that the addition of H_2 does not open new significantly contributing pathways for the population and deactivation of $N_2(B)$, respectively. The exothermicity of reactions NH + N → N_2 + H (6.5 eV) and NH_2 + N → N_2 + H_2 (6.9 eV) (NIST-JANAF Thermochemical Tables) is not sufficient to yield an $N_2(B)$ state, requiring 7.4 eV. On the other hand, quenching of $N_2(B)$ by N_2 and H_2 has similar rate constants [189]. Therefore, the same α can be used for mixtures of nitrogen and hydrogen.

In Fig. 8.3 L OES spectra are shown, taken at z = 2 cm on post-discharges from DBDs in N_2 with or without added H_2. While all bands of the FPS are significantly attenuated already by addition of 0.1 % H_2, the bands are still visible at 4 % H_2. Interestingly, bands originating from higher vibrational levels such as the 11-7 band at 580 nm are more greatly reduced than bands from lower levels such as, for example, the Δv = 1 bands from levels 1 to 3 between 850 and 900 nm. Nitrogen atom concentrations for N_2 + y % H_2 at different values of z are shown in

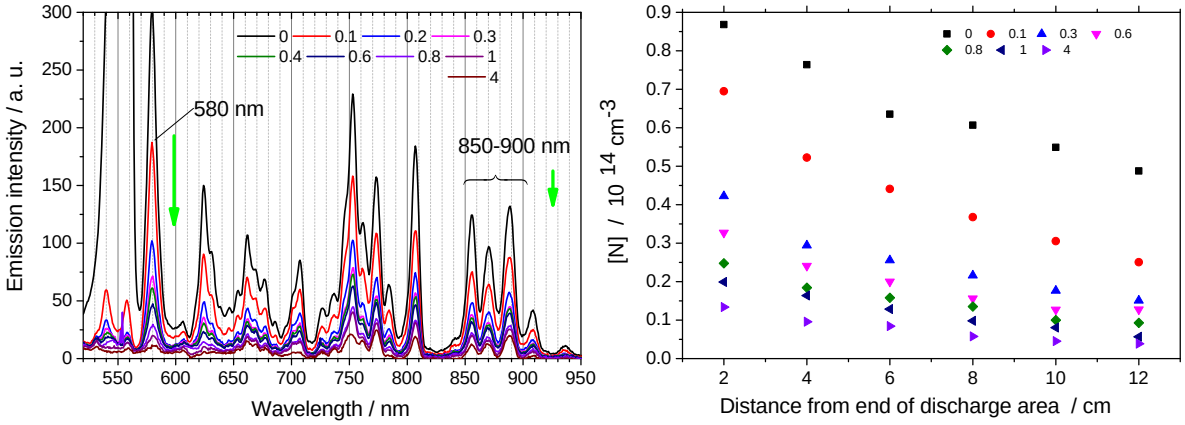

Figure 8.3: Left: OES spectra taken at z = 2 cm from post-discharges from DBDs in N_2 with or without added H_2, percentages indicated in the inserted legend. Right: N atom concentrations determined from the emission at 580 nm vs. z at hydrogen percentages indicated in the legend.

Fig. 8.3 R. While there is a general decrease of [N] with rising y, differences are always larger between y = 0 and y = 0.1 than between y = 1 and y = 4. Using the chemical kinetic modelling, the decrease of [N] by a factor of 6.3 at z = 2 and y = 4 should be due to a H atom mole fraction x_H of about 10^{-5} at z = 0, comparable to x_N(z=0) and significantly less than x_H observed, e.g., from a discharge in Ar + 4 % H_2 [190]. The decrease of [N] might be responsible for generally observed decreasing incorporation of functional groups beyond y = 0.1 %.

The addition of 0.1 % H_2 is sufficient to reduce the Aurora band at 557.6 by a factor of about 100 while the effects of even larger y are not as pronounced. We tentatively attribute this observation to a radical change of the chemistry within the post-discharge which is potentially also responsible for the vanishing of the amide-carbonyl-related absorption band at 1695 cm^{-1}, observed by FTIR-ATR (see section 5.1.4 and Fig. 5.8 L). This coincidence gives an interesting hint to the role of oxygen atoms in the formation of amides during the polymer surface treatment.

8.3 OES at post-discharges of N_2 + y % H_2 + x % O_2

We completed optical emission studies of the effects of O_2 traces (x = 0.01 % and 1 %) and H_2 admixtures y = 0, 1, and 4 % (flammability limit) on nominally pure N_2. The emission intensities of 11-7 bands of the FPS of N_2 in nitrogen-hydrogen and oxygen mixtures at a constant position along the afterglow are depicted in Fig. 8.4. The position is chosen 2 cm from the discharge area. The constant input power of 50 watts is applied. Additionally, the emission intensity change of the green band (557.7 nm) via different gas mixtures is seen. The intensities of both bands rapidly decrease by adding 1 % of hydrogen into the nitrogen. Adding 0.01 % of oxygen does not change significantly the emission intensities of FPS N_2 and the green band. However, reducing the 557.7 nm band in the case of nitrogen-hydrogen mixtures with y = 0.1 proves the main role of hydrogen to passivate oxygen or oxygen-derived species.

Based on the outlined experimental results we are lead to conclude that

- OES measurement analyzes reveal that the H_2 additions reduced the concentration of oxygen atoms because they possibly reacted to H_2O. This corroborates the FTIR-ATR results of plasma treatment using nitrogen-hydrogen mixtures in which no amide was able to be formed, see section 5.1.2 and 5.1.4.

- The "negative role" of H_2 additions is to reduce concentrations of N atoms by a mechanism already put forward by Brown in 1973 [191]

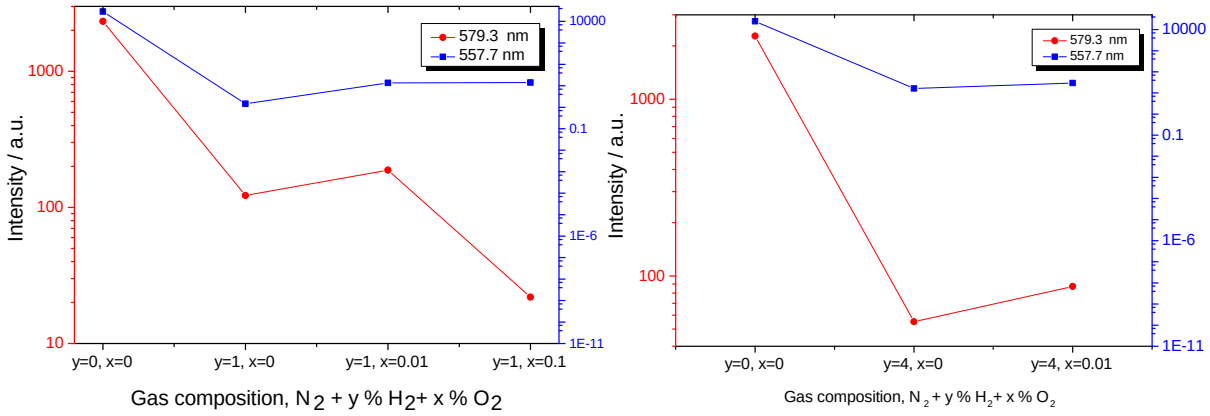

Figure 8.4: Emission intensity of $\lambda = 579.3$ nm (11-7) and $N_2O(^1S)$ $\lambda = 557.7$ nm in terms of gas composition N_2 + y % H_2 + x % O_2, input power 50 W.

9 Conclusions

9.1 Summary

In situ FTIR-ATR measurements during afterglow plasma treatments of freshly spin-coated ultrathin polyethylene films were performed to monitor chemical surface changes. The LDPE films were treated in the post-discharges from dielectric barrier discharges (DBDs) in N_2 + x % H_2 (x = 0 to 4) using different exposure durations. Curve fitting of the FTIR spectra of plasma-treated PE surfaces in the region of 1750-1450 cm^{-1} showed three absorption peaks in the case of pure nitrogen and five peaks after hydrogen was added. In this region, different functional groups, such as X=Y stretching vibrations and X-H bending vibrations are expected to occur.

In order to separate the vibrational signature of primary amines from overlapping stretching vibrations of double bonds, an exchange of the nitrogen-bonded hydrogen against deuterium was applied. Primary amine groups (-NH_2) typically show a bending vibration absorbance near 1620 cm^{-1} which shifts to about 1200 cm^{-1} when replaced by D, thereby forming ND_2. However, *in situ* FTIR measurements of treated films after exposure to D_2O and H_2O vapors in a nitrogen atmosphere showed no vibration due to ND_2. (The detection limit was about 0.3 groups per nm^{-2}.). It was inferred that virtually no primary amine functionalization occurred.

Plasma-treated thin films were exposed to TFBA vapor and an *in situ* ATR monitoring of the chemical reaction between TFBA and the surface was performed. Surprisingly, plasma-treated LDPE surfaces exhibited considerable bonding of the 4-trifluoromethylphenyl moiety, although no primary amine had been found before. These unexpected results led us to conclude that other nitrogen functionalities were present, showing IR absorption bands in the region between 1800 and 1550 cm^{-1} and being able to bind substantial amounts of aromatic aldehydes.

Imino groups derived either from aldehyde (aldimine -CH=N-) or from ketone (ketimine >C=N-) groups were considered to be suitable candidates. From a close inspection of the available literature and several of our own experiments, we found that imines are able to react with TFBA. The

hypothesis that imino groups were actually present after plasma treatment was supported by nucleophilic derivatization of treated surfaces using nucleophilic reagents such as 2-mercaptoethanol (ME), 4-(trifluoromethyl)phenylhydrazine (TFMPH), and 4-(trifluoromethyl)benzylamine (TFMBA). According to XPS and FTIR ATR analyzes performed *ex situ* on treated PE foils, the above reagents were able to bind to the plasma-treated surface. Moreover, near-edge X-ray absorption fine structure (NEXAFS) measurements confirmed that imine or other moieties with carbon-nitrogen double bonds are indeed present on such plasma-treated surfaces.

In addition, several experiments provided clear evidence that trifluoroacetic anhydride (TFAA) as a derivatization reagent not only indicates the presence of O-H groups and N-H moieties of primary or secondary amines (as it was supposed for a long time), but also imines. We concluded that the myth of primary-amine selectivity of aromatic aldehydes as well as amine and hydroxyl selectivity of TFAA must be refuted. Indeed, the reactivity of these reagents with other nitrogen-containing functional groups, formed as a result of plasma treatment in an N_2, NH_3, and N_2-H_2 mixtures, was disregarded in a large number of published papers in recent decades.

There are several conclusions made in this thesis:

- Traditional derivatization reagents, especially the prototypic electrophilic TFBA and TFAA are actually indicating imines - besides amines, and, in the case of TFAA, hydroxy groups.

- The hypothesis that imines are formed by the plasma treatment was confirmed by nucleophilic derivatization and NEXAFS results.

- FTIR ATR results of surfaces treated in N_2 + x % O_2 + y % H_2 DBD post-discharges as well as OES measurements demonstrated that adding a small percentage of hydrogen into nitrogen led to passivation of oxygen traces by hydrogen (probably by formation of gaseous H_2O). Indeed, oxygen atoms are responsible for amide formation observed in afterglows from DBDs in pure N_2.

- OES analyzes of N_2 + y % H_2 demonstrated that nitrogen atoms and excited nitrogen molecules in the triplet state $N_2(A)$, which are most probably responsive for nitrogen functionalization in pure N_2, still exist in the post-discharge. It must be noted that, although hydrogen addition prevented amide formation, it led to a decrease in the concentrations of nitrogen atoms.

9.2 Outlook and future work

H-D experiment of several model compounds to investigate the exchangeable functional groups formed on the treated surface

The research begs the question which functional group(s) is/are responsible for showing the exchangeable product formed on the plasma-treated polymer surfaces in contact with H_2O and D_2O, respectively. H-D exchange experiments of model compounds of moieties which were taken into consideration as candidates for functional groups formed by post-discharge-exposure of the surfaces, should provide a lot of information. For this purpose, in addition to urea (section 5.3.3), hydrogen and deuterium forms of several functional groups like primary and secondary amides as well as amidines should be studied using FTIR-ATR to get more insight into the processes during hydrolysis and surface functionalization.

***Ex situ* H-D exchange on plasma-treated LDPE foils**

The findings of our work were mainly based on PE surfaces treated in afterglows of DBDs in N_2 + H_2. From a scientific point of view, but even more under application-related aspects it is important to know if similar results will be obtained with polymer foils treated in a direct DBD discharge of N_2 (+ H_2 + O_2) in the corresponding gas atmosphere. Recently, the results of *ex situ* H-D isotope exchange on directly-plasma-treated LDPE foils was published by the IOT group [156]. The foils were treated using a newly developed "plasma-printing" setup with 1 % hydrogen in the N_2 + H_2 mixture. It was pointed out that no primary amine was formed.

***In situ* nucleophilic derivatization of plasma-treated films using FTIR-ATR**

TFMPH (and ME) derivatization of treated surfaces *in situ* under exclusion of ambient oxygen and water will provide more reliable and informative results to clarify the major reaction pathways more precisely. The effects of impurities in the polymer can largely be excluded and also the reason for nitrogen loss can probably be clarified. In addition, investigations of model imines would help to elucidate the main reaction routes followed under typical derivatization conditions and would support the *in situ* FTIR ATR analyzes of such surfaces.

***In situ* electrophilic derivatization: Trifluoroacetylation**

Why N-H or O-H stretching vibrations at wavenumbers beyond the origin 3200 cm^{-1} on the plasma-treated surfaces are present, is as yet unclear. Trifluoroacetylation is a proposed process which is able to differentiate amides, alcoholic groups and -NH groups of secondary amines or of N-H imines. Amides are not expected to react with TFAA under sufficiently mild conditions while TFAA undergoes reactions with alcoholic groups and -NH groups of secondary amines or of N-H imines. Such reactions result in the formation of ester and amides of trifluoroacetic acid,

respectively. A secure identification method could be based on both XPS analyzes and *in situ* H-D isotope exchange on treated surface using FTIR ATR.

NEXAFS measurement of imine reference compounds

There is still a lack of suitable reference NEXAFS data for C=N bonds in aliphatic saturated or unsaturated imines. In our study, the reason for the NEXAFS result of imine model compounds used to compare with our measurements on plasma-treated PE is not yet clear. It is, therefore, suggested that similar investigations be repeated on several unsaturated imine compounds. Careful consideration should be made to minimize both contact with the ambient atmosphere and the interval time between preparation and sample measurement.

Abbreviations

ATR	Attenuated total reflectance
at%	Atomic percent
BE	Binding energy
CD	Chemical derivatization
CD-XPS	Chemical derivatization X-ray photoelectron spectroscopy
DBD	Dielectric barrier discharge
FTIR	Fourier transform infrared spectroscopy
FWHM	Full width at half maximum
FPS	First positive system
HMDSO	Hexamethyldisiloxane
IB	Isobutyraldehyde
IRE	Internal reflection element
LDPE	Low-density polyethylene
LLDPE	Linear low-density polyethylene
ME	2-Mercaptoethanol
NEXAFS	Near-edge X-ray absorption fine structure
OES	Optical emission spectroscopy
PET	Polyethylene terephthalate
PE	Polyethylene
PFB	Pentafluorobenzaldehyde
ppm	Parts per million
PS-AM-NH_2	Aminomethylated polystyrene
PS	Polystyrene
PTFE	Polytetrafluoroethylene
rpm	Revolutions per minute
STP	Standard temperature and pressure
TFAA	Trifluoroaceticanhydride
TFBA	4-(Trifluoromethyl)benzaldehyde
TFMBA	4-(Trifluoromethyl)benzylamine
TFMBA	4-(Trifluoromethyl)benzylamine
VUV	Vacuum-ultraviolet
XPS	X-ray photoelectron spectroscopy

Bibliography

[1] C.-P. Klages, A. Hinze, and Z. Khosravi, "Nitrogen plasma modification and chemical derivatization of polyethylene surfaces - An in situ study using FTIR-ATR spectroscopy," *Plasma Process. Polym.*, vol. 10, no. 11, pp. 948–958, 2013.

[2] C.-P. Klages, Z. Khosravi, and A. Hinze, "Some remarks on chemical derivatization of polymer surfaces after exposure to nitrogen-containing plasmas," *Plasma Process. Polym.*, vol. 10, no. 4, pp. 307–312, 2013.

[3] Z. Khosravi and C.-P. Klages, "Nucleophilic derivatization of polyethylene surfaces treated in ambient-pressure N_2-H_2 DBD post discharges," *Plasma Chem. Plasma Process.*, vol. 34, pp. 661–669, 2014.

[4] L. J. Stief, F. L. Nesbitt, W. A. Payne, S. C. Kuo, W. Tao, and R. B. Klemm, "Rate constant and reaction channels for the reaction of atomic nitrogen with the ethyl radical," *J. Chem. Phys.*, vol. 102, no. 13, pp. 5309–5317, 1995.

[5] U. Kogelschatz, B. Eliasson, and W. Egli, "Dielectric-barrier discharges. Principle and applications," *J. Phys IV Fr.*, vol. 7, no. C4, pp. 47–66, 1997.

[6] G. Socrates, *Infrared and Raman characteristic group frequencies: Tables and charts*. Hoboken, NJ, USA: John Wiley & Sons. Ltd,, 2004.

[7] N. Shahidzadeh, M. M. Chehimi, F. Arefi-Khonsari, J. Amouroux, and M. Delamar, "Evaluation of acid-base properties of ammonia plasma-treated polypropylene by means of XPS," *Plasmas Polym.*, vol. 1, pp. 27–45, 1996.

[8] Y. Nakayama, T. Takahagi, and F. Soeda, "XPS analysis of NH_3, plasma-treated polystyrene films utilizing gas phase chemical modification," *J. Polym. Sci., Part A Polym. Chem.*, vol. 26, pp. 559–572, 1988.

[9] C. Girardeaux, N. Zammatteo, M. Art, B. Gillon, J. Pireaux, and R. Caudano, "Amination of poly(ethylene-terephtalate)," *Plasmas Polym.*, vol. 1, no. 4, pp. 327–346, 1996.

[10] A. A. Meyer-Plath, B. Finke, K. Schröder, and A. Ohl, "Pulsed and cw microwave plasma excitation for surface functionalization in nitrogen-containing gases," *Surf. Coat. Technol.*, vol. 175, pp. 877–881, 2003.

[11] J. M. Grace and L. J. Gerenser, "Plasma treatment of polymers," *J. Dispers. Sci. Technol.*, vol. 24, no. 3-4, pp. 305–341, 2003.

[12] J. R. Hollahan and B. B. Stafford, "Attachment of amino groups to polymer surfaces by radiofrequency plasmas," *J. Appl. Polym. Sci.*, vol. 13, no. 4, pp. 807–816, 1969.

[13] K. Schröder, A. Meyer-Plath, D. Keller, B. W, G. Babucke, and A. Ohl, "Plasma-induced surface functionalization of polymeric biomaterials in ammonia plasma," *Contrib. Plasma Phys.*, vol. 41, no. 6, pp. 562–572, 2001.

[14] P. Favia, M. V. Stendardo, and R. D'Agostino, "Selective grafting of amine groups on polyethylene by means of NH_3-H_2 RF glow discharges," *Plasmas Polym.*, vol. 1, no. 2, pp. 91–112, 1996.

[15] M. Thomas and K. L. Mittal, *Atmospheric pressure plasma treatment of polymers: relevance to adhesion*. Hoboken, NJ, USA: John Wiley & Sons, Inc., 2013.

[16] G. J. Courval, D. G. Gray, and D. A. I. Goring, "Chemical modification of polyethylene surfaces in a nitrogen corona," *Polym. Lett. Ed.*, vol. 14, pp. 231–235, 1976.

[17] J. M. Pochan, L. J. Gerenser, and J. F. Elman, "An e.s.c.a. study of the gas-phase derivatization of poly (ethyleneterephthalate) treated by dry-air and dry-nitrogen corona discharge," *Polymer*, vol. 27, pp. 1–5, 1986.

[18] J. L. Weininger, "Reaction of active nitrogen with polyethylene," *Nature*, vol. 186, pp. 546–547, 1960.

[19] J. L. Weininger, "The reactions of active nitrogen with polyolefins," *J. Phys. Chem*, vol. 65, no. 6, pp. 941–943, 1961.

[20] D. T. Clark, A. Dilks, and H. R. Thomas, "ESCA applied to polymers . XXI. Investigation of sample-charging phenomena," *J. Polym. Sci., Polym. Chem. Ed.*, vol. 16, pp. 1461–1474, 1978.

[21] D. T. Clark and H. R. Thomas, "Applications of ESCA to polymer chemistry. XVII. Systematic investigation of the core levels of simple homopolymers," *J. Polym. Sci., Polym. Chem. Ed.*, vol. 16, pp. 791–820, 1978.

[22] D. T. Clark and A. Dilks, "ESCA applied to polymers. XV. RF Glow-discharge modification of polymers, studied by means of ESCA in terms of a direct and radiative energy-transfer model," *J. Polym. Sci., Polym. Chem. Ed.*, vol. 15, pp. 2321–2345, 1977.

[23] D. T. Clark and W. J. Feast, "Application of electron spectroscopy for chemical applications (ESCA) to studies of structure and bonding in polymeric systems," *J. Macromol. Sci., Rev. Macromol. Chem.*, vol. C12, no. 2, pp. 191–286, 1975.

[24] J. R. Hollahan and A. T. Bell, *Techniques and applications of plasma chemistry.* New York: Wiley, 1974.

[25] H. Yasuda, N. Morosoff, E. S. Brandt, and C. N. Reilley, "Plasma polymerization of tetrafluoroethylene. I. Inductive radio frequency discharge," *J. Appl. Polym. Sci.*, vol. 23, no. 4, pp. 1003–1011, 1979.

[26] N. Morosoff and H. Yasuda, "Plasma polymerization of tetrafluoroethylene. III. Capacitive audio frequency (10 kHz) and ac discharge," *J. Appl. Polym. Sci.*, vol. 23, pp. 3471–3488, 1979.

[27] N. Morosoff, H. Yasuda, E. S. Brandt, and C. N. Reilley, "Plasma polymerization of tetrafluoroethylene. II. Capacitive radio frequency discharge," *J. Appl. Polym. Sci.*, vol. 23, pp. 3449–3470, 1979.

[28] M. Buddhadasa and P.-L. Girard-Lauriault, "Plasma co-polymerisation of ethylene, 1,3-butadiene and ammonia mixtures : Amine content and water stability," *Thin Solid Films*, vol. 591, pp. 76–85, 2015.

[29] D. S. Everhart and C. N. Reilley, "Chemical derivatization in electron spectroscopy for chemical analysis of surface functional groups introduced on low-density polyethylene film," *Anal. Chem.*, vol. 53, no. 4, pp. 665–676, 1981.

[30] C. K. Ingold, "The additive formation of four-membered rings. Part VII. The synthesis and division of some dimethylene-1:3-oxaimines," *J. Chem. Soc.*, vol. 127, pp. 1141–1145, 1925.

[31] R. W. Layer, "The chemistry of imines," *Chem. Rev.*, vol. 63, no. 5, pp. 489–510, 1963.

[32] S. Patai, *The chemistry of the carbon-nitrogen double bonds.* Chichester-New York-Brisbane-Toronto: John Wiley & Sons Ltd, 1970.

[33] D. Briggs and C. R. Kendall, "Derivatization of discharge-treated LDPE: an extension of XPS analysis and a probe of specific interactions in adhesion," *Int. J. Adhes. Adhes.*, vol. 2, no. 1, pp. 13–17, 1982.

[34] J. G. A. Terlingen, L. M. Bernneisen, H. T. J. Super, A. P. Pijpers, A. S. Hoffman, and J. Feijen, "Introduction of amine groups on poly(ethylene) by plasma immobilization of a preadsorbed layer of decylamine hydrochloride," *J. Biomater. Sci., Polym. Ed.*, vol. 4, no. 3, pp. 165–181, 1993.

[35] M. Mavadat, M. Ghasemzadeh-Barvarz, S. Turgeon, C. Duchesne, and L. Gaetan, "Correlation between the plasma characteristics and the surface chemistry of plasma-treated polymers through partial least-squares analysis," *Langmuir*, vol. 29, no. 51, pp. 15859–15867, 2013.

[36] F. Fally, C. Doneux, J. Riga, and J. J. Verbist, "Quantification of the functional groups present at the surface of plasma polymers deposited from propylamine, allylamine, and propargylamine," *J. Appl. Polym. Sci.*, vol. 56, no. 5, pp. 597–614, 1995.

[37] A. Choukourov, J. Kousal, D. Slavínská, H. Biederman, E. R. Fuoco, S. Tepavcevic, J. Saucedo, and L. Hanley, "Growth of primary and secondary amine films from polyatomic ion deposition," *Vacuum*, vol. 75, no. 3, pp. 195–205, 2004.

[38] A. A. Meyer-Plath, K. Schröder, B. Finke, and A. Ohl, "Current trends in biomaterial surface functionalization - Nitrogen-containing plasma assisted processes with enhanced selectivity," *Vacuum*, vol. 71, pp. 391–406, 2003.

[39] J. C. Ruiz, A. St-Georges-Robillard, C. Thérésy, S. Lerouge, and M. R. Wertheimer, "Fabrication and characterisation of amine-rich organic thin films: Focus on stability," *Plasma Process. Polym.*, vol. 7, no. 9-10, pp. 737–753, 2010.

[40] U. Kogelschatz, "Process technologies for water treatment," in *Adv. Ozone Gener.*, ch. Advanced O, pp. 87–118, New York: Springer US, plenum pre ed., 1988.

[41] W. Siemens, "Ueber die elektrostatische Induction und die Verzoegerung des Stroms in Flaschendraehten," *Poggendorff's Ann. der Phys. und Chemie*, vol. 102, pp. 66–122, 1857.

[42] N. Inagaki and Y. Kubokawa, "Plasma polymerization of ethylene glycol monomethylether and water-vapor permeability," *J. Polym. Sci., Part A Polym. Chem.*, vol. 27, pp. 795–805, 1989.

[43] V. Krishnamurthy, I. L. Kamel, and Y. Wei, "Analysis of plasma polymerization of allylamine by FTIR," *J. Polym. Sci. Part A Polym. Chem.*, vol. 27, no. 4, pp. 1211–1224, 1989.

[44] H. Yasuda, *Plasma polymerization.* New York: Academic Press, 1985.

[45] A. Choukourov, H. Biederman, D. Slavinska, L. Hanley, A. Grinevich, H. Boldyryeva, and A. Mackova, "Mechanistic studies of plasma polymerization of allylamine.," *J. Phys. Chem. B*, vol. 109, no. 48, pp. 23086–23095, 2005.

[46] P. Favia and R. D'Agostino, "Plasma treatments and plasma deposition of polymers for biomedical applications," *Surf. Coat. Technol.*, vol. 98, pp. 1102–1106, 1998.

[47] G. Fridman, M. Peddinghaus, H. Ayan, A. Fridman, M. Balasubramanian, A. Gutsol, A. Brooks, and G. Friedman, "Blood coagulation and living tissue sterilization by floating-electrode dielectric barrier discharge in air," in *33rd IEEE Int. Conf. Plasma Sci. ICOPS 2006. IEEE*, vol. 26, pp. 425–442, 2006.

[48] F. Rossi, O. Kylián, H. Rauscher, D. Gilliland, and L. Sirghi, "Use of a low-pressure plasma discharge for the decontamination and sterilization of medical devices," *Pure Appl. Chem*, vol. 80, no. 9, pp. 1939–1951, 2008.

[49] E. Piskin, "Plasma processing of biomaterials," *J. Biomater. Sci. Polym. Ed.*, vol. 4, no. 1, pp. 45–60, 1993.

[50] P. Rajasekaran, *Atmospheric-pressure dielectric barrier discharge (DBD) in air: Plasma characterisation for skin therapy.* PhD thesis, Bochum, Germany, 2011.

[51] E. Stoffels, a. J. Flikweert, W. W. Stoffels, and G. M. W. Kroesen, "Plasma needle: a non-destructive atmospheric plasma source for fine surface treatment of (bio) materials," *Plasma Sources Sci. Technol.*, vol. 11, no. 4, pp. 383–388, 2002.

[52] J. Janca, L. Zajickova, M. Klima, and P. Slavicek, "Diagnostics and application of the high frequency plasma pencil," *Plasma Chem. Plasma Process.*, vol. 21, no. 4, pp. 565–579, 2001.

[53] S. Kühn, N. Bibinov, R. Gesche, and P. Awakowicz, "Non-thermal atmospheric pressure HF plasma source: generation of nitric oxide and ozone for bio-medical applications," *Plasma Sources Sci. Technol.*, vol. 19, no. 1, p. 015013 (8pp), 2010.

[54] R. B. Gadri, J. Roth, T. C. Montie, K. Kelly-Wintenberg, P. P.-Y. Tsai, D. J. Helfritch, P. Feldman, D. M. Sherman, F. Karakaya, and Z. Chen, "Sterilization and plasma processing of room temperature surfaces with a one atmosphere uniform glow discharge plasma (OAUGDP)," *Surf. Coatings Technol.*, vol. 131, pp. 528–541, 2000.

[55] A. J. Wagner, D. H. Fairbrother, and F. Reniers, "A comparison of PE surfaces modified by plasma generated neutral nitrogen species and nitrogen ions," *Plasma Polym.*, vol. 8, no. 2, pp. 119–134, 2003.

[56] J. Friedrich, P. Rohrer, W. Saur, T. Gross, A. Lippitz, and W. Unger, "Improvement in polymer adhesivity by low and normal pressure plasma surface modification," *Surf. Coatings Technol.*, vol. 59, no. 1-3, pp. 371–378, 1993.

[57] M. Kawakami, Y. Yamashita, M. Iwamoto, and S. Kagawa, "Modification of gas permeabilities of polymer membranes by plasma coating," *J. Memb. Sci.*, vol. 19, no. 3, pp. 249–258, 1984.

[58] M. Stamm, *Polymer surfaces and interfaces: characterization, modification and applications.* Leibniz Institute of Polymer Research Dresden: Springer, 2008.

[59] R. Foerch, N. S. Mcintyre, R. N. S. Sodhi, and D. H. Hunter, "Nitrogen plasma treatment of polyethylene and polystyrene in a remote plasma reactor," *J. Appl. Polym. Sci.*, vol. 40, pp. 1903–1915, 1990.

[60] M. J. Shenton, M. C. Lovell-Hoare, and G. C. Stevens, "Adhesion enhancement of polymer," *J. Phys. D Appl. Phys.*, vol. 34, pp. 2754–2760, 2001.

[61] K. H. Becker, U. Kogelschatz, K. H. Schoenbach, and R. J. Barker, *Non-equilibrium air plasmas at atmospheric pressure.* London: CRC Press, 2004.

[62] H. V. Boeing, *Plasma science and technology.* New York: Cornell University Press, 1982.

[63] M. Parvinzadeh Gashti, D. Hegemann, M. Stir, and J. Hulliger, "Thin film plasma functionalization of polyethylene terephthalate to induce bone-like hydroxyapatite nanocrystals," *Plasma Process. Polym.*, vol. 11, no. 1, pp. 37–43, 2014.

[64] F. Taraballi, S. Zanini, C. Lupo, S. Panseri, C. Cunha, C. Riccardi, M. Marcacci, M. Campione, and L. Cipolla, "Amino and carboxyl plasma functionalization of collagen films for tissue engineering applications," *J. Colloid Interface Sci.*, vol. 394, no. 1, pp. 590–597, 2013.

[65] A. Boulares-Pender, A. Prager, S. Reichelt, C. Elsner, and M. R. Buchmeiser, "Functionalization of plasma-treated polymer surfaces with glycidol," *J. Appl. Polym. Sci.*, vol. 121, pp. 2543–2550, 2011.

[66] H. Shonhorn and R. H. Hansen, "Surface treatment of polymers for adhesive bonding," *J. Appl. Polym. Sci*, vol. 11, no. 8, pp. 1461–1474, 1967.

[67] F. Massines, R. Messaoudi, and C. Mayoux, "Comparison between air filamentary and helium glow dielectric barrier discharges for the polypropylene surface treatment," *Plasmas Polym.*, vol. 3, no. 1, pp. 43–59, 1998.

[68] V. Švorčík, K. Koláova, P. Slepička, A. Macková, M. Novotná, and V. Hnatowicz, "Modification of surface properties of high and low density polyethylene by Ar plasma discharge," *Polym. Degrad. Stab.*, vol. 91, pp. 1219–1225, 2006.

[69] T. G. Shikova, V. V. Rybkin, V. A. Titov, and H.-S. Choi, "Reaction of oxygen plasma active species with polyethylene," *High Energy Chem.*, vol. 40, no. 5, pp. 396–400, 2006.

[70] A. Vesel and M. Mozetic, "Modification of PET surface by nitrogen plasma treatment," *J. Phys. Conf. Ser.*, vol. 100, no. 1, p. 012027 (4pp), 2008.

[71] N. Inagaki, K. Narushim, N. Tuchida, and K. Miyazaki, "Surface characterization of plasma-modified poly(ethylene terephthalate) film surfaces," *J. Polym. Sci. Part B Polym. Phys.*, vol. 42, no. 20, pp. 3727–3740, 2004.

[72] R. Morent, G. De Geyter, S. Van Vlierberghe, P. Dubruel, C. Leys, L. Gengembre, E. Schacht, and E. Payen, "Deposition of HMDSO-based coatings on PET substrates using an atmospheric pressure dielectric barrier discharge," *Prog. Org. Coat.*, vol. 64, pp. 304–310, 2009.

[73] M. Alami, M. Charbonnier, and M. Romand, "Interest of NH_3 and N_2 plasmas for polymer treatment before electroless metallization," *Plasma Polym.*, vol. 1, no. 2, pp. 113–126, 1996.

[74] S. Kreitz, C. Penache, M. Thomas, and C.-P. Klages, "Patterned DBD treatment for area-selective metallization of polymers-plasma printing," *Surf. Coatings Technol.*, vol. 200, pp. 676–679, 2005.

[75] C.-P. Klages, A. Hinze, P. Willich, and M. Thomas, "Atmospheric-pressure plasma amination of polymer surfaces," *J. Adhes. Sci. Technol.*, vol. 24, pp. 1167–1180, 2010.

[76] S. Kotula, M. Lüdemann, J. Philipp, M. Thomas, and C.-P. Klages, "Plasma nitrogenation of polymer surfaces with a new type of combinatorial plasma-printing reactor," *Plasma Process. Polym.*, vol. 9999, pp. 1–12, 2016.

[77] H.-E. Wagner, R. Brandenburg, K. Kozlov, A. Sonnenfeld, P. Michel, and J. Behnke, "The barrier discharge: basic properties and applications to surface treatment," *Vacuum*, vol. 71, no. 3, pp. 417–436, 2003.

[78] J. R. Roth, *Industrial plasma engineering, Vol. 2, Application to nonthermal plasma processing.* UK: IOP Publishing: CRC Press, 2001.

[79] U. Kogelschatz, "Filamentary, patterned, and diffuse barrier discharges," *IEEE Trans. Plasma Sci.*, vol. 30, no. 4, pp. 1400–1408, 2002.

[80] B. Eliasson and U. Kogelschatz, "Nonequilibrium volume plasma chemical processing," *IEEE Trans. Plasma Sci.*, vol. 19, no. 6, pp. 1063–1077, 1991.

[81] F. Massines, C. Sarra-Bournet, F. Fanelli, N. Naudé, and N. Gherardi, "Atmospheric pressure low temperature direct plasma technology: Status and challenges for thin film deposition," *Plasma Process. Polym.*, vol. 9, no. 11-12, pp. 1041–1073, 2012.

[82] F. Massines, N. Gherardi, N. Naude, and P. Segur, "Recent advances in the understanding of homogeneous dielectric barrier discharges," *Eur. Phys. J. Appl. Phys. Appl. Phys.*, vol. 47, no. 2, pp. 22805–22815, 2009.

[83] S. Kanazawa, M. Kogoma, T. Moriwaki, and S. Okazaki, "Stable glow plasma at atmospheric pressure," *J. Phys. D. Appl. Phys.*, vol. 21, pp. 838–840, 1988.

[84] F. Massines and G. Gouda, "A comparison of polypropylene-surface treatment by filamentary, homogeneous and glow discharges in helium at atmospheric pressure," *J. Phys. D. Appl. Phys.*, vol. 31, pp. 3411–3420, 1998.

[85] N. Gherardi, G. Gouda, E. Gat, A. Ricard, and F. Massines, "Transition from glow silent discharge to micro-discharges in nitrogen gas," *Plasma Sources Sci. Technol.*, vol. 9, pp. 340–346, 2000.

[86] R. Brandenburg, Z. Navrátil, J. Jánský, P. St'ahel, D. Trunec, and H.-E. Wagner, "The transition between different modes of barrier discharges at atmospheric pressure," *J. Phys. D. Appl. Phys.*, vol. 42, pp. 085208–085217, 2009.

[87] F. Massines, N. Gherardi, N. Naudé, and P. Ségur, "Glow and Townsend dielectric barrier discharge in various atmosphere," *Plasma Phys. Control. Fusion*, vol. 47, pp. B577–B588, 2005.

[88] C. Meyer, S. Müller, E. L. Gurevich, and J. Franzke, "Dielectric barrier discharges in analytical chemistry," *Analyst*, vol. 136, no. 12, pp. 2427–2440, 2011.

[89] D. Hegemann, B. Hanselmann, S. Guimond, G. Fortunato, M. N. Giraud, and A. G. Guex, "Considering the degradation effects of amino-functional plasma polymer coatings for biomedical application," *Surf. Coatings Technol.*, vol. 255, pp. 90–95, 2014.

[90] R. Foerch, J. Izawa, and G. Spears, "A comparative study of the effects of remote nitrogen plasma, remote oxygen plasma, and corona discharge treatments on the surface properties of polyethylene," *J. Adhes. Sci. Technol.*, vol. 5, no. 7, pp. 549–564, 1991.

[91] E. Panousis, A. Ricard, F. Gaboriau, F. Clement, E. Lecoq, J.-F. Loiseau, and B. Held, "Active species in the afterglow of an atmospheric pressure DBD under bipolar pulsed HV excitation," in *2008 17th Int. Conf. Gas Discharges Their Appl.*, pp. 285–288, 2008.

[92] A. M. Diamy, L. Hochard, J. C. Legrand, and A. Ricard, "Concentrations of active species in the flowing afterglow of a nitrogen microwave plasma," *Plasma Chem. Plasma Process.*, vol. 18, no. 4, pp. 447–460, 1998.

[93] A. Ricard, E. Panousis, F. Clement, T. Sindzigre, and J. F. Loiseau, "Production of active species in a N_2 DBD plasma afterglow at atmospheric gas pressure," *Eur. Phys. J. Appl. Phys.*, vol. 42, pp. 63–66, 2008.

[94] Mitra, *Active Nitrogen-A New Theory.* India: Calcutta, 1945.

[95] K. R. Jennings, J. W. Linnett, and M. A. D. Phil, "Active nitrogen," *Q. Rev. Chem. Soc.*, vol. 12, pp. 116–132, 1958.

[96] S. E. Babayan, G. Ding, G. R. Nowling, X. Yang, and R. F. Hicks, "Characterization of the active species in the afterglow of a nitrogen and helium atmospheric-pressure plasma," *Plasma Chem. Plasma Process.*, vol. 22, no. 2, pp. 255–269, 2002.

[97] N. J. Harrick and F. K. du Pre, "Effective thickness of bulk materials and of thin films for internal reflection spectroscopy," *Appl. Opt.*, vol. 5, no. 11, pp. 1739–1743, 1966.

[98] J. Schmitt and H.-C. Flemming, "FTIR-spectroscopy in microbial and material analysis," *Int. Biodeterior. Biodegrad.*, vol. 41, pp. 1–11, 1998.

[99] N. J. Harrick and A. I. Carlson, "Internal reflection spectroscopy: Validity of effective thickness equations," *Appl. Opt.*, vol. 10, no. 1, pp. 19–23, 1971.

[100] V. P. Tolstoy, I. V. Chernyshova, and V. A. Skryshevsky, *Handbook of infrared spectroscopy of ultrathin films.* Hoboken, NJ, USA: John Wiley & Sons, Inc, 2003.

[101] D. A. Ramsay, "Intensities and shapes of infrared absorption bands of substances in the liquid phase," *J. Am. Chem. Soc.*, vol. 74, no. 1, pp. 72–80, 1952.

[102] A. S. Wexler, "Integrated intensities of absorption bands in infrared spectroscopy," *Appl. Spectrosc. Rev.*, vol. 1, no. 1, pp. 29–98, 1967.

[103] M. R. Yagudaev and Y. N. Sheinker, "Integral intensity of deformational vibration bands of the primary amino group," *Transl. from Dokl. Akad. Nauk SSSR*, vol. 144, no. 1, pp. 279–381, 1962.

[104] K. U. Linderstrom-Lang, "Deuterium exchange and protein structure," in *Symp. Protein Struct.*, (London), pp. 23–24, Chemical Society, 1958.

[105] A. Hvidt and K. U. Linderstrom-Lang, "Exchange of hydrogen atoms in insulin with deuterium atoms in aqueous solutions," *Biochim Biophys Acta.*, vol. 14, no. 4, pp. 574–575, 1954.

[106] H. Lenormant and E. R. Blout, "Origin of the absorption band at 1,550 cm-1 in proteins," *Nature*, vol. 172, p. 770, 1953.

[107] E. R. Blout, C. De Lozé, and A. Asadourian, "The deuterium exchange of water-soluble polypeptides and proteins as measured by infrared spectroscopy," *J. Am. Chem. Soc.*, vol. 83, no. 8, pp. 1895–1900, 1961.

[108] G. H. Haggis, "Proton-deuteron exchange in protein and nucleoprotein molecules surrounded by heavy water," *Biochim. Biophys. Acta*, vol. 23, pp. 494–503, 1957.

[109] F. S. Parker and K. R. Bhaskar, "Infrared studies of hydrogen-deuterium exchange in biological molecules," *Appl. Spectrosc. Rev.*, vol. 3, pp. 91–137, 1970.

[110] J. E. DeVries, "Surface characterization methods-XPS, TOF-SIMS, and SAM a complimentary ensemble of tools," *J. Mater. Eng. Perform.*, vol. 7, no. 3, pp. 303–311, 1998.

[111] D. T. Clark and A. Dilks, "ESCA applied to polymers. XXIII. RF glow discharge modification of polymers in helium, neon, argon, and krypton," *J. Polym. Sci., Polym. Chem. Ed.*, vol. 17, pp. 957–976, 1979.

[112] R. M. France and R. D. Short, "Plasma treatment of polymers: The effects of energy transfer from an argon plasma on the surface chemistry of polystyrene, and polypropylene. A high-energy resolution X-ray photoelectron spectroscopy study," *Society*, vol. 14, no. 9, pp. 4827–4835, 1998.

[113] H. Yasuda, H. C. Marsh, S. Brandt, and C. N. Reilly, "ESCA study of polymer surfaces treated by plasma," *J. Polym. Sci.*, vol. 15, no. 4, pp. 991–1019, 1977.

[114] A. Dilks, "The identification of peroxy-features at polymer surfaces by ESCA," *J. Polym. Sci.*, vol. 19, pp. 1319–1327, 1981.

[115] L. J. Gerenser, "X-Ray photoemission study of plasma modified polyethylene surfaces," *J. Adhes. Sci. Tech*, vol. 1, no. 4, pp. 303–318, 1987.

[116] B. Mutel, J. Grimblot, O. Dessaux, and P. Goudmand, "XPS investigations of nitrogen-plasma-treated polypropylene in a reactor coupled to the spectrometer," *Surf. Interface Anal.*, vol. 30, pp. 401–406, 2000.

[117] L. J. Gerenser, "An x-ray photoemission spectroscopy study of chemical interactions at silver/plasma modified polyethylene interfaces: Correlations with adhesion," *J. Vac. Sci. Technol. A Vacuum, Surfaces, Film.*, vol. 6, no. 5, pp. 2897–2903, 1988.

[118] D. Briggs, D. G. Rance, C. R. Kendall, and A. R. Blythe, "Surface modification of poly (ethylene terephthalate) by electrical discharge treatment," *Polymer*, vol. 21, pp. 895–900, 1980.

[119] M. Nitschke and J. Meichsner, "Low-pressure plasma polymer modification from the FTIR point of view," *J. Appl. Polym. Sci. Polym. Chem. Ed. f Appl. Polym. Sci.*, vol. 65, no. 2, pp. 381–390, 1996.

[120] A. Hollaender, S. Kroepke, and F. Pippig, "Chemical analysis of functionalized polymer surfaces," *Surf. Interface Anal.*, vol. 40, pp. 379–385, 2008.

[121] A. Hollaender, F. Pippig, M. Dubreuil, and D. Vangeneugden, "Distinguishing surface OH and NHx using TFAA derivatization and XPS," *Plasma Process. Polym.*, vol. 5, pp. 345–349, 2008.

[122] A. Chilkoti and B. D. Ratner, "An X-ray photoelectron spectroscopic investigation of the selectivity of hydroxyl derivatization reactions," *Surf. Interface Anal.*, vol. 17, pp. 567–574, 1991.

[123] A. Choukourov, H. Biederman, D. Slavinska, M. Trchova, and A. Hollander, "The influence of pulse parameters on film composition during pulsed plasma polymerization of diaminocyclohexane," *Surf. Coatings Technol.*, vol. 174 -175, pp. 863–866, 2003.

[124] C.-P. Klages and A. Grishin, "Quantitative ATR FT-IR analysis of chemically derivatized plasma-modified polymer surfaces," *Plasma Process. Polym.*, vol. 5, pp. 359–367, 2008.

[125] J. Stöhr, *NEXAFS spectroscopy.* Berlin: Springer-V, 1992.

[126] S. G. Urquhart, A. P. Hitchcock, A. P. Smith, H. W. Ade, W. Lidy, E. G. Rightor, and G. E. Mitchell, "NEXAFS spectromicroscopy of polymers: overview and quantitative analysis of polyurethane polymers," *J. Electron Spectros. Relat. Phenomena*, vol. 100, pp. 119–135, 1999.

[127] J. Kikuma and B. P. Tonner, "XANES spectra of a variety of widely used organic polymers at the C K-edge," *J. Electron Spectros. Relat. Phenomena*, vol. 82, pp. 53–60, 1996.

[128] W. E. S. Unger, A. Lippitz, C. Wöll, and W. Heckmann, "X-ray absorption spectroscopy (NEXFAS) of polymer surfaces," *Fresenius J. Anal. Chem.*, vol. 358, pp. 89–92, 1997.

[129] H. Ade, A. Smith, H. Zhang, G. Zhuang, J. Kirz, E. Rightor, and A. Hitchcock, "X-ray spectromicroscopy of polymers and tribological surfaces at beamline X1A at the NSLS," *J. Electron Spectros. Relat. Phenomena*, vol. 84, pp. 53–72, 1997.

[130] T. Hemraj-Benny, S. Banerjee, S. Sambasivan, M. Balasubramanian, D. A. Fischer, G. Eres, A. A. Puretzky, D. B. Geohegan, D. H. Lowndes, W. Han, J. A. Misewich, and S. S. Wong, "Near-edge X-ray absorption fine structure spectroscopy as a tool for investigating nanomaterials," *Small*, vol. 2, no. 1, pp. 26–35, 2006.

[131] G. Hähner, "Near edge X-ray absorption fine structure spectroscopy as a tool to probe electronic and structural properties of thin organic films and liquids," *Chem. Soc. Rev.*, vol. 35, pp. 1244–1255, 2006.

[132] A. Ricard, A. Besner, J. Hubert, and M. Moisant, "High nitrogen atom yield downstream of an atmospheric pressure flowing Ar-N_2, microwave discharge," *J. Phys. B At. Mol. Opt. Phys*, vol. 21, pp. L579–L583, 1988.

[133] S. E. Babayan, G. Ding, and R. F. Hicks, "Determination of the nitrogen atom density in the afterglow of a nitrogen and helium, nonequilibrium, atmospheric pressure plasma," *Plasma Chem. Plasma Process.*, vol. 21, no. 4, pp. 505–521, 2001.

[134] Z. Khosravi and C.-P. Klages, "Investigation of imine formation on PE surfaces treated in ambient-pressure nitrogen/hydrogen DBD afterglow," in *Int. Conf. Plasma Surf. Eng. PSE*, (Garmisch-Partenkirchen), 2014.

[135] Z. Khosravi, A. Hinze, and C.-P. Klages, "In-situ FTIR-ATR spectroscopic investigations of atmospheric-pressure plasma modification of polyolefin thin films-where are the primary amino groups?," in *Int. Conf. Plasma Surf. Eng. PSE*, (Garmisch-Partenkirchen), 2012.

[136] W. Hertl, "Surface chemical properties of zinc sulfide," *Langmuir*, vol. 4, no. 3, pp. 594–598, 1988.

[137] M. Strobel, C. S. Lyons, and K. L. Mittal, *Plasma surface modification of polymers: Relevance to adhesion*. VSP, 1994.

[138] G. Hawkins and R. Hunneman, "The temperature-dependent spectral properties of filter substrate materials in the far-infrared (6-40 micron)," *Infrared Phys. Technol.*, vol. 45, no. 1, pp. 69–79, 2004.

[139] H. Kukimoto, S. Shionoya, T. Koda, and R. Hioki, "Infrared absorption due to donor in ZnS crystals," *J. Phys. Chem. Solids*, vol. 29, pp. 935–944, 1968.

[140] J. Friedrich, J. Gaehde, H. Frommelt, and H. Wittrich, "Modification of the surface of solids by high-frequency discharge for purposes of adhesion.," *Faserforsch. und Textiltechnik*, vol. 27, p. 604, 1976.

[141] D. Mantovani, M. Castonguay, J. F. Pageau, M. Fiset, and G. Laroche, "Ammonia RF-plasma treatment of tubular ePTFE vascular prostheses," *Plasma Polym.*, vol. 4, no. 2/3, pp. 207–228, 1999.

[142] J. R. Durig and C. Zheng, "Infrared spectra of krypton solutions of methylamine," *Struct. Chem.*, vol. 12, no. 2, pp. 137–148, 2001.

[143] G. M. Barrow, "The infrared spectra of oriented rhombic sulfur crystals with polarized radiation," *J. Chem. Phys.*, vol. 21, pp. 219–222, 1953.

[144] V. Krishnamurthy and I. L. Kamel, "Analysis of plasma polymerization of allylamine by FTIR," *J. Polym. Sci., Part A Polym. Chem.*, vol. 27, pp. 1211–1224, 1989.

[145] D. Lin-Vien, N. B. Colthup, W. G. Fateley, and J. G. Grasselli, *The handbook of infrared and Raman characteristic frequencies of organic molecules.* elsevier, ed., 1991.

[146] D. Meakins and R. J. Moss, "The antisymmetric stretching band of carbodi-imides," *J. Chem. Soc.*, vol. 1957, pp. 993–997, 1957.

[147] P. H. Mogul, *The physical and optical properties of carbodiimides.* Doctor of philosophy, Iowa State University of Science and Technology Ames, Iowa, 1967.

[148] H. Ulrich, *Chemistry and technology of carbodiimides*, vol. 179. West Sussex: John Wiley & Sons, Ltd, 2007.

[149] D. Bégué, G. G. Qiao, and C. Wentrup, "Nitrile imines: Matrix isolation, IR spectra, structures, and rearrangement to carbodiimides," *J. Am. Chem. Soc.*, vol. 134, pp. 5339–5350, 2012.

[150] E. M. Kosower and T. S. Sorensen, "Some unsaturated imines," *J. Org. Chem.*, vol. 28, no. 3, pp. 692–695, 1963.

[151] A. D. J. Calow, J. J. Carbó, J. Cid, E. Fernández, and A. Whiting, "Understanding α,β-unsaturated imine formation from amine additions to α,β-unsaturated aldehydes and ketones: An analytical and theoretical investigation," *J. Org. Chem.*, vol. 79, no. 11, pp. 5163–5172, 2014.

[152] Y. Amatatsu, Y. Hamada, and M. Tsuboi, "FTIR detection of unstable molecules: Infrared spectrum of 2-azabutadiene," *J. Mol. Spectrosc.*, vol. 123, no. 2, pp. 276–285, 1987.

[153] J. C. Guillemin, J. M. Denis, and A. Lablache-Combier, "1-Azetine: Thermal ring opening to 2-azabutadiene," *J. Am. Chem. Soc.*, vol. 103, pp. 469–471, 1981.

[154] R. H. Hasek, E. U. Elam, and J. C. Martin, "Reaction of secondary and tertiary aldehydes with ammonia," *J. Org. Chem.*, vol. 26, no. 6, pp. 1822–1825, 1961.

[155] A. G. Shard, J. D. Whittle, A. J. Beck, P. N. Brookes, N. A. Bullett, R. A. Talib, A. Mistry, D. Barton, and S. L. McArthur, "A NEXAFS examination of unsaturation in plasma polymers of allylamine and propylamine," *J. Phys. Chem. B*, vol. 108, no. 33, pp. 12472–12480, 2004.

[156] C.-P. Klages and S. Kotula, "Critical remarks on chemical derivatization analysis of plasma-treated polymer surfaces and plasma polymers," *Plasma Process. Polym.*, vol. 13, pp. 1213–1223, 2016.

[157] D. Zeroka, J. O. Jensen, and A. C. Samuels, "Infrared spectra of some isotopomers of ethylamine and the ethylammonium ion: A theoretical study," *J. Mol. Struct. Theochem*, vol. 465, no. 2-3, pp. 119–139, 1999.

[158] S. Pinchas and I. Laulicht, *Infrared spectra of labelled compounds*. academic p ed., 1971.

[159] J. Fabian and M. Legrand, "Imine intensities," *Bull. Soc. Chim. Fr.*, vol. 23, p. 1461, 1956.

[160] Z. Bascik, N. Ahlsten, A. Ziadi, G. Zhao, A. E. Garcia-Bennett, B. Martín-Matute, and N. Hedin, "Mechanisms and kinetics for sorption of CO2 on bicontinuous mesoporous silica modified with n-propylamine," *Langmuir*, vol. 27, pp. 11118–11128, 2011.

[161] C. D. Batich, "Chemical derivatization and surface analysis," *Appl. Surf. Sci.*, vol. 32, no. 1-2, pp. 57–73, 1988.

[162] J. E. Klemberg-Sapieha, O. M. Küttel, L. Martinu, and M. R. Wertheimer, "Dual frequency N_2 and NH_3 plasma modificaion of polyethylene and polyimide," *J. Vac. Sci. Technol. A*, vol. 9, no. 6, pp. 2975–2981, 1991.

[163] H. Rojas-Saenz, G. V. Uarez-Moreno, I. Ramos-Garcia, E. Duarte-Hernandez, A. M. Mijangos, A. Pena-Hueso, R. Contreras, and A. Flores-Parra, "1,4-Dialkyl-1,4-diazabutadienes: : Their reactions with aluminum and indium halides," *New J. Chem.*, vol. 38, p. 391, 2014.

[164] A. Harada, H. Fujii, and M. Kamachi, "Polymerization of azabutadiene (azine) derivatives. Preparation of a stereoregular polymer from propionaldehyde azine," *Macromolecules*, vol. 24, pp. 5504–5507, 1991.

[165] G. Abbiati, A. Contini, D. Nava, and E. Rossi, "Cycloaddition reactions of 1,3-diazabuta-1,3-dienes with alkynyl ketenes," *Tetrahedron*, vol. 65, no. 24, pp. 4664–4670, 2009.

[166] R. Fuks, D. Baudoux, C. Piccinni-Leopardi, J. P. Declercq, and M. Van Meerssche, "A new and facile synthesis of ketene imines and their 2-iminoazetidine dimer from nitriles via their nitrilium salts," *J. Org. Chem.*, vol. 53, pp. 18–22, 1988.

[167] E. Orton, S. T. Collins, and G. C. Pimentel, "Molecular structure of the nitrile ylide derived from 3-phenyl-2H-azirine in a nitrogen matrix," *J. Phys. Chem*, vol. 90, no. 23, pp. 6139–6143, 1986.

[168] P.-L. Girard-Lauriault, P. Dietrich, T. Gross, and W. E. S. Unger, "Is quantitative chemical derivatization XPS of plasma deposited organic coatings a valid analytical procedure?," *Surf. Interface Anal.*, vol. 44, pp. 1135–1140, 2012.

[169] G. Reddelien and H. Danilof, "Über die Spaltbarkeit der Anile," *Berichte*, vol. 54, pp. 3132–3142, 1921.

[170] C. K. Ingold and H. A. Piggott, "The additive formation of four-membered rings. Part I. The synthesis and division of derivatives from 1:3 dimethindiazidine," *J. Chem. Soc., Trans.*, vol. 121, pp. 2793–2804, 1922.

[171] H. Breederveld, "The chemistry of the n-alkylaldimines," *Recueil*, vol. 79, pp. 401–407, 1960.

[172] D. E. Tosunyan, S. V. Verin, and E. V. Kuznetsov, "2-benzopyrylium salts. Interaction of 2-benzopyrylium salts and their monocyclic analogs with imines of ketones," *Chem. HeterocTclic Compd.*, vol. 30, pp. 1015–1023, 1994.

[173] V. B. Ivanov, J. Behnisch, A. Hollander, F. Mehdorn, and H. Zimmermann, "Determination of functional groups on polymer surfaces using fluorescence labelling," *Surf. Interface Anal.*, vol. 24, pp. 257–262, 1996.

[174] R. Huisgen, M. Morikawa, D. S. Breslow, and R. Grashey, "Reaktionen der azomethine mit isothiocyanaten und schwefelkohlenstoff," *Chem. Ber.*, vol. 100, pp. 1602–1615, 1967.

[175] R. Mahrwald, "unpublished,"

[176] F. Pippig, S. Sarghini, A. Hollaender, S. Paulussen, and H. Terryn, "TFAA chemical derivatization and XPS analysis of OH and NHx polymers," *Surf. Interface Anal.*, vol. 41, pp. 421–429, 2009.

[177] J. C. Ruiz, S. Taheri, A. Michelmore, D. E. Robinson, R. D. Short, K. Vasilev, and R. Förch, "Approaches to quantify amine groups in the presence of hydroxyl functional groups in plasma polymerized thin films," *Plasma Process. Polym.*, vol. 11, pp. 888–896, 2014.

[178] L. Gerenser, J. Elman, M. Mason, and J. Pochan, "E.s.c.a. studies of corona-discharge-treated polyethylene surfaces by use of gas-phase derivatization," *Polymer*, vol. 26, pp. 1162–1166, 1985.

[179] R. Schulte-Ladbeck, R. Lindahl, J. O. Levin, and U. Karst, "Characterization of chemical interferences in the determination of unsaturated aldehydes using aromatic hydrazine reagents and liquid chromatography," *J. Environ. Monit.*, vol. 3, no. 3, pp. 306–310, 2001.

[180] F. Shirini and J. Albadi, "Melamine trisulfonic acid as a new, efficient and reusable catalyst for the chemoselective oxathioacetalyzation of aldehydes," *Bull. Korean Chem. Soc.*, vol. 31, no. 5, pp. 1119–1120, 2010.

[181] Z. Khosravi, S. Kotula, A. Lippitz, W. Unger, and C.-P. Klages, "IR- and NEXAFS-spectroscopic Characterization of Plasma-nitrogenated Polyolefin Surfaces," *Prep.*, 2017.

[182] Z. Khosravi, S. Kotula, and C.-P. Klages, "ISPC 22 - 22nd International Symposium on Plasma Chemistry," in *ISPC 22 - 22nd Int. Symp. Plasma Chem.*, (Antwerp), 2015.

[183] A. J. Beck, J. D. Whittle, N. A. Bullett, P. Eves, S. Mac Neil, S. L. McArthur, and A. G. Shard, "Plasma co-polymerisation of two strongly interacting monomers: Acrylic acid and allylamine," *Plasma Process. Polym.*, vol. 2, pp. 641–649, 2005.

[184] M. F. Golde and A. Thrush, "Afterglows," *Rep. Prog. Phys.*, vol. 36, pp. 1285–1364, 1973.

[185] G. Black, R. L. Sharpless, and T. G. Slanger, "Collision-induced emission from O(^{1}S) by He, Ar, N_2, H_2, Kr, and Xe," *J. Chem. Phys.*, vol. 63, pp. 4546–4550, 1975.

[186] A. Ricard, S.-g. Oh, and V. Guerra, "Line-ratio determination of atomic oxygen and molecular nitrogen metastable absolute densities in an RF nitrogen late afterglow," *Plasma Sources Sci. Technol.*, vol. 22, no. 3, p. 035009, 2013.

[187] M. A. A. Clyne and D. H. Stedman, "Rate of recombination of nitrogen atoms," vol. 71, no. 9, pp. 3071–3073, 1967.

[188] A. Ricard, C. Jaoul, F. Gaboriau, N. Gherardi, and S. Villeger, "Production of N, H, O, and C atoms in flowing microwave discharges," *Surf. Coat. Tech.*, vol. 188-189, pp. 287–293, 2004.

[189] L. G. Piper, "Energy transfer studies on N_2(X $^1\Sigma_g^+$,v) and N_2(B $^3\Pi_g$)," *J. Chem. Phys.*, vol. 97, pp. 270–275, 1992.

[190] C.-P. Klages and B. Hergelova, "to be published," 2017.

[191] R. L. Brown, "A measurement of the rate of the reaction N + H + M to NH + M," *Int. J. Chem. Kinet.*, vol. v, pp. 663–667, 1973.